EXOSOMES SECRETED BY MICROGLIA CONTRIBUTE TO VIRUS PERSISTENCE AND DEMYELINATING DISEASE

A DISSERTATION

SUBMITTED TO THE FACULTY OF THE

UNIVERSITY OF MINNESOTA

BY

NHUNGOC HONG LUONG

IN PARTIAL FULFILLMENT OF THE REQUIREMENTS

FOR THE DEGREE OF

DOCTOR OF PHILOSOPHY

Julie K. Olson

Adviser

September 2020

ACKNOWLEDGMENTS

I would like to thank the following people, with whom this work would not have been achieved:

1. My advisor, Dr. Julie K. Olson, for her endless mentorship and support on my journey to obtain my doctoral degree. I would like to send my deepest gratitude to her willingness to welcome me to her laboratory and giving me so much independence in choosing my research interest. She has always supported me in attending conferences and meetings, which allowed me to share my research as well as expand my network. Dr. Olson has also been an outstanding role model for me when it comes to demonstrating what it is like and what it takes to be a woman in science. Her encouragements during difficult times truly helped me stay positive and stay persistent when overcoming seemingly insurmountable obstacles.
2. My committee members: Dr. Michael Murtaugh, Dr. Thomas Molitor, Dr. James Lokensgard, and Dr. Mark Schleiss for their support and feedback on my work. I want to especially thank Dr. Michael Murtaugh for all the memories that we had since my first day of becoming a graduate student. I used to be intimidated by tough questions, but these questions were only meant to train me to be more critical of my experimental designs and better at public speaking.
3. Dr. Jennifer Lenz, for her tremendous contribution to the study of exosomes from tumor cells. She was an incredible lab mate and friend.

She made sure that I would not belittle myself when work and personal life did not go the way that I wanted.

4. Neighbor lab members, Dr. Karen Ross, Dr. Bruno Lima, Dr. Brittany Nair, and Dr. Deb Ghose, for their technical support and help. Thank you for seeing me as an “adopted lab member” and more importantly, a friend and sister.
5. My T32 training grant (DA007097) and the program coordinator, Yorie Smart, for financially supporting my work and providing a trusted and safe environment for me to express my concerns, share my future endeavors, and ask for advices.
6. My mom, Thanhtung Nguyen, and my brothers, Tri Luong and Thuc Luong for their love and understanding. They have always been proud of me and supported my decisions, including pursuing a doctoral degree.
7. Last but not least, my husband, Gordon Ruan for his tremendous support, love, and sacrifice. Thank you for coming to my life during the last and most challenging year of my PhD journey.

ABSTRACT

Multiple sclerosis (MS) is a chronic autoimmune-mediated demyelinating disease that affects more than 2.3 million people worldwide, especially young adults. The etiology is unknown, and effective treatments are unavailable. Viral infection(s) has been postulated to play a critical role in the initiation and progression of MS. My study utilizes a mouse model called Theiler's murine encephalomyelitis virus-induced demyelinating disease (TMEV-IDD) to better understand human MS. In TMEV-IDD, *microglia, a resident macrophage in the central nervous system (CNS), are* persistently infected with TMEV. As a result, the infected microglia produce an innate immune response that has been shown to contribute to bystander damage, bystander activation, and inflammation in the CNS, ultimately leading to demyelination. My central hypothesis is that exosomes secreted by microglia during TMEV infection may play an important role in sustaining persistence of virus and inflammation in the CNS, contributing to the development of demyelinating disease. We found that exosomes secreted by microglia during the acute phase (2 days post infection, dpi) and chronic phase (starting at 63dpi) of TMEV infection have altered surface markers and importantly, contain viral RNA/genome. We discovered that these exosomes are able to transfer viral RNA to uninfected CNS and infiltrating bystander cells to activate an innate immune response including expression of type I IFNs, pro-inflammatory cytokines, chemokines, and effector molecules. This activation was prominently triggered by the recognition viral RNA in exosomes by innate immune receptors. Naïve mice injected with exosomes secreted by microglia

during TMEV infection showed microglia activation, neuroinflammation, and demyelination. In summary, these findings shed light on the role of exosomes in maintaining viral persistence and sustaining inflammation which are crucial in the development of virus-induced demyelinating disease in mice, and possibly human MS. The knowledge from this work may allow for identification of new therapeutic targets or disease-modifying strategies to treat demyelinating disease in human MS.

TABLE OF CONTENTS

LIST OF TABLES

LIST OF FIGURES

LIST OF ABBREVIATIONS

1. BBB, blood-brain barrier
2. CNS, central nervous system
3. EVs, extracellular vesicles
4. MS, multiple sclerosis
5. PLP, proteolipid protein
6. TMEV, Theiler's murine encephalomyelitis virus
7. TMEV-IDD, Theiler's murine encephalomyelitis virus induced demyelinating disease

CHAPTER 1

Background and literature review

1. MULTIPLE SCLEROSIS (MS)

MS is a chronic, inflammatory demyelinating disease of the central nervous system (CNS). In MS, the myelin sheet surrounding the axon is impaired, which results in a breakdown of communication between neurons and progressive and permanent nerve deterioration. The incidence of MS is highest in people ages 20 to 40, with the incidence among women compared to men being significantly higher at a 3:1 ratio respectively[1, 2]. MS in the pediatric population is rare and occurs in 1 every 100,000 cases [3]. The diagnosis of MS is difficult because it is primarily a clinical diagnosis that requires an objective demonstration of dissemination of CNS in both space and time. Clinical manifestations are dependent on the location and stage of lesion/damage with symptoms such as tremors, focal or multifocal neurologic deficits, facial paresthesia, diplopia, dysarthria, bladder dysfunction, ataxia, or spastic paralysis [4]. Imaging with magnetic resonance imaging (MRI) can be helpful and is the preferred imaging test to identify whether patients have CNS plaques or lesions at different regions in both white and grey matter of the brain and spinal cord. Diagnosis of MS is thus based upon clinical findings alone or a combination of clinical and magnetic resonance imaging (MRI) findings. MS is a complex disease with heterogeneous phenotypes that are categorized into four main types[5]. The most common (~87%) form of MS is relapse-remitting (RRMS), which is described by episodes of reversible neurological attacks. Once the

attacks become more frequent and protuberant, the patients can develop secondary progressive MS (SPMS). On the other hand, primary progressive MS (PPMS) (~10%) is the most severe phenotype with irreversible progressive clinical symptoms. PPMS lesions tend to locate in the spinal cord rather than the brain and are associated with more serious symptoms such as ataxia and paralysis[5].

There is no cure for MS and existing treatment is focused on reducing the severity of attacks or relapses, expediting recovery, or slowing disease progression. Current therapies employ temporary immunomodulation and/or immunosuppression, which need to be administered regularly and have adverse side effects that increase the patient's risk for infection and malignancy[6]. Immune reconstitution therapy using embryonic or mesenchymal stem cells has shown promising long-lasting outcomes in some patients but carries significant mortality due to its high adverse effect profile[7]. More research is needed to understand the pathophysiology of MS so that new therapeutics can be developed to ultimately improve patient outcomes

2. MS PATHOGENESIS

The cause of MS is unknown, and the combination of environmental agents, genetic predisposition, and immunological components have been suggested to contribute to the disease pathogenesis[5, 8, 9]. Among those, viral infections contracted during childhood (the first 15 years of life) that act as potential triggers have been extensively studied[9-11]. In recent years, ubiquitous viruses belonging to the herpesvirus family such as Epstein-Barr virus (EBV) and

human herpesvirus 6 (HHV 6) have gained significant interest. Studies have shown that high titer of antibodies against EBV and increased circulating HHV-6 proteins are consistently detected in body fluids of MS patients during relapse and progression [12, 13].

Traditionally, MS has been classified as an autoimmune disease associated with myelin-specific T cells and B cells. However, recent studies have suggested that the role of these adaptive immune cells is likely the result of another upstream process[14, 15]. Our hypothesis is that there is a viral etiology that causes CNS-resident inflammatory immune cells, mainly microglia, to activate and induce infiltration of peripheral lymphocytes, including myelin-specific T cell and B cells, which result in the death of myelin-producing oligodendrocytes and neuron apoptosis. Our work focuses on further exploring a viral etiology as a cause for MS.

3. MICROGLIA

Microglia Development and Function

The CNS was once thought to be the immune-privileged organ until the discovery of the lymphatic drainage system[16]. The CNS equips itself with the specialized innate immune cell called microglia to rapidly respond to pathogenic infections and injury, minimize unnecessary crosstalk with peripheral cells, thus maintaining homeostasis and tissue vigilance [17]. Microglia make up approximately 15% of CNS cells and have the ability to self-regenerate. These cells are commonly known as the CNS-resident macrophages due to their shared immunological functions, phenotypes, and morphology. Since microglia and

monocytes/macrophages express similar surface markers (CD45, CD11b, Iba1, CD68, and CX3CR1, and others), distinguishing one from the other has been a great challenge for researchers. Nonetheless, microglia originate from the yolk sac and migrate the CNS at early development (embryonic day 9.5, E9.5) and reside strictly in the parenchyma[18, 19]. On the other hand, monocytes/ macrophages are derived from post-natal bone marrow cells and populate peripherally including choroid plexus, perivascular space, and meninges[18]. Under normal conditions, microglia stay quiescent and stationary, using their elongated and fine processes to patrol the extracellular space and maintain homeostasis by performing tasks such as CNS debris/plaque scavenging, neuronal repair, and synaptic pruning.

As innate immune cells, microglia also serve as the first line of defense in the CNS against pathogens. Upon viral infections, microglia become activated to secrete type I interferons (INFs, IFNα, and IFNβ), chemokines(CCL2, CCL3, and CCL5), pro-inflammatory cytokines (interleukin (IL)- 1β, IL-6, IL-12, and TNFα) as well as anti-inflammatory cytokines (IL-10 and arginase) to recruit and activate other immune cells at the infection site to combat the virus and remove apoptotic bodies[20, 21]. On the surface, microglia express co-stimulatory molecules CD80, CD86 and CD40 and both major histocompatibility complex (MHC) class I and II, and thus are able to present foreign antigens to $CD4^+$ and $CD8^+$ T cells to orchestrate T cell-mediated and direct killing of infected cells[21]. The phenotypic plasticity of the microglia enables them to perform both inflammatory and anti-

inflammatory functions, thus, their role in disease pathogenesis is often controversial.

Microglia in MS

Microglial activation and inflammation are the gold standard hallmarks of MS pathology. Clinical studies found clusters of activated microglia not only in the active/demyelinating lesions but also in the intact white matter of MS patients, which were termed “pre-active lesions”[22]. These pre-active lesions are void of infiltrating lymphocytes and often progress into active lesions[23]. Activated microglia stained positive for myelin degradation products such as myelin basic protein (MBP) and proteolipid protein (PLP) are detected consistently throughout early demyelinating and post demyelinating lesions[23]. Transmembrane protein 119, TMEM119 has been proposed to be the microglia specific marker present in the active lesion[24]. About 43% of phagocytes are TMEM119 positive and ionized calcium-binding adaptor molecule 1 (Iba1) positive, and these double-positive microglia are present at the border of mixed active/inactive lesions, indicating that microglia may play a key role in MS progression[25].

In both human MS and murine demyelinating disease models, microglia have been shown to upregulate their expression of pro-inflammatory cytokines such as IL-1β, IL-18, IL-6, and chemokines CCL2 and CCL5, to recruit and activate T cells, thereby contributing to CNS inflammation and neurodegeneration. Reactive oxygen species (ROS) and reactive nitrogen species (RNS) secreted from microglia can act on oligodendrocytes and neurons to induce impaired remyelination and axonal damage, respectively. Overall,

these clinical studies agree with animal experimental studies, suggesting that microglia are indeed involved in the initiation, progression, and even remyelination of MS lesions. However, the trigger(s) remain undetermined. Targeting microglia could potentially be a new therapeutic option for MS.

4. THEILER'S MURINE ENCEPHALOMYELITIS VIRUS-INDUCED DEMYELINATING DISEASE (TMEV-IDD)

TMEV is a positive sense, single-stranded (ss) which belongs to the Piconaviridae family. Infection of TMEV (BeAn 8386 strain) in susceptible mouse strain (Swiss Jim Lambert, SJL) can lead to viral persistence in microglia and development of chronic progressive demyelinating disease associated with proteolipid peptide $(PLP)_{139-151}$ -specific $CD4^{+}Th_1$ type T cells, approximately 55 days post-infection (dpi)[21, 26-28]. Clinical symptoms in mice can be observed around 35 dpi, which include spastic paralysis in the hind limbs and gaiting difficulty[29, 30]. The demyelination seen in the TMEV-IDD appears to not be due to the cytolytic effect in glial cells but rather immune-mediated, which closely recapitulates the immunopathology seen in human MS. Hence, TMEV-IDD is an appropriate mouse model for studying the virologic and mechanisms involved in human chronic progressive MS.

Both the innate and adaptive immune responses play inevitable roles in driving the development and progression of TMEV-IDD through mechanisms including bystander activation, bystander damage, and epitope spreading[31]. Interestingly, a comprehensive transcriptional study demonstrated that although the expression of the adaptive immune response was upregulated early (30dpi)

in TMEV-IDD, the innate immune genes were more prominent at the late chronic stage (165dpi) of TMEV-IDD[32]. This seemingly counterintuitive observation suggests that more research is needed in investigating the activity of the innate immune cells in sustaining neuroinflammation during the chronic stage.

Role of the CNS innate immune response to TMEV infection and demyelination.

The innate immune response becomes activated by the recognition of pathogen-associated molecular patterns (PAMPs) through innate immune receptors, predominantly Toll-like receptors (TLRs) which are expressed in most cells. TLR7 and TLR8 were shown to recognize viral ssRNA, while TLR3, intracellular melanoma differentiation-associated protein 5 (MDA5) and retinoic acid-inducible gene 1 (RIG-I) recognize viral dsRNA[33-37]. TLR7 signals through a common adaptor protein myeloid differentiation primary response gene 88 (MyD88) resulting in downstream activation of the NF-kB family of transcription factors[38]. Meanwhile, TLR3 signals through TIR-domain-containing adaptor-inducing interferon β (TRIF) adaptor which leads to the cascade of interferon regulatory factor (IRF)-3 and IRF-7[39]. MDA5 and RIG-I also involve activation of IRF-3[40]. All of these engagements result in transcriptional expression of cytokines, chemokines, and effector molecules contributing to an inflammatory milieu.

Inflammation is the hallmark of demyelinating diseases including MS. The susceptibility to demyelinating disease development in mice is greatly dependent on the magnitude of the innate immune response following TMEV infection[41].

Shortly after intracranial inoculation of TMEV, type I IFNs (IFNβ and IFNα) are immediately produced by the CNS innate immune cells. Type I IFNS are prominent antiviral mediators such as promoting blastogenesis and proliferation of natural killer (NK) cells independent of IL-2 pathway, as well as enhancing their cytolytic effect on infected cells [42]. Type I IFNs also mediate the adaptive immune response by driving $CD4^+$ T cells toward the Th1 type response and induce IFNγ secretion by T cells to promote expression of MHC class I and II on antigen-presenting cells (APCs), macrophage activation, and B cell class switching (IgG2a)[43-45]. Studies from our lab have shown that administration of IFNβ, not IFNα, shortly post-infection reduced the development and slowed the progression of TMEV-IDD and was associated with a decrease in pro-inflammatory cytokines, mononuclear cells infiltration, and myelin-specific $CD4^+$ T cells response[41]. In contrast, the administration of an antibody against IFNβ correlates with an increase in disease severity of the demyelinating disease[41].

Role of the adaptive immune response in TMEV infection and demyelination.

Persistent infection due to inefficient viral clearance is another central condition in demyelinating disease development. After one week of post-TMEV infection, peripheral immune cells are recruited into the CNS as the blood-brain barrier (BBB) integrity is compromised by the cytokines and chemokines released by innate immune cells. Viral clearance clearly showed the importance of disease initiation as $CD8^+$T cell depleted-resistant mice or β2-microglobulin-deficient mice develop chronic infection and demyelination after TMEV

challenge[30, 46]. In addition, an insufficient immune response from virus-specific $CD8^+$T cells is linked to the H-2K locus on the MHC class I genes in susceptible mouse strands[47]. However, $CD8^+$T cells appeared to minimally contribute to the progression of TMEV-demyelinating disease as the deletion of $CD8^+$T cells did not rescue susceptible mice from disease development[48].

In TMEV-IDD, there are TMEV-specific $CD4^+$T cells and myelin-specific $CD4^+$T cells, and their involvements are significant in disease development. MHC class II-restricted, TMEV-specific $CD4^+$T cells play a role in the initiation of the disease because the rise of these cells happens as early as 5 dpi and their peak (14dpi) coincides with the clinical disease onset[49, 50]. The immune response from viral-specific $CD4^+$ T cells may have a *bystander damage effect on surrounding* myelinated neurons[30]. Induced toleration of $CD4^+$T cells with TMEV antigens leads to reduced severity of disease and secretion of Th1-type pro-inflammatory cytokines[51]. On the other hand, myelin-specific $CD4^+$T cells are found to be involved in the chronic demyelinating phase of TMEV-IDD as these cells do not arise until 50-55dpi[49]. Autoreactive $CD4^+$T against $PLP_{139-151}$ was consistently isolated from the CNS of mice during TMEV-IDD. Not only that, reactivity to myelin epitopes of $CD4^+$T cells progresses in order (PLP_{56-70}, myelin oligodendrocyte glycoprotein $(MOG)_{92-106}$, $PLP_{178-191}$, myelin basic protein $(MBP)_{84-104}$), introducing the concept of *epitope spreading*. Most importantly, peripheral tolerance of PLP and MBP using recombinant fusion protein halts the disease progression.

Role of microglia in TMEV-IDD development and progression

Microglia have been implicated in the pathogenesis of mouse TMEV-IDD and human MS due to their pro-inflammatory nature. They are the first cells to arrive at the infection site and express innate immune receptors which enable them to rapidly respond to pathogens invading the CNS. Microglia are persistently infected with TMEV and become activated through the innate immune receptors to express cytokines, chemokines, and effector molecules[20]. We have previously shown that TMEV infection of microglia leads to rapid expression of IFNα and IFNβ[41]. We have also shown that microglia infected with TMEV become activated to express pro-inflammatory cytokines, IL-1 β, IL-6, IL-12, TNFα, chemokines, CCL2, CCL3, CCL5, and effector molecules like inducible nitric oxide (iNOS)[41]. TMEV- infected microglia also become activated antigen-presenting cells that can present viral antigens and myelin antigens to $CD4^+$ T cells[21]. Hence, we are compelled to understand more about how microglia are involved in maintaining viral persistence, neuroinflammation, and demyelination following TMEV infection.

5. EXOSOMES

Exosome biogenesis

Almost all eukaryotic cells constitutively release extracellular vesicles (EVs) that can be taken up by other cells, thus mediating intercellular communication. The exosome is a subset of EVs, classified by its nanoscopic size (30-160 nanometers, nm) and distinct biogenesis. These nanovesicles are generated by the clathrin-mediated inward budding of the endosomal membrane to form multivesicular bodies (MVBs). Before being released into the extracellular space,

they are called intraluminal vesicles (ILVs). Once the ILVs are released by the fusion of MVBs with the cell membrane, they become *exosomes*. The exosome membranes resemble the lipid bilayer membrane containing cell-specific makers as well as exosome-specific markers such as tetraspanin (CD63, CD81, and CD9) and syndecans[52, 53]. Exosomes contain proteins, lipids, and nucleic acids, including mRNA, microRNA, and DNA[54]. The composition of the exosomal membrane allows them to securely transfer various materials across stringent structures such as the BBB and prevent the degradation from surrounding RNAse and proteases[55]. Studies have suggested that the exosomal content sorting and delivery destination are rather programmed and not arbitrary as previously thought. The sorting of exosomal content and packaging require proteins of the endosomal sorting complex (ESCRT), ALG2 interacting protein X (ALIX), and tumor susceptibility genes (TSG101)[56, 57]. The cellular markers expressed on exosomes may steer exosomes to target specific cells and the uptake is dependent on the cell type [58, 59]. Nonetheless, this area of exosome research needs more investigation

Roles of exosomes in diseases

Recent studies have revealed the important role of exosomes in the pathogenesis of neurodegenerative diseases via the transfer of miRNAs, pathogenic, and misfolded proteins from rafts to recipient cells[55, 60]. Some efforts were delegated on studying the role of exosomes in MS, mainly by using experimental autoimmune encephalitis (EAE), a mouse model of human relapse-

remitting MS. Thus, how exosomes are involved in the chronic progressive MS remains a substantial gap in knowledge.

More recently, exosomes represent a novel pathway in pathogenesis and immune evasion of viruses. Exosomes isolated from the sera of chronically infected hepatitis C virus (HCV) patients showed to contain replication-competent viral RNA[61]. Further, exosome-packaged HCV could induce the phenotype and cytokine profile switch in recipient macrophage[62]. Another study demonstrated that exosomes secreted by human immunodeficient virus (HIV)1–infected cells contained trans activator of transcription (Tat) protein promote bystander neurotoxicity seen in with HIV-associated neurocognitive diseases[63]. Once packaged inside the exosomes, viruses and their components would be protected from antibodies, thus possibly enhancing viral transmission and persistence.

Another topic of interest is pathogenic roles of extracellular EVs, specifically exosomes, in cancer metastasis. Tumor-derived exosomes have shown to contribute to the formation of a premetastatic niche and determine specific organotrophic metastasis via exosomal integrins. Exosomal integrins mediate the interaction of tumor-derived exosomes and the resident cells, and uptake of tumor-derived exosomes leads to activation of proto-oncogene tyrosine-protein kinase Src (Src) phosphorylation and pro-inflammatory S100 gene expression[64]. Tumor-derived exosomes can deliver critical miRNAs, lncRNAs, and proteins that contribute to angiogenesis and acquisition of tumor-associated cell phenotype[65]. Moreover, exosomes prepare the surrounding

microenvironment to be amenable for tumor colonization. Epithelial ovarian cancer cells have been shown to transfer miRNA that inhibit the activity of STAT3 and cause an imbalance of Treg and Th17 cells that lead to an immune-suppressive microenvironment[66]. Thus, we attempted to explore whether EVs secreted by tumors contribute to the suppressive phenotypes of monocytes in the tumor environment.

CHAPTER 2

Exosomes secreted by microglia during virus infection in the central nervous system activate an inflammatory response in bystander cells and promote CNS inflammation

Authors: Nhungoc Luong and Julie K. Olson

*This work was submitted for publication in the Journal of Virology.

BACKGROUND

Theiler's murine encephalomyelitis virus (TMEV) is a natural mouse pathogen that can establish a persistent virus infection in the central nervous system (CNS). TMEV is a picornavirus which has a single positive- stranded RNA genome and has no envelope. TMEV infection of susceptible mice, such as SJL mice, establishes a persistent infection in the microglia/macrophage in the brain and spinal cord[21, 26]. The persistent infection leads to the development of a chronic, progressive demyelinating disease beginning with clinical disease around day 35 to 40 days post infection[11, 30]. TMEV-induced demyelinating disease has been shown to be associated with an inflammatory immune response in the CNS and development of autoimmune $CD4^+$ T cell response directed against myelin antigen, proteolipid protein, $PLP_{139-151}$[27, 28]. We have previously shown that the innate immune response to virus infection influences the development and progression of demyelinating disease[41, 67]. TMEV- induced

demyelinating disease has several immunological and pathological similarities to multiple sclerosis (MS) in humans[68, 69].

Microglia are the resident immune cells of the CNS that originate from the yolk sac during development. Microglia express innate immune receptors which enable them to rapidly respond to pathogens invading the CNS[20]. Microglia become activated through the innate immune receptors to express cytokines, chemokines, and effector molecules. We have previously shown that TMEV infection of microglia leads to a rapid expression of type I interferons, IFNα and IFNβ[21]. We have also shown that microglia infected with TMEV become activated to express pro-inflammatory cytokines, IL1β, IL-6, IL-12, TNFα, chemokines, CCL2, CCL3, CCL5, and effector molecules, inducible nitric oxide (iNOS)[20, 21]. TMEV-infected microglia also become activated antigen presenting cells that can present viral antigens and myelin antigens to $CD4^+$ T cells[21].

Exosomes are derived from microvesicular bodies (80-120nm) within the cell and are then released from the cell. Exosomes secreted from one cell can fuse with target cells releasing the components of the exosome into the target cell, thus exosomes provide a means of communication between cells. Exosomes contain proteins, lipids, and nucleic acids, including mRNA, microRNA, and DNA[54]. The exosome membranes resemble the lipid bilayer membrane containing exosome-specific markers such as tetraspanin (CD63, CD81) and syndecans[52, 53]. The exosomal structure allows them to securely transfer various materials across the blood-brain barrier and prevent the degradation from surrounding RNAse and proteases[55]. Recent studies have

revealed the important role of exosomes in the pathogenesis of neurodegenerative diseases via the transfer of miRNAs, pathogenic, and misfolded proteins from rafts to recipient cells[55, 60]. More recently, exosomes have been isolated from the sera of chronically infected hepatitis C virus (HCV) patients and shown to contain replication-competent viral RNA [61]. Further studies showed that exosome-packaged HCV could induce phenotype and cytokine profile switch in recipient macrophages[62].

Exosomes represent a novel pathway for communication between cells, thus exosomes secreted by microglia may play an important role in communication between cells in the CNS. Microglia have been shown to be infected during TMEV infection, thus we wanted to determine whether TMEV-infected microglia secrete exosomes which may contribute to persistent viral infection and inflammation in the CNS. Our studies determined that exosomes secreted from microglia during TMEV infection do not contain TMEV viral particles but do contain the viral RNA genome which can be transferred to uninfected CNS resident cells such as microglia, astrocytes, and neurons. More importantly, these exosomes activated bystander CNS cells to express type I interferons and pro-inflammatory cytokines and chemokines through innate immune receptor recognition of the viral RNA. Further, exosomes secreted by microglia in the brain during TMEV infection did not contain viral particles but contained viral RNA which could be transferred to naïve mice activating an inflammatory immune response in the recipient mice. The results from these studies suggest a new pathway via exosomes by which viral RNA can be

transferred during persistent infection in the CNS independent of viral particles and by which neuroinflammation can be maintained during persistent virus infection in the CNS.

RESULTS

Microglia infected with TMEV secrete exosomes that contain viral RNA

Microglia secrete exosomes under normal conditions, therefore, we wanted to determine whether exosomes secreted by microglia during TMEV infection have altered contents. Microglia were infected with TMEV, and exosomes were isolated after 24 hours. The isolation of exosomes was determined based on expression of exosome specific proteins such as CD63, shown by flow cytometry (Figure 1 A, F), and CD9, CD81, TSG101, and Rab proteins, as determined by mass spectrometry (Table I). The exosomes also lacked the expression of Grp94, calnexin, cytochrome C, histones, and argonaute/RISC complex which are associated with other types of extracellular vesicles. The exosomes were further examined by TEM and Nanosight to determine purity and size with average size about 120nm (Figure 1K and Figure 2A). These analyses confirmed the isolation and definition of exosomes for publication as determined by the International Society for Extracellular Vesicles[70]. Furthermore, the exosomes isolated from TMEV- infected microglia do not contain viral particles based on TEM analysis which showed no viral particles inside the exosomes or associated with exosomes, viral plaque assays of exosome isolations which resulted in no plaques on BHK cells, mass spectrometric analysis of isolated exosomes which detected no viral proteins

present in exosomes, and Nanosight particle size of exosomes which showed no particles smaller than 60 nm (TMEV is 30-40nm) (Figure 1K, Figure 2A, B, C, and Table 1). Next, we wanted to determine whether exosomes secreted from microglia contain surface proteins similar to microglia. Exosomes isolated from both uninfected and infected microglia have CD11b on the surface (Figure 1B and G). Exosomes from uninfected microglia have low levels of co-stimulatory molecules, CD80 and CD86, and do not have MHC class II (Figure 1 C, D, E, H, I, J). Interestingly, exosomes from TMEV-infected microglia have higher levels of co-stimulatory molecules and have MHC class II compared to exosomes from uninfected microglia.

Exosomes have been shown to contain RNA, therefore, we wanted to determine whether exosomes from TMEV-infected microglia contain viral RNA. The exosomes were isolated from TMEV-infected microglia and examined for viral RNA. First, primers for a short piece at the beginning of the viral genome were used to generate a 200bp product which showed that viral RNA was present in the exosomes from TMEV-infected exosomes similar to microglia infected with TMEV (Figure 3A). Since TMEV is a small positive- strand RNA virus, we wanted to determine whether the entire genome was present in the exosomes. Primers were used to generate a long piece which includes the coding region of the viral genome. Exosomes from TMEV-infected microglia contained the viral genome similar to TMEV-infected microglia (Figure 3A).

Since the exosomes secreted from TMEV-infected microglia contain viral RNA and exosomes can be taken up by other cells, we wanted to determine

whether exosomes from TMEV-infected microglia can be taken up by uninfected microglia, bystander cells, thus transferring viral RNA. First, exosomes from TMEV-infected microglia were isolated and labeled with green fluorescence before being place on uninfected microglia to determine whether the exosomes were taken up by the uninfected microglia (Figure 3B). Next, the RNA inside the exosomes isolated from TMEV-infected microglia was labeled with fluorescence dye before exosomes were placed on bystander microglia (Figure 3C, D). The RNA from the TMEV-infected exosomes can be observed inside the cytoplasm of the bystander microglia and over time can be observed spreading around in the cytoplasm of the bystander microglia. To further determine whether the viral RNA was transferred to uninfected bystander microglia, the exosomes from the TMEV-infected microglia were added to the bystander microglia, and after 24 hours, the bystander microglia were lysed and analyzed for viral RNA inside the cells. The bystander microglia contained viral RNA, although at lower levels than microglia directly infected with TMEV (Figure 3F). To ensure the viral RNA was inside the exosomes, the exosomes isolated from TMEV- infected microglia were treated with RNAse or proteinase cocktail after isolation and then analyzed for viral RNA. These treated exosomes had similar levels of viral RNA as untreated exosomes indicating viral RNA was inside the exosomes (Figure 3E). Furthermore, when these treated exosomes were placed on bystander microglia, the microglia contained similar levels of viral RNA after 24 hours compared to untreated exosomes from TMEV infected microglia (Figure 3G). Finally, we wanted to determine whether the viral RNA that was transferred by the

exosomes to the bystander microglia was able replicate in the recipient cells. The exosomes were isolated from TMEV- infected microglia and placed on bystander microglia for 4 hours, the exosomes were removed, and the cells were washed. The bystander microglia were incubated an additional 0, 4, 8, or 20 hours before being lysed and analyzed for viral RNA. The viral RNA in the bystander microglia increased over time indicating viral replication occurred in the recipient cells (Figure 3H).

Exosomes secreted by virus- infected microglia activate bystander CNS cells

We have previously shown that microglia infected with TMEV become activated immune cells and express innate immune cytokines, including pro-inflammatory cytokines[21]. We wanted to determine whether the exosomes secreted by the TMEV- infected microglia could activate uninfected bystander microglia. We have shown above that exosomes secreted by TMEV- infected microglia contain viral RNA but do not contain viral proteins. Exosomes were isolated from TMEV- infected microglia and placed on uninfected bystander microglia. After 24 hours, the recipient microglia were analyzed for expression of cytokines and chemokines. Bystander microglia exposed to exosomes from TMEV-infected microglia increased the expression of type I interferons, IFNα and IFNβ, cytokines, IL-6, IL-12, and TNFα, and increased chemokines, CCL2, compared to bystander microglia exposed to exosomes from uninfected microglia (Figure 4). The quantity of exosomes added to the bystander microglia (100μg per $1x10^6$ cells) was determined based on a dose response to varying amounts

of exosomes based on approximately 200μg of exosomes being isolated from $1x10^6$ TMEV-infected microglia (Figure 5). Furthermore, exosomes secreted from TMEV-infected microglia that were treated with RNAse or proteinase cocktail prior to their addition to the bystander microglia showed a similar activation of bystander microglia as compared to untreated exosomes (Figure 6). These results show that the contents inside the exosomes are activating the bystander microglia to increase expression of cytokines and chemokines. To determine activation time course, exosomes were isolated from TMEV-infected microglia and added to bystander microglia. After 4 hours, the microglia cultures were washed to remove any exosomes that were not taken up. The microglia were incubated for an additional 0, 4, 8, or 20 hours and then lysed for analysis of expression of cytokines and chemokines. The bystander microglia increased expression of cytokines and chemokines over time (Figure 7).

The CNS has several resident cells, including astrocytes and neurons, which could also take up exosomes secreted by microglia. Thus, exosomes isolated from TMEV- infected microglia were placed on uninfected bystander astrocytes. After 24 hours, the astrocytes were examined for viral RNA and were also analyzed for the expression of cytokines and chemokines (Figure 8). Exosomes from TMEV-infected microglia transferred viral RNA to the bystander astrocytes and activated the astrocytes to express type I interferons, IFNα and IFNβ, as well as increase the expression of cytokines, IL-6, IL-12, and TNFα, and chemokines, CCL2. Similarly, exosomes from TMEV- infected microglia were placed on uninfected bystander neurons. After 24 hours, the neurons were

examined for viral RNA and for expression of cytokines and chemokines (Figure 9). Exosomes from TMEV-infected microglia transferred viral RNA to neurons and activated the neurons to express type I interferons, IFNα and IFNβ, cytokines, IL-6, IL-12, and TNFα, and chemokines, CCL2.

Bystander microglia are activated by the viral RNA in exosomes from TMEV-infected microglia

Since the exosomes contain viral RNA and viral RNA has been shown to be recognized by innate immune receptors to activate an innate immune response, we wanted to determine whether the viral RNA in the exosomes was activating the bystander microglia. Since TMEV is a single stranded RNA virus, the innate immune receptors that recognize single stranded RNA include TLR7 which signals through MyD88[71]. Double stranded RNA is recognized by TLR3 which signals through TLR adaptor molecule 1 (Ticam1) to induce expression of type I interferons. Double stranded RNA is also recognized by melanoma differentiation- associated protein 5 (MDA5) which signals through mitochondrial antiviral- signaling protein (MAVS) to induce expression of type I interferons and cytokines[71]. Thus, microglia were silenced for MyD88, Ticam1, or MAVS prior to incubation with exosomes from TMEV-infected microglia (Figure 10). After 24 hours, the microglia were analyzed for expression of type I interferons and cytokines. Microglia that were silenced for MyD88 and MAVS had greatly reduced expression of IFNα and IFNβ after exposure to TMEV- infected exosomes while there was no difference in type I interferon in microglia silenced for Ticam1. In addition, microglia silenced for MyD88 and MAVS also had

reduced expression of cytokines, IL-6 and TNFα after exposure to TMEV-infected exosomes. These results show that MyD88 and MAVS which are important signaling pathways in the innate immune response to viral RNA were necessary for microglia to become activated to express type I interferons and cytokines in response to TMEV-infected exosomes.

Because the inflammatory response induced by exosomes from TMEV-infected microglia on bystander cells was prominent and promising, we wanted to see if the exosomes alone could generate a similar effect in the CNS of mice as seen with direct TMEV infection. In order to observe pathology of demyelinating disease, 4 doses of exosomes were given to mice, one dose every other day. Intrathecal injection procedure was carefully chosen over intracerebral injection because of its less invasiveness. Two days after the last injection, mice brains and spinal cords were collected and processed for immunohistochemistry staining and RNA Scope in situ hybridization. First, tissue sections were stained for myelin peptide, PLP, and microglia marker, Iba1. Myelin loss and significant increase in Iba1 expression in the brains and spinal cords of mice injected with exosomes from TMEV-infected microglia were observed (Figure 11B, D, F). Besides the increase in quantity, microglia from the mice exhibited the typical ameboid morphology associated activation status. In comparison, mice injected with exosomes isolated from uninfected microglia showed intact myelin and without sign of microglia activation (Figure 11A, C, E). Although Iba1 is the standard marker for microglia in the CNS during normal condition, events such as infections and injuries would compromise the integrity of the BBB to allow the

CNS infiltration of monocytes/macrophages, which also express Iba1. Thus, the Iba1$^+$ cells could represent both microglia and those infiltrating blood mononuclear cells. RNA Scope in situ hybridization was used to detect viral RNA (Figure 11F) and pro-inflammatory cytokines (Figure 11G) in the lumbar sections of mice injected with exosomes from TMEV-infected microglia. Cells in the CNS were co-labeled with viral RNA. More interestingly, those cells and the neighbor cells expressed high level mRNA for pro-inflammatory cytokine, Il-1β. Overall, these data support previous findings in which viral RNA in exosomes from microglia can be taken up by CNS bystander cells. These cells can become activated to initiate bystander activation and bystander damage, contributing to the demyelinating process.

Microglia secrete exosomes during TMEV infection in mice that contain viral RNA and activate bystander CNS cells

The *in vitro* data showed that microglia infected with TMEV secrete exosomes that contain viral RNA that can activate bystander CNS cells, including microglia, astrocytes, and neurons to express type I interferons and cytokines. Next, we wanted to determine whether microglia infected with TMEV in mice also secrete exosomes that contain viral RNA. SJL mice were infected with TMEV or mock infected, and at 2 days post infection, the brain was removed, and exosomes were isolated. The exosomes were analyzed by flow cytometry for expression of CD63, exosome marker, and CD11b, microglia (Figure 12A, B). Approximately 60% of the exosomes isolated from the brain were derived from microglia as determined by CD11b expression, and this was consistent between

TMEV- infected and mock- infected mice. Further analysis of the exosomes from TMEV- infected mice determined that the exosomes had MHC class II on the surface while exosomes from mock infected mice did not have MHC class II (Figure 12C, D). These results are similar to MHC class II expression on microglia during TMEV infection in the brain. The exosomes isolated from the TMEV- infected mice were then sorted based on CD11b expression to isolate exosomes derived specifically from microglia. The exosomes isolated from TMEV infected mice brains did not contain viral particles as determined by plaque assay and mass spectrometric analysis (Figure 2B, C, and Table 1). The $CD11b^+$ exosomes from TMEV-infected mice contained viral RNA while $CD11b^-$ exosomes had very little viral RNA (Figure 12F). Most significantly, the $CD11b^+$ exosomes contained the viral genome (Figure 12E). Next, the $CD11b^+$ exosomes from TMEV- infected mice were placed on uninfected microglia *in vitro* to determine whether the viral RNA could be transferred to bystander microglia. The $CD11b^+$ exosomes from TMEV-infected mice transferred the viral RNA to bystander microglia including the viral genome, while the $CD11b^-$ exosomes transferred minimal viral RNA (Figure 12E, G). Furthermore, $CD11b^+$ exosomes from TMEV-infected mice were placed on bystander astrocytes and neurons *in vitro*. Similarly, the $CD11b^+$ exosomes from TMEV-infected mice were able to transfer the viral RNA to the bystander astrocytes and neurons (Figure 12 H, I). These results show that during TMEV infection of mice microglia secrete exosomes that contain viral RNA but not infectious virus particles or viral

proteins, and these exosomes can transfer viral RNA to bystander, uninfected CNS cells.

Since the exosomes secreted from TMEV-infected microglia *in vitro* activated bystander microglia, we wanted to determine whether the exosomes secreted by microglia during TMEV infection in mice could activate uninfected bystander microglia. The $CD11b^+$ exosomes isolated from TMEV-infected mice at 2 days post infection were transferred to uninfected bystander microglia. After 24 hours, the microglia were examined for expression of type I interferons, cytokines, and chemokines (Figure 13). The microglia that were incubated with $CD11b^+$ exosomes from TMEV- infected mice increased the expression of type I interferons, IFNα and IFNβ, cytokines, IL-6, IL-12, and TNFα, and chemokines, CCL2. Meanwhile, $CD11b^-$ exosomes isolated from TMEV-infected mice only slightly increased the expression of type I interferons and IL-6 in bystander microglia. Similarly, when $CD11b^+$ exosomes from TMEV-infected mice were transferred to bystander astrocytes (Figure 14A-F) and neurons (Figure 14G-L), the $CD11b^+$ exosomes increased the expression of type I interferons, cytokines, and chemokines in the bystander cells. These results show that $CD11b^+$ exosomes secreted during TMEV infection in mice activate bystander microglia, astrocytes, and neurons to express type I interferons, IFNα and IFNβ, cytokines, IL-6, IL-12, TNFα, and chemokines, CCL2.

Since the exosomes secreted by microglia during TMEV infection in mice activated bystander cells *in vitro*, we wanted to determine whether these exosomes could activate an inflammatory response in the brain of a naïve

mouse. $CD11b^+$ exosomes were isolated from TMEV- infected mice at 2 days post infection, the $CD11b^+$ exosomes were injected into the brain of naïve mouse. At 2 days post injection, the brains were removed and examined for expression of viral RNA (Figure 15). The mice that received the $CD11b^+$ exosomes from the TMEV- infected mouse had viral RNA in the brain although at a lower level compared to mice directly infected with TMEV. More interestingly, the $CD11b^+$ exosomes injected in the naïve mice brains activated the expression of type I interferons, IFNα and IFNβ, as well as induced the expression of inflammatory cytokines, IL-6 and TNFα (Figure 15). Although the levels of expression of the cytokines were less compared to directly infected mice, the levels of cytokines were significantly increased over the mice that had been injected with $CD11b^+$ exosomes from naïve mice. These results show that exosomes secreted by $CD11b^+$ microglia during TMEV infection can transfer viral RNA and promote an inflammatory immune response in uninfected mice.

DATAS

Proteins Present in Exosomes	Proteins Absent in Exosomes
CD63 antigen	Grp94 (HSP90B1)
Integrin alpha-1 (Itga1)	Clanexin (CANX)
CD81 antigen	Golgi (GM130)
CD9 antigen	cytochrome C (cytC)
Tumor susceptibility gene 101 protein (Tsg101)	histones (HIST*H*)
Ras-related protein Rab-14 (Rab14)	Argonaute/RISC complex (AGO*)
Putative uncharacterized protein (Rab5c)	
Ras-related protein Rab-5A (Rab5a)	TMEV viral capsid protein 3 (VP3)
Ras-related protein Rab-5B (Rab5b)	TMEV viral protein 3C
Ras-related protein Rab-2A (Rab2a)	TMEV viral protein 2C
Ras-related protein Rab-10 (Rab10)	
Ras-related protein Rab-18 (Rab18)	
Ras-related protein Rab-7a (Rab7a)	
Ras-related protein Rab-14 (Rab14)	
Annexin A2 (Anxa2)	
Cell adhesion molecule 3 (Cadm3)	
BDNF/NT-3 growth factors receptor (Ntrk2)	
Annexin A5 (Anxa5)	

Table 1: Protein analysis in identification of exosomes. Exosomes were isolated and purified from TMEV-infected microglia. Mass spectrometry was used to analyze protein contact on both surface and inside of exosomes.

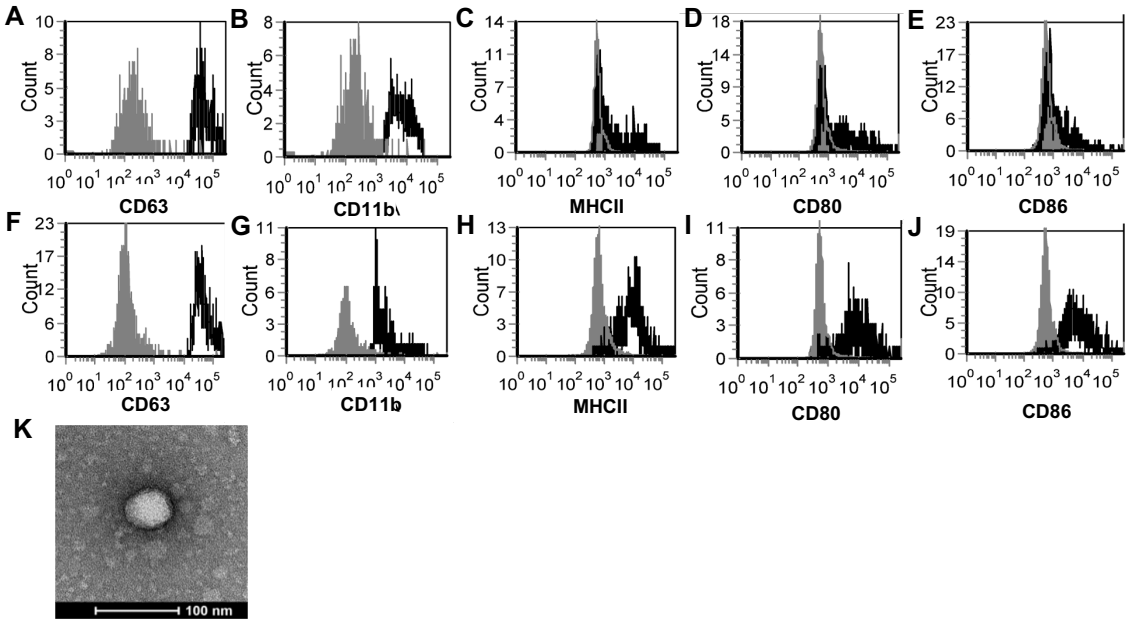

Figure 1. TMEV-infected microglia secrete exosomes that contain activation markers.

Exosomes were isolated from uninfected (A-E) or TMEV infected microglia (F-J). The exosomes were labeled with fluorescently labeled antibodies for CD63 (A and F), CD11b (B and G), MHC class II (C and H), CD80 (D and I), and CD86 (E and J). The exosomes were analyzed by flow cytometry for expression of specific markers as shown in the black line compared to isotype control antibodies in the gray line. (K) Isolated exosomes were analyzed by transmission electron microscopy and determined to be 40-80nm. One representative image is shown. These are representative graphs and images from one experiment of four independent repeated experiments.

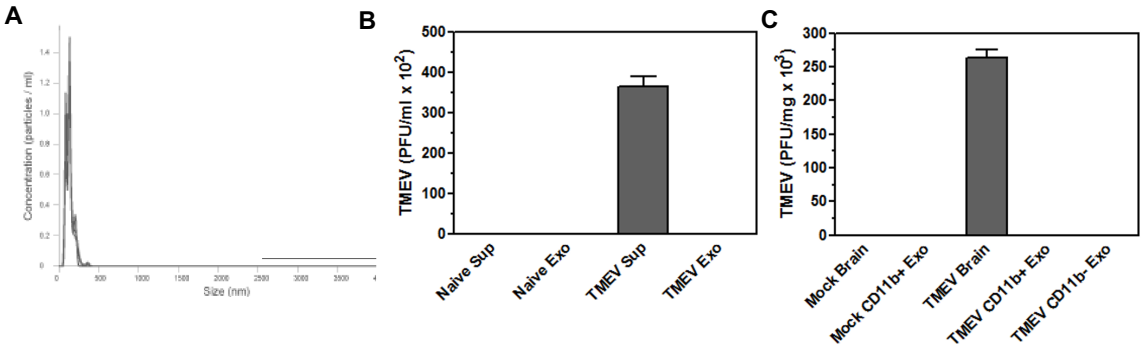

Figure 2. Exosomes isolated from TMEV- infected microglia do not contain infectious viral particles.

Exosomes were isolated from TMEV-infected microglia or mock infected microglia. The exosomes were analyzed by Nanosight for particle size (A). The supernatant removed from TMEV-infected microglia (TMEV Sup) or mock infected microglia (Mock Sup), and the exosomes isolated from TMEV-infected microglia (TMEV Exo) or mock infected microglia (Mock Exo) were used in a plaque assay with BHK cells. Plaque forming units (PFU) were determined per ml of starting supernatant. The brain was removed from TMEV-infected mice at 2 days post infection (TMEV brain) or from mock infected mice (Mock brain) and homogenized. The exosomes were isolated from the brains of TMEV infected mice at 2 days post infection and then sorted into CD11b+ exosomes (TMEV CD11b+ Exo) and CD11b- exosomes (TMEV CD11b- Exo). Exosomes were also isolated from mock infected mice brains (Mock Exo). The brain homogenates and isolated exosomes were used in a plaque assay and plaque forming units (PFU) were counted based on mg of starting brain tissue.

.

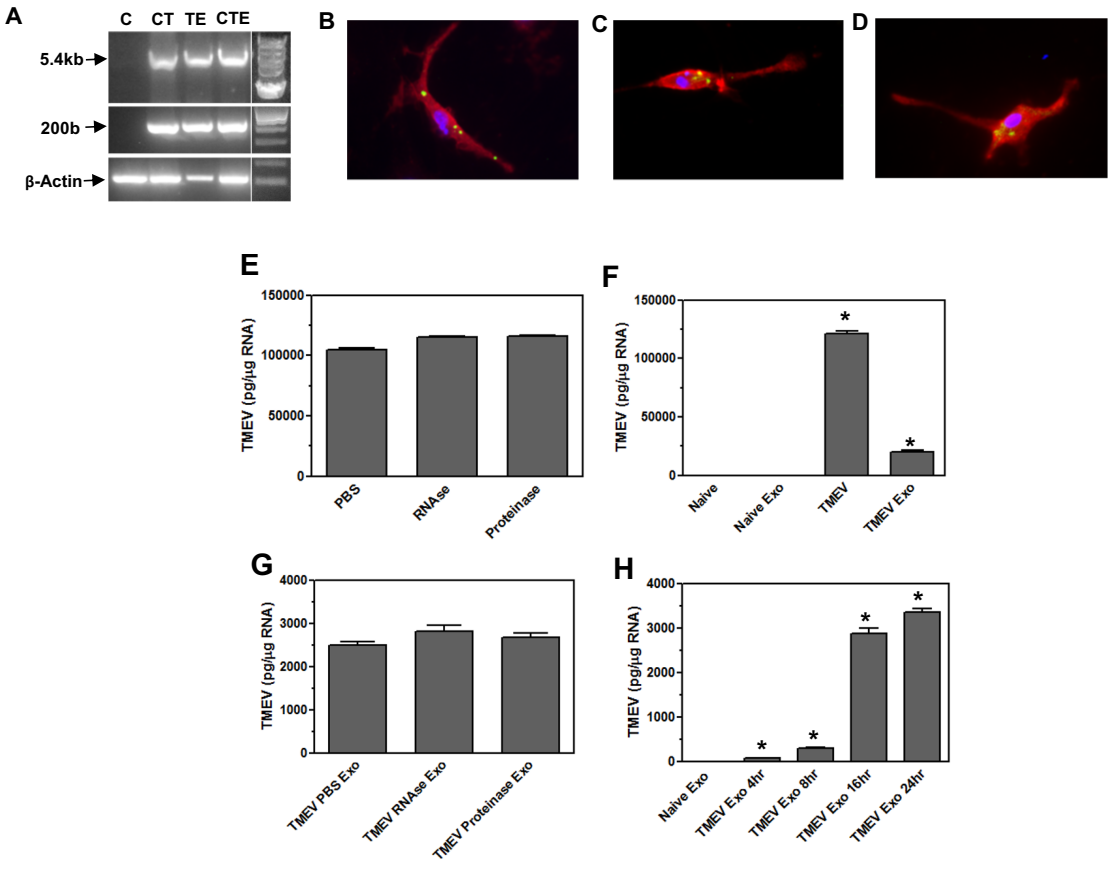

Figure 3. Exosomes from TMEV-infected microglia contain viral RNA that is transferred to bystander microglia.

(A) Microglia were infected with TMEV and exosomes were isolated (lane TE). Microglia ($1x10^6$) were uninfected (lane C), infected with TMEV (lane CT), or incubated with exosomes (100ug) from TMEV- infected microglia (lane CTE). The cells were lysed 24 hours later, RNA isolated, converted to cDNA, and used in PCR analysis with primers for TMEV long (5.4kbp) or short (200bp) products or with primers for β-actin. (B) Exosomes isolated from TMEV-infected microglia were fluorescently labeled with 2uM CFSE (green). The exosomes were placed in culture with naive microglia for 2 hours, and the microglia were fixed and incubated with fluorescently labeled antibody for CD11b (red). Exosomes

isolated from TMEV- infected microglia were incubated with RNA stain (green) and placed on microglia for 2 hours (C) or 4 hours (D). Microglia were fixed and incubated with fluorescently labeled antibody for CD11b (red). Cells were analyzed by confocal microscopy. (E) Exosomes from TMEV-infected microglia were isolated and control treated (PBS), RNAse treated, or proteinase treated. The RNA was isolated from the exosomes, converted to cDNA, and used in real time PCR with primers for TMEV. (F) Microglia were uninfected (naïve) or infected with TMEV. Microglia were incubated with exosomes isolated from TMEV-infected microglia or uninfected microglia. The microglia were lysed 24 hours later, RNA isolated, converted to cDNA, and real time PCR conducted with primers for TMEV. (G) Exosomes were isolated from TMEV- infected microglia and control treated (PBS), RNAse treated or proteinase treated prior to putting the exosomes into culture with naïve microglia. The microglia were lysed 24 hours later and analyzed by real time PCR for TMEV. (H) Exosomes were isolated from TMEV- infected microglia and placed on naïve microglia. After 4 hours, the exosomes were removed and the cells were washed and incubated for an additional 0, 4, 12, or 20 hours before being lysed and analyzed by real time PCR for TMEV. Significant difference was determined by one-way ANOVA and Bonferroni's multiple comparison test ($p<0.001$) based on expression by naïve microglia. These are representative graphs from one experiment of six independent repeated experiments.

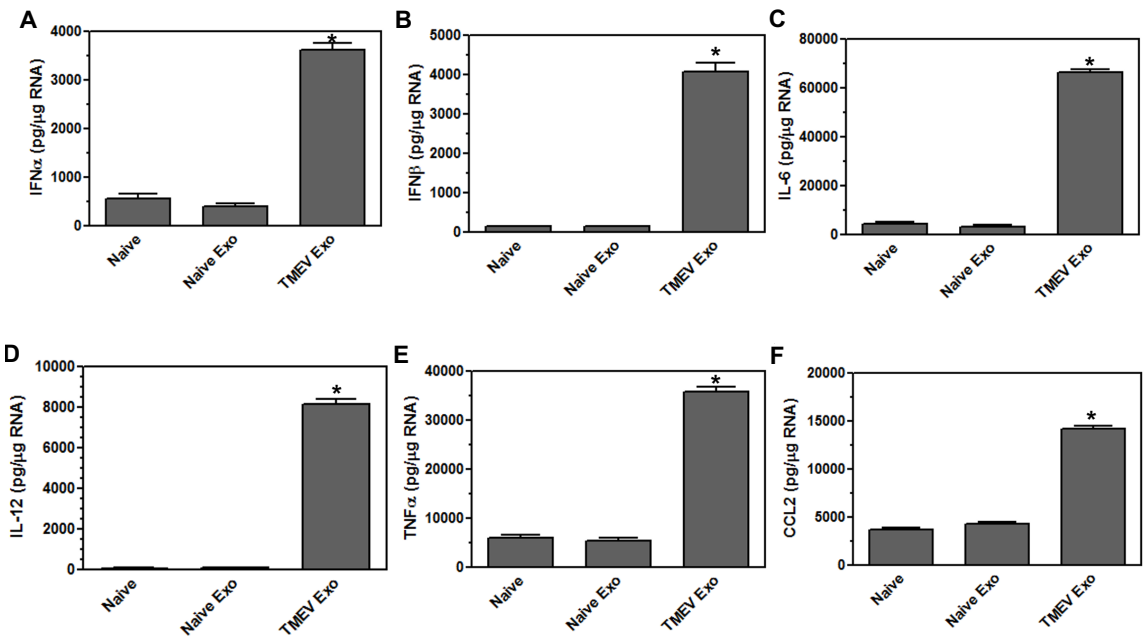

Figure 4. Exosomes from TMEV- infected microglia activate bystander microglia to express type I interferons and pro-inflammatory cytokines. Exosomes were isolated from TMEV-infected microglia or uninfected (naïve) microglia (100 ug) and placed on naive microglia ($1x10^6$) for 24 hours. Microglia were lysed, RNA isolated, converted to cDNA, and analyzed by real time PCR for expression of IFNα (A), IFNβ (B), IL-6 (C), IL-12 (D), TNFα (E), and CCL2 (F). Significant difference was determined by the one-way ANOVA and Bonferroni's multiple comparison test ($p<0.001$) based on unstimulated microglia. These are representative graphs from one experiment of five independent repeated experiments.

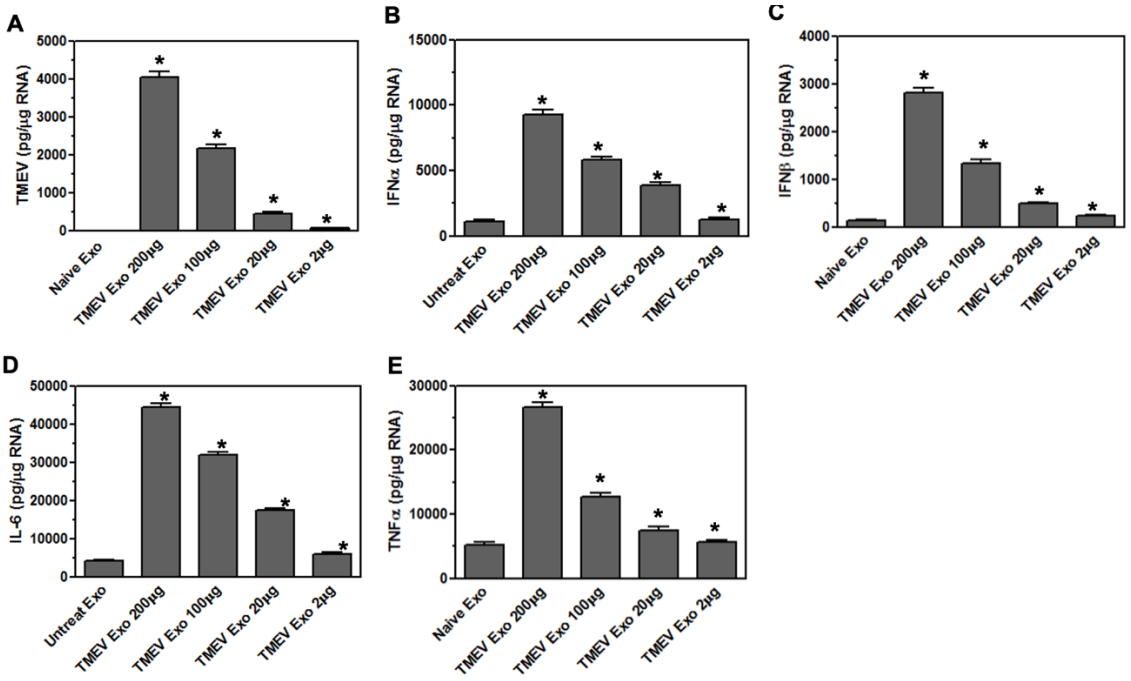

Figure 5. Exosomes from TMEV-infected microglia activate bystander microglia in dose dependent manner.

Exosomes were isolated from TMEV-infected microglia or mock infected microglia. The exosomes from TMEV- infected microglia were quantified and placed on unstimulated microglia ($1x10^6$) at concentration of 200ug, 100ug, 20ug, or 2ug for 24 hours. Microglia were lysed, RNA isolated, converted to cDNA, and analyzed by real time PCR for expression of TMEV (A), IFNα (B), IFNβ (C), IL-6 (D), and TNFα (E). Significant difference was determined by the one-way ANOVA and Bonferroni's multiple comparison test ($p<0.001$) based on unstimulated microglia. These are representative graphs from one experiment of four independent repeated experiments.

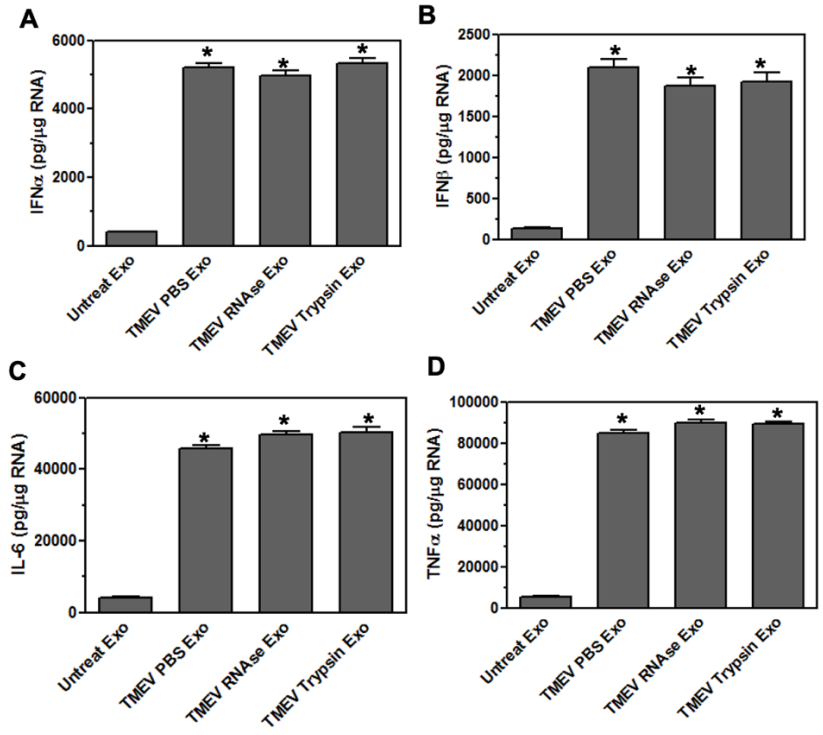

Figure 6. The content inside of exosomes from TMEV-infected microglia activate bystander microglia.

The exosomes (200ug) from TMEV-infected microglia were control treated, RNAse treated, or proteinase treated. The exosomes were then placed in culture with naïve microglia for 24 hours. After 24 hours, the microglia were lysed, RNA isolated, converted to cDNA, and analyzed by real time PCR for expression of TNFα (A), IFNβ (B), IL-6 (C), and TNFα (D). Significant difference was determined by the one-way ANOVA and Bonferroni's multiple comparison test ($p<0.001$) based on unstimulated microglia. These are representative graphs from one experiment of four independent repeated experiments.

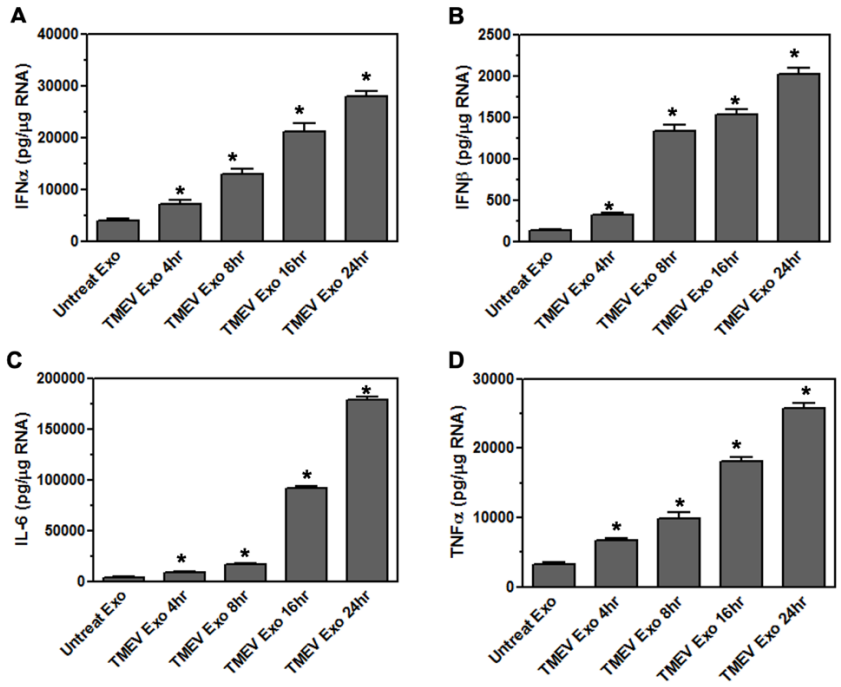

Figure 7. The expression of type I interferons and pro-inflammatory cytokines increased over time in bystander microglia exposed to exosomes from TMEV-infected microglia, starting at 4 hours.

Exosomes (200ug) were isolated from TMEV- infected microglia and placed on naïve microglia. After 4 hours, the exosomes were removed, and the cells were washed. The microglia were incubated for an additional 0, 4, 8, or 12 hours before being lysed and analyzed by real time PCR for expression of IFNα (A), IFNβ (B), IL-6 (C), and TNFα (D). Significant difference was determined by the one-way ANOVA and Bonferroni's multiple comparison test ($p<0.001$) based on unstimulated microglia. These are representative graphs from one experiment of four independent repeated experiments.

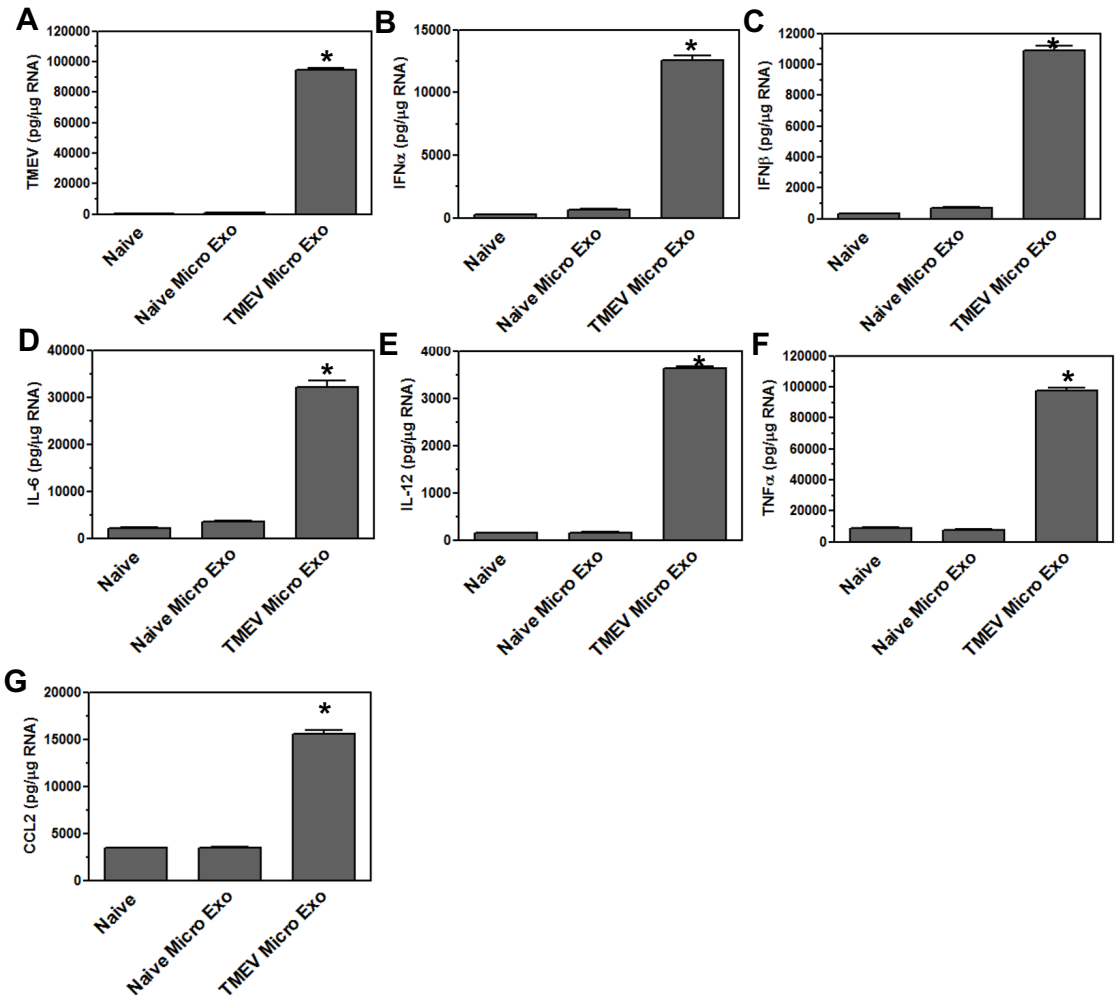

Figure 8. Exosomes from TMEV-infected microglia activate bystander astrocytes.

Exosomes were isolated from uninfected (naïve) microglia or TMEV-infected microglia and placed on naive astrocytes for 24 hours. Astrocytes were lysed, RNA isolated, converted to cDNA, and analyzed by real time PCR for expression of TMEV (A), IFNα (B), IFNβ (C), IL-6 (D), IL-12 (E), TNFα (F) and CCL2 (G). Significant difference was determined by the one-way ANOVA and Bonferroni's multiple comparison test ($p<0.001$) based on unstimulated microglia. These are

representative graphs from one experiment of four independent repeated experiments.

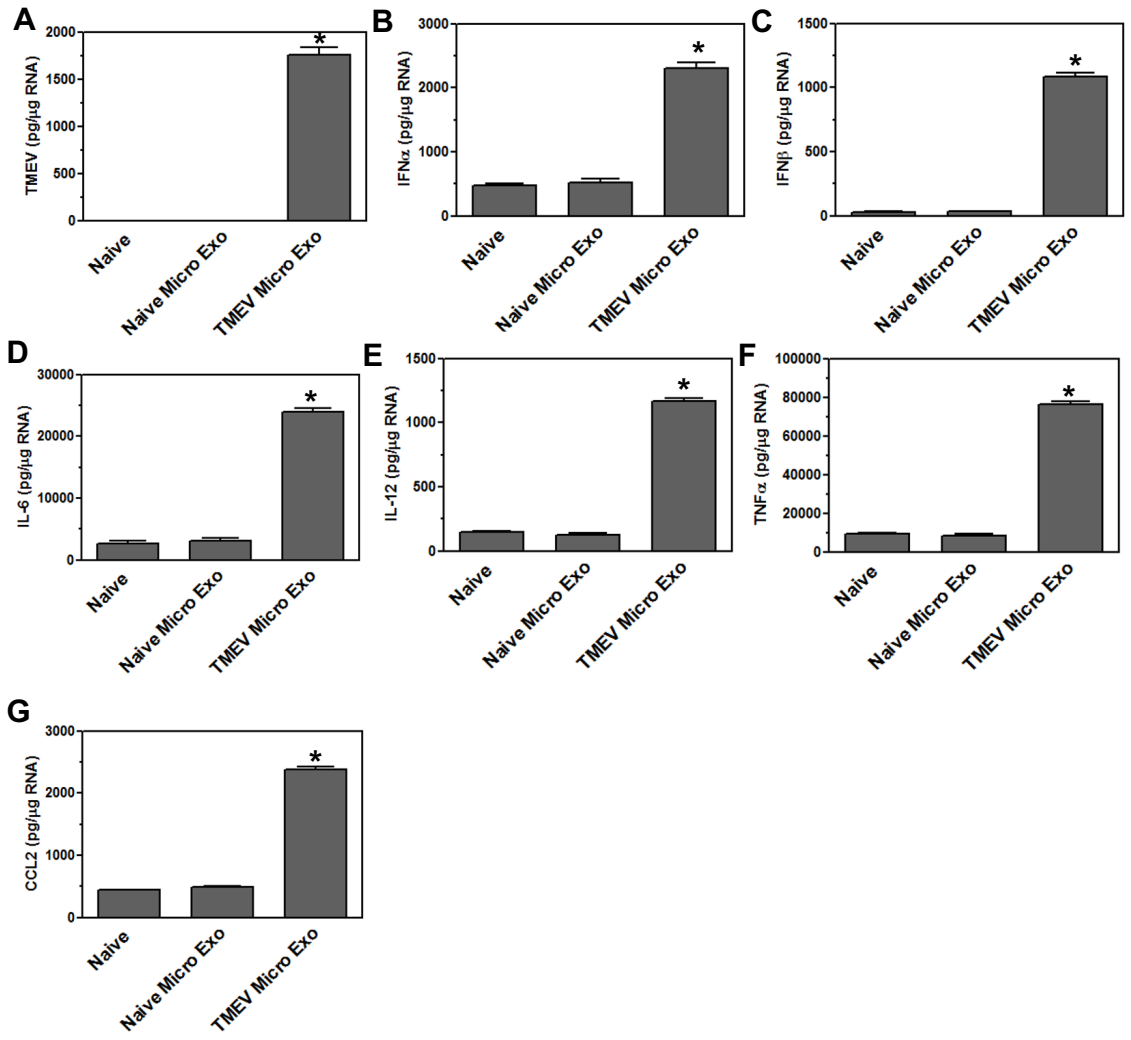

Figure 9. Exosomes from TMEV-infected microglia activate bystander neurons.

Exosomes were isolated from uninfected (naïve) microglia or TMEV-infected microglia and placed on naive neurons for 24 hours. Neurons were lysed, RNA isolated, converted to cDNA, and analyzed by real time PCR for expression of TMEV (A), IFNα (B), IFNβ (C), IL-6 (D), IL-12 (E), TNFα (F) and CCL2 (G).

Significant difference was determined by the one-way ANOVA and Bonferroni's multiple comparison test ($p<0.001$) based on unstimulated microglia. These are representative graphs from one experiment of three independent repeated experiments.

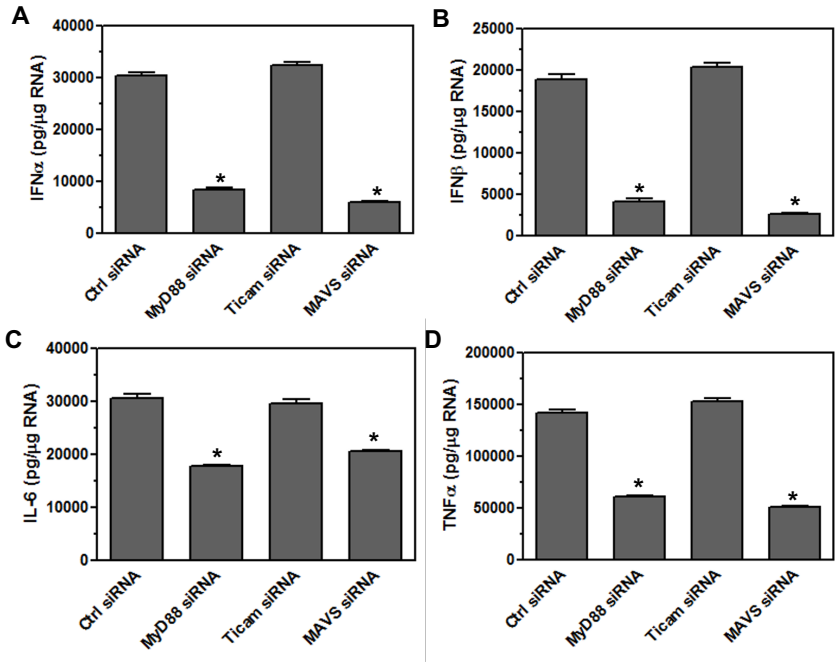

Figure 10. Bystander microglia are activated by viral RNA in exosomes from TMEV-infected microglia via innate immune receptors.

Microglia were transfected with siRNA for MyD88, TICAM-1, MAVS, or control (6 hours). Exosomes were isolated from TMEV- infected microglia and placed on the transfected microglia for 24 hours. Microglia were lysed, RNA isolated, converted to cDNA, and analyzed by real time PCR for expression of IFNα (A), IFNβ (B), IL-6 (C), and TNFα (D). Significant difference was determined by the one-way ANOVA and Bonferroni's multiple comparison test ($p<0.001$) based on

control siRNA transfected microglia. These are representative graphs from one experiment of three independent repeated experiments.

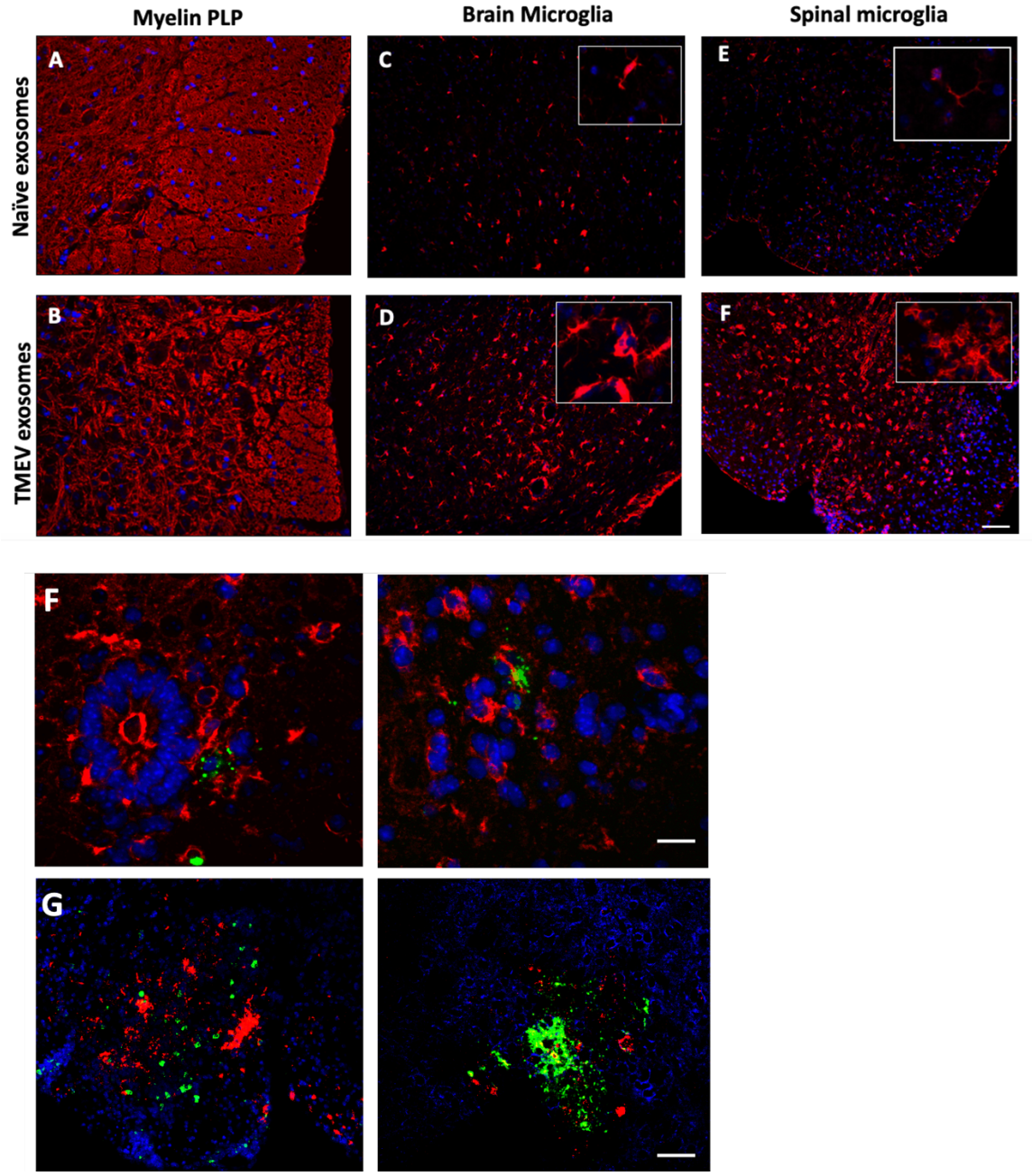

Figure 11. Exosomes from TMEV-infected microglia transfer viral RNA to bystander cells, promote microglia activation, myelin loss, and inflammation in the CNS of mice.

Naïve mice were injected intrathecally with 100ug exosomes from TMEV-infected microglia (TMEV exosomes, B, D, F) or unstimulated microglia (naïve exosomes, A, C, E) for every other day for the total of 4 injections. Mice (3 mice/group) were sacrificed 2 days after the last injection. Brains and spinal cords were sectioned and fluorescently stained for proteolipid protein (PLP, red) or Iba1 (microglia marker, red), and DAPI (blue). Images were taken at 10x magnification. Scale bar=80um. (F and G) RNAScope *in situ* hybridization technique was done on lumbar sections from mice injected with exosomes from TMEV-infected microglia. (F) TMEV RNA (green) was detected in microglia (red), DAPI (blue). (G) TMEV RNA (green) and IL-1β (red) are localized in microglia (blue). Images was taken with a confocal microscope, scale bar=20um (F) and 40um (G).

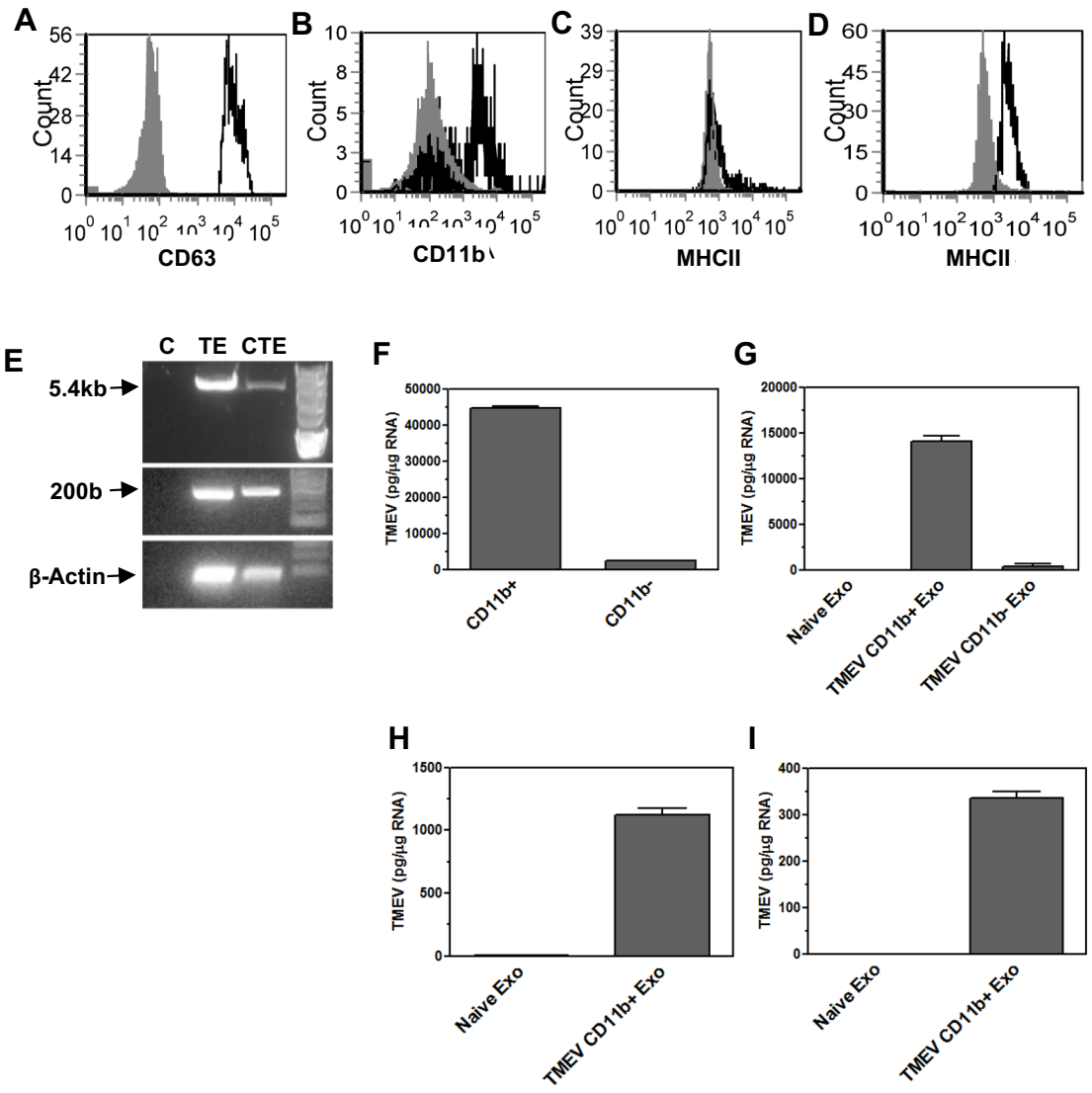

Figure 12. Exosomes secreted by microglia during TMEV infection of mice contain viral RNA that can be transferred to bystander CNS cells.

Exosomes were isolated from the brains of TMEV- infected mice at day 2 post infection (3 mice per group). The exosomes were labeled with fluorescently labeled antibodies for CD63, CD11b, and MHC class II. The exosomes were analyzed by flow cytometry for CD63 (A) and CD11b (B) and MHC class II in $CD11b^-$ exosomes (C) and $CD11b^+$ exosomes (D) with the specific antibodies in black lines and isotype control antibodies in gray. (E) Mice were infected or

mock infected with TMEV. At 2 days post infection, exosomes were isolated from the brains and sorted for $CD11b^+$ exosomes. RNA was isolated from the $CD11b^+$ exosomes from mock infected mice (C) and TMEV-infected mice (TE). RNA was converted to cDNA and used in PCR analysis with primers for TMEV long (5.4kbp) or short (200bp) products or with primers for β-actin. Microglia were incubated with $CD11b^+$ exosomes isolated from the brains of TMEV-infected mice (lane CTE). The cells were lysed 24 hours later and RNA isolated, converted to cDNA and used in PCR analysis. (F) At day 2 post infection, exosomes were isolated from TMEV- infected mice brains and sorted into $CD11b^+$ and $CD11b^-$ exosomes. The exosomes were analyzed for TMEV using real time PCR. (G-I) The exosomes isolated from TMEV- infected mice brains were sorted into $CD11b^+$ and $CD11b^-$ exosomes and placed on unstimulated cultures of microglia, astrocytes, and neurons. After 24 hours, the cells were lysed, RNA isolated, converted to cDNA and analyzed by real time PCR for TMEV in microglia (G), astrocytes (H), and neurons (I). These are representative graphs from one experiment of four independent repeated experiments.

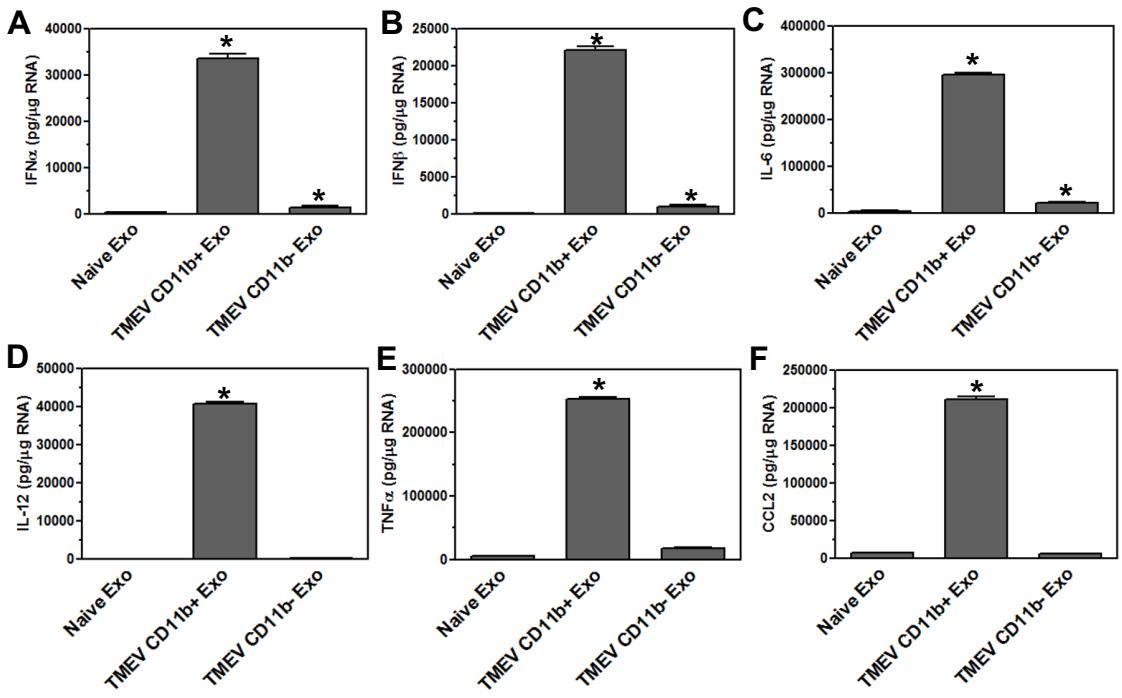

Figure 13. Exosomes secreted by microglia during TMEV infection in mice activate bystander microglia.

Exosomes were isolated from the brains of TMEV- infected mice at 2 days post infection (3 mice per group). The exosomes from the brains of TMEV- infected mice and naïve mice were sorted for $CD11b^+$ and $CD11b^-$ exosomes which were then placed on unstimulated microglia. After 24 hours, the microglia were lysed, RNA isolated, converted to cDNA, and used in real time PCR with primers for IFNα (A), IFNβ (B), IL-6 (C), IL-12 (D), TNFα (E), and CCL2 (F). Significant difference was determined by the one-way ANOVA and Bonferroni's multiple comparison test ($p<0.001$) based on microglia that were incubated with exosomes secreted by microglia in naive mice. These are representative graphs from one experiment of four independent repeated experiments.

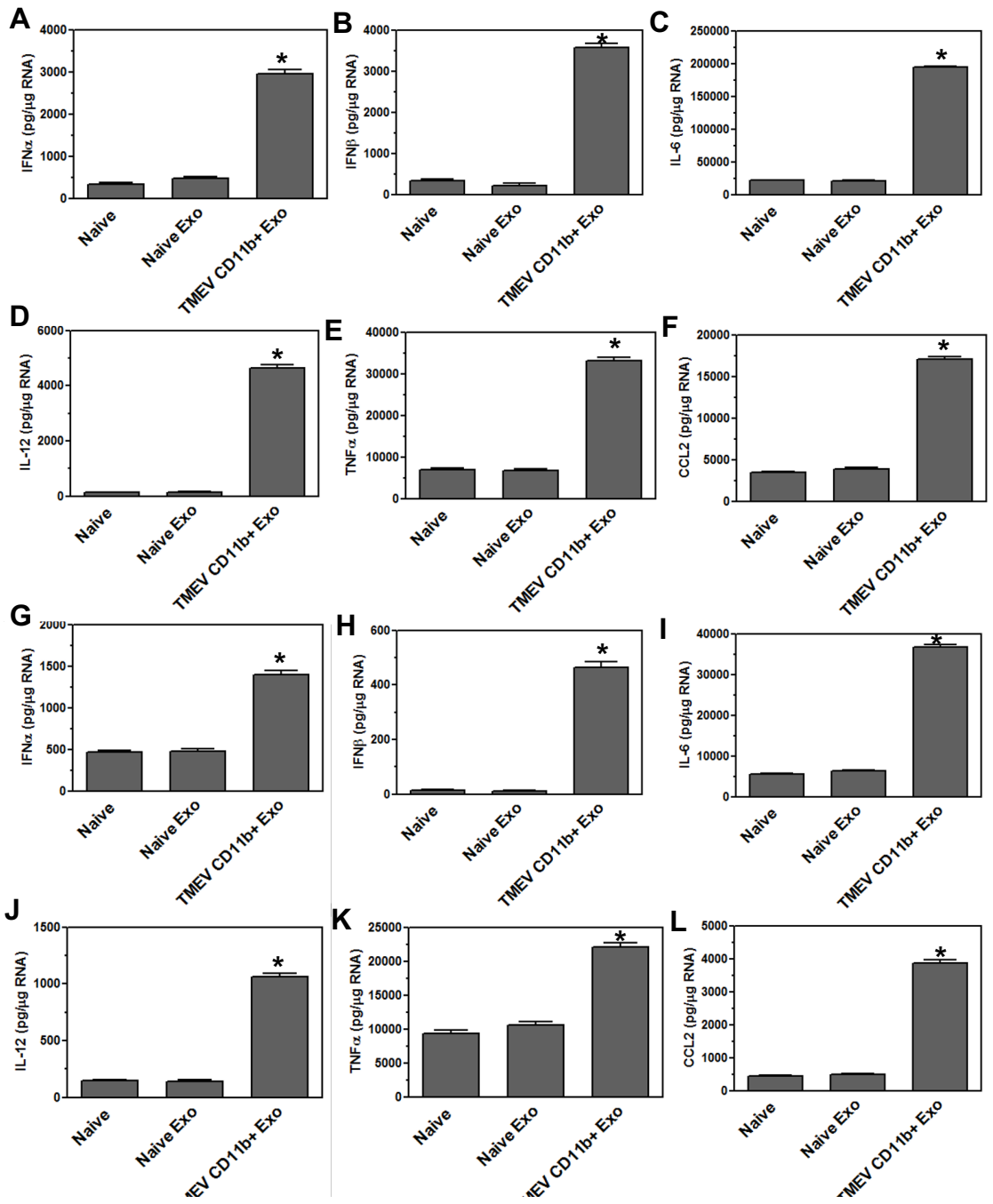

Figure 14. Exosomes secreted by microglia during TMEV infection in mice activate bystander CNS cells.

Exosomes were isolated from the brains of TMEV- infected mice at 2 days post infection or from naïve mice (3 mice per group). The exosomes were sorted for $CD11b^{+}$ exosomes which were placed on unstimulated astrocytes and neurons.

After 24 hours, the astrocytes (A-F) and neurons (G-L) were lysed, RNA isolated, converted to cDNA, and used in real time PCR with primers for IFNα (A and G), IFNβ (B and H), IL-6 (C and I), IL-12 (D and J), TNFα (E and K), and CCL2 (F and L). Significant difference was determined by the one-way ANOVA and Bonferroni's multiple comparison test ($p<0.001$) based on naive astrocytes or neurons. These are representative graphs from one experiment of three independent repeated experiments.

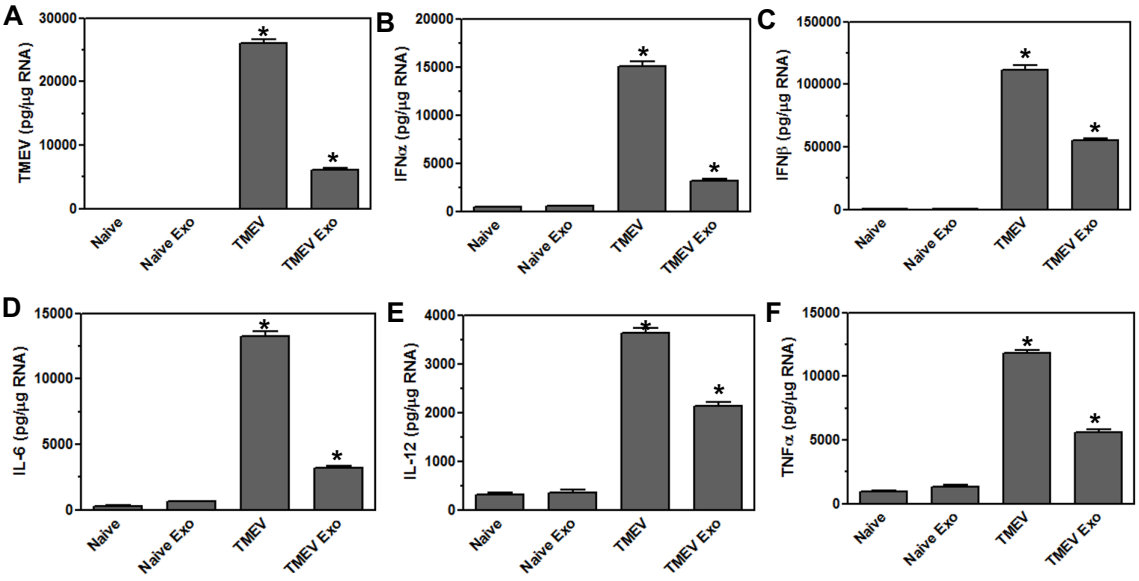

Figure 15. Exosomes secreted by microglia during TMEV infection in mice activate an inflammatory response in naïve mice.

Exosomes were isolated from the brains of TMEV- infected mice at 2 days post infection or from naïve mice (3 mice per group). The exosomes were sorted for $CD11b^+$ exosomes, and the $CD11b^+$ exosomes were injected into the brain of naïve mice. At 2 days post injection, the brains were removed from the mice (3 mice per group), and RNA was isolated, converted to cDNA and used in real time

PCR with primers for TMEV (A), IFNα (B), IFNβ (C), IL-6 (D), IL-12 (E), and TNFα (F). As comparison, the brains were removed from naïve mice or mice at 2 days post TMEV infection, and RNA was isolated, converted to cDNA and used in real time PCR. Significant difference was determined by the one-way ANOVA and Bonferroni's multiple comparison test ($p<0.001$) based on the naïve mouse brain.

DISCUSSION

Microglia are the immune resident population of the CNS. We have previously shown that microglia become persistently infected with TMEV. These studies show that TMEV-infected microglia secrete exosomes that contain viral RNA which can be transferred to uninfected CNS resident cells, including microglia, astrocytes, and neurons. We have previously shown that TMEV-infected microglia become activated to express type I interferons and pro-inflammatory cytokines and chemokines[20, 21]. In these studies, we show that exosomes from TMEV- infected microglia contain viral RNA but do not contain viral particles or viral proteins. These exosomes can be taken up by uninfected bystander microglia, and the viral RNA in the exosomes were recognized by innate immune receptors in the uninfected bystander microglia which activated the microglia to express type I interferons and pro-inflammatory cytokines. Likewise, exosomes secreted from TMEV- infected microglia also activated other CNS bystander cells including astrocytes and neurons to express type I interferons and pro-inflammatory cytokines and chemokines. Since the *in vitro* studies were promising, we wanted to validate whether exosomes secreted by microglia during TMEV infection in mice could have similar effects on bystander

cells. Exosomes from microglia were isolated from the brains of mice by sorting isolated exosomes for $CD11b^+$ exosomes. These studies showed that exosomes secreted by microglia during TMEV infection in mice contain viral RNA but do not contain viral particles or viral proteins. The exosomes secreted by microglia during TMEV infection could activate bystander microglia, astrocytes, and neurons to secrete type I interferons and pro-inflammatory cytokines. Most importantly, exosomes secreted by microglia during TMEV infection in mice could induce an inflammatory immune response when injected into a naïve mouse. These results showed that TMEV- infected microglia secrete exosomes that not only transfer viral RNA to bystander uninfected CNS cells but also activates bystander cells to express pro-inflammatory cytokines and chemokines associated with neuroinflammation.

Following TMEV infection in SJL mice, infectious virus loads are very high in the brain for the first 1-3 days post infection followed by a rapid spread to the spinal cord. The virus remains persistent in both the brain and spinal cord throughout the lifetime of the animal[26]. Microglia have been shown to be the persistently infected cells during TMEV, however, microglia produce very few infectious viral particles during infection[72]. Since microglia play an important role in the persistent virus infection, these studies focused on TMEV-infected microglia. We wanted to determine whether TMEV- infected microglia secrete exosomes that may contain viral products. In order to isolate exosomes that excluded viral particles, we used a method to isolate exosomes that does not include high speed centrifugation which would pellet the viral particles. TMEV is

a non-enveloped virus around 40-50nm in size. Our method yielded purified exosomes as verified by TEM staining for morphology, as verified for CD63 expression by flow cytometry and mass spectrometry, and as verified for particle size by Nanosight (120nm). The isolated exosomes did not contain viral particles as verified by TEM staining which showed no viral particles isolated with the exosomes and no viral particles in exosomes, by plaque assays which showed no infectious particles isolated with the exosomes and no viral particles in exosomes, and by mass spectrometry which showed no viral proteins in exosomes. Since the exosomes do not contain viral particles, we wanted to determine whether the exosomes from TMEV-infected microglia contain viral RNA. TMEV is a small positive single- stranded RNA virus. The exosomes secreted from TMEV- infected microglia contained not only viral RNA but the whole viral genome. To further determine whether microglia were secreting exosomes during TMEV infection in mice, we isolated exosomes from the brains of TMEV infected mice at 2 days post infection. Since exosomes from microglia were determined to have CD11b on their surface, we sorted microglia-secreted exosomes from the whole brain exosomes using CD11b as a marker. Most interestingly, the exosomes secreted by microglia during TMEV infection in the brain contain viral RNA, including the entire TMEV genome. Meanwhile, the exosomes from the brain of TMEV- infected mice that were secreted by other cells (CD11b-), not microglia, contained little or no viral RNA suggesting the main source of exosomes that contain viral RNA in the brain during TMEV infection are secreted by microglia. The exosomes secreted by microglia during TMEV

infection could transfer the viral RNA to uninfected microglia, and the viral RNA replicated in the recipient cells. Similarly, exosomes secreted by microglia during TMEV infection could transfer viral RNA to uninfected bystander astrocytes and neurons. These results show that exosomes secreted by microglia during TMEV infection can transfer viral RNA to uninfected cells independent of viral particles. Furthermore, the viral RNA transferred by the exosomes could replicate in the recipient bystander cells. Most interestingly, exosomes may transport viral RNA between cells during TMEV infection as a means to evade the immune response, especially virus-specific antibodies, and enable virus persistence.

Microglia infected with TMEV produce type I interferons which have been shown to have a direct effect on development of TMEV- induced demyelinating disease[41]. The exosomes secreted by microglia during TMEV infection could activate the expression of type I interferons, IFNα and IFNβ, in the uninfected bystander microglia. We have previously shown that microglia express several innate immune receptors that recognize viral RNA[20]. Since TMEV is a single stranded RNA virus, the innate immune receptors that could recognize the RNA include TLR3, TLR7 and MDA5. Each of these receptors activates a distinct signaling pathway to promote transcription of type I interferons. Silencing MyD88 which is activated by TLR7 or silencing MAVS which is activated by MDA5 led to reduced expression of type I interferons in microglia that were exposed to exosomes secreted by microglia during TMEV infection. These results show that viral RNA in the exosomes were recognized by innate immune receptors in the bystander microglia which activated the expression of type I interferons. Further,

exosomes secreted by microglia during TMEV infection could also activate the expression of type I interferons in bystander astrocytes and neurons. Type I interferons have direct anti-viral activity, thus, the expression of type I interferons in these bystander cells may protect these cells from a damaging virus infection, especially for neurons.

Microglia infected with TMEV become activated to express pro-inflammatory cytokines, chemokines, and effector molecules associated with neuroinflammation. The exosomes secreted by microglia during TMEV infection could also induce the expression of pro-inflammatory cytokines, IL-6, IL-12 and TNFα, and chemokines, CCL2, in bystander uninfected microglia. The expression of cytokines and chemokines was reduced when innate immune signaling pathways involved in recognition of viral RNA were silenced, however, the expression was not completely reduced. This suggests that some expression of cytokines and chemokines is induced by the innate immune response to viral RNA, however, there are many other components in the exosomes secreted by microglia during TMEV infection, including miRNA and proteins, which may be also be activating the expression of cytokines and chemokines in the bystander cells. However, exosomes secreted by other cell types in the CNS (CD11b-) during TMEV infection were unable to activate bystander microglia. Further, the exosomes secreted by microglia during TMEV infection could also activate bystander astrocytes and neurons to express cytokines and chemokines. These results show that exosomes secreted by microglia during TMEV infection activate

bystander uninfected cells to express pro-inflammatory cytokines and chemokines which may contribute to neuroinflammation during infection.

We have previously shown that microglia become activated following TMEV infection to increase expression of co-stimulatory molecules and MHC class II[21]. Interestingly, exosomes secreted by microglia during TMEV infection had increased levels of co-stimulatory molecules, CD80, CD86, CD40, on the surface compared to exosomes secreted by microglia during mock infection. Further, exosomes secreted by microglia during TMEV infection have MHC class II. These results suggest that exosomes can also have proteins on their surface which are similar to the activation state of the cells from which they are derived. In addition, the exosomes isolated from the brain of TMEV infected mice were about 60% $CD11b^+$ which suggests that the majority of exosomes in the CNS are derived from microglia but also suggests that other CNS cells also secrete exosomes which may have an effect during virus infection. For this reason, these studies isolated $CD11b^+$ exosomes to focus on exosomes secreted from microglia.

TMEV infection in mice leads to neuroinflammation which contributes to the development of demyelinating disease. Exosomes secreted by microglia during TMEV infection were shown to activate uninfected bystander microglia, astrocytes, and neurons to express pro-inflammatory cytokines and chemokines associated with neuroinflammation. However, to determine the effect of exosomes on neuroinflammation in the brain, the exosomes secreted by microglia during TMEV infection in mice were injected into naïve mice. First,

multiple intrathecal injections of exosomes from TMEV-infected microglia into naïve mice could induce similar consequences seen with direct TMEV infection including microglia/monocyte/macrophage activation and myelin loss. Since Iba1 labels monocytes and macrophages as well, we could not rule out the possibility that exosomes from infected microglia could promote an influx of immune cells into the CNS, and additional works are needed to help distinguish between these cell types. Viral RNA were also detected in the same area with high IL-1β expression. In a different experiment, exosomes secreted by microglia isolated from mice during TMEV infection promoted the expression of pro-inflammatory cytokines and chemokines in the naïve mouse with a single intracerebral injection. In addition, the exosomes secreted by microglia during TMEV infection could transfer viral RNA and induce the expression of type I interferons in the brain of the naïve mice. These results show that exosomes secreted by microglia during TMEV infection can transfer viral RNA and can promote neuroinflammation in a naïve mouse brain suggesting that exosomes may play an important role in virus persistence and neuroinflammation during TMEV infection. These results suggest that exosomes secreted by microglia during persistent virus infection can promote neuroinflammation associated with development of neurological diseases. Thus, exosomes secreted by microglia may represent a novel mechanism for viral persistence and chronic neuroinflammation.

MATERIALS AND METHODS

Mice

Female SJL mice age 5-6 weeks were purchased from Envigo (Madison, WI). Pregnant SJL/J mice (15-17 days) were purchased from Enivgo. Neonatal SJL mice were used for primary cell isolation. The mice were housed at University of Minnesota Research Animal Resource Center accredited by the American Association for Accreditation of Laboratory Animal Care. The animals are handled according to university and Animal Care and Use Committee approved protocols.

Isolation and culture of CNS cells

Isolation of primary glial cultures from neonatal mice was performed, as previously described[21]. Briefly, brains were removed from 1 to 3 days old mice, and the meninges were removed. The left and right hemispheres of the brain were gently dissociated in a nylon mesh bag. The cells were resuspended in DMEM-F12 media (Lonza) supplemented with 10% FCS (Invitrogen Life Technologies) and 100U/ml penicillin and 100µg/ml streptomycin (Invitrogen Life Technologies). The cells were seeded in poly(D-lysine) (Sigma- Aldrich) coated tissue culture flasks and incubated at 37C. After 10-14 days of incubation, microglia were removed from the astroglial layer by shaking the flasks on an orbital shaker for 24 hours. The primary microglia were removed from the flask and placed in DMEM (Invitrogen Life Technologies) supplemented with 10% exosome free FCS and 3ng/ml rGM-CSF (R&D Systems). The microglia were seeded in 24-well plates coated with poly(D)lysine. Astrocytes were cultured in supplemented DMEM-F12 media with exosome free FCS as described above. For neurons, the brain tissue was dissociated with 0.25% trypsin for 15 minutes,

and the cell suspension was placed in laminin coated flasks with B27 supplemented neurobasal media (Gibco, Invitrogen). The microglia were transfected with siRNA specific for MyD88, Ticam1, or MAVS, SMARTpool siRNA (5μM), or siCONTROL (Dharmacon) using Dharmafect 4 following the protocol provided by Dharmacon.

TMEV infection

SJL female mice were intracranially injected with $2X10^6$ PFU of BeAn strain of TMEV. Microglia were infected with the BeAN strain of TMEV at a multiplicity of infection of 5 in serum- limited DMEM for 24 hours as previously described[21].

Exosome isolation and analysis

Cell culture media was removed from the cells and centrifuged at 2,000xg to remove cellular debris. Total exosome isolation reagent for cell culture (Invitrogen) was added to the supernatant (1:2 ratio) and incubated overnight at 4°C. The exosomes were pelleted the next day by centrifuging at 10,000xg for one hour per the protocol (Invitrogen). For isolating exosomes from brains, the brains were dissociated through a 70μM filter into 3ml Hank's balanced salt solution. The homogenate was then centrifuged two times at 2,000xg to remove cells and debris. The exosomes were isolated from the cleared homogenate with the isolation reagent as described above. The exosomes were then incubated with antibody for CD11b conjugated to magnetic beads and separated on a column per manufacturer protocol (Miltenyi). To determine the size of the

exosomes, exosomes were resuspended in PBS and analyzed on a Nanosight N300 (Malvern). To determine purity, exosomes were imaged on a transmission electron microscope (TEM). Briefly, the exosomes were fixed with 2% glutaraldehyde for one hour and then absorbed onto a glow discharged carbon-Formvar coated 200-mesh copper grids for 5 minutes. Grids were washed twice with water and stained with 2% uranyl acetate twice for 30 seconds. TEM imaging was performed on a Tecnai G2 F30 instrument. Exosomes were analyzed by flow cytometry for surface protein expression. Briefly, exosomes were incubated with aldehyde/sulfate latex beads (Invitrogen) per the manufacturer protocol. The exosomes were then incubated with fluorescently labeled antibodies for CD45, CD11b, CD63, I-As, CD80, and CD86. The exosomes were washed and analyzed on LSRII (BD). Isolated exosomes were also analyzed for CD63 by western blot (BioRad) following lysis using Total Exosome RNA and protein isolation kit (Life Sciences). Florescent imaging of exosomes was conducted by labeling exosomes with carboxyfluorescein succinimidyl ester (2μM) or SYTO RNA select (Thermo Fisher Scientific). Microglia were labeled with fluorescently labeled antibody for CD11b and imaged on Olympus confocal microscope. Additional protein analysis was conducted using mass spectrometry. Proteins were separated on 4-12% Bis-Tris gels (Invitrogen). Cysteine bonds were reduced and alkylated with 10nM DTT in 50mM ammonium bicarbonate and 55mM iodoacetamide:50mM NH_4HCO_3. Proteins were digested in 50mM NH_4HCO_3, 5mM $CaCl_2$, 5ng/μl trypsin. The samples were eluted with 60:40 acetonitrile: H2O, 0.1% trifluoroacetic acid

before analysis on Thermo Orbitrap Elite mass spectrometer at the University of Minnesota Center for Mass Spectrometry. To determine concentration of exosomes, Bradford assay was performed. Isolated exosomes were incubated with RNAse (100ng/ml) (Thermo Fisher Scientific), or trypsin (1mg/ml) (Mediatech) and pepsin (10µg/ml) (Sigma) for 10 minutes at 37C and then washed with PBS before analysis or adding to the cells. Isolated exosomes (100µg) were added to cultured cells ($1x10^6$) or injected intracranially (500µg) into a mouse.

Multiple intrathecal injections, Immunohistochemistry staining (IHC), and RNA SCope

Exosomes were isolated from TMEV-infected microglia or uninfected microglia. 100ug exosomes were intrathecally injected into naïve mice every other day, for 8 days. On day 10, mice were sacrificed, brains and spinal cords were perfused with cold PBS and fixed with 4% paraformaldehyde. Tissues were paraffin-embedded, sectioned at 5 micron-thick, and stained for microglia marker Iba1 (Wako, 1:1000) and PLP (Abcam, 1:1000). For RNA Scope was used to detect TMEV RNA, Igtam (microglia marker), and IL-1β according to the manufacturer (ACD Bio). Images were captured with an Olympus BX51 confocal microscope.

RNA isolation and PCR analysis

RNA was isolated from exosomes using the Total Exosome RNA and protein isolation kit (Life Sciences). RNA was isolated from microglia, astrocytes,

and neurons using SV Total RNA Isolation kit which contains a DNAse reaction (Promega). RNA was isolated from brain tissue using Trizol protocol followed by DNAse digestion (Thermo Fisher Scientific). First strand cDNA was generated from 1µg of total RNA using oligo$(dT)_{12\text{-}18}$ primers and Advantage for RT-PCR kit in a final volume of 100µl (Clontech). Real- time PCR was conducted in triplicate with Rotor-Gene SYBR green RT-PCR kit (Qiagen). Briefly, 0.5µM primers, 1X SYBR Green reagent, and 2µl of cDNA were combined in 10µl reactions. The primers for TMEV, cytokines, chemokines, and effector molecules were previously described (2, 11). Real time PCR was conducted on a Rotor-Gene Qiagen Q instrument using hot start with cycle combinations, 40 cycles: 95°C for 15s; 60°C for 20s; 72°C for 15s, followed by a melt from 75°C to 95°C. Quantitation of the mRNA was based on standard curves derived from cDNA standards for each primer pair. Positive and negative cDNA controls were used for each primer pair using cells known to express or not express the specific mRNA. Samples from different groups were normalized based on expression of β-actin. All samples were run in triplicate for each primer pair. Statistical analysis comparison between groups was determined by one-way ANOVA and Bonferroni's multiple comparison test ($p<0.001$). PCR for viral genomes was conducted using cDNA in 25µl reactions with TMEV primers (0.5µM), dNTPs (200µM), 1X reaction buffer, and Q5 high fidelity DNA polymerase (0.02U/µl) (New England BioLabs) on Eppendorf Mastercycler with a hot start and 40 cycles: 95°C for 30s; 60°C for 30s; 72°C for 8m, followed by a 20-minute

extension. PCR products were separated on 0.8% agarose gel with Sybr Safe (Thermo Fisher Scientific) and imaged.

CHAPTER 3

Exosomes from microglia sustain viral persistence and neuroinflammation during TMEV-induced demyelinating disease in mice

Authors: Nhungoc Luong and Julie K. Olson

*The manuscript for this work is being prepared.

BACKGROUND

Viral persistence is important in sustaining inflammatory cues that lead to irreversible damage and development of neurological diseases such as MS[73]. TMEV is a ssRNA virus that belongs to the Picornavirus family and is naturally neurotropic in mice. TMEV (BeAn 8386 strain) infection of susceptible mice (SJL strain) leads to persistent infection of microglia and development of chronic progressive demyelinating disease in the central nervous system (CNS) of mice[73]. TMEV-induced demyelinating disease (TMEV-IDD) has been a useful murine model to study the pathogenesis of MS, particularly the primary progressive type. The clinical symptoms in TMEV-IDD including spastic hindlimb paralysis is comparable to progressive MS in human[74]. TMEV-IDD is described as a biphasic disease[11]. In the acute phase of infection, the immune response against the virus is driven primarily by activation of innate immune cells and TMEV-specific $CD4^+$T cells[49]. Nevertheless, viral clearance is inefficient in susceptible mice, which leads to viral persistence and development of a chronic

phase causing demyelination due to neuroinflammation and myelin-specific $CD4^+$T cells[49].

Microglia are self-regenerative CNS-resident macrophages that migrate to the brain and spinal cord during early development[18]. As innate immune cells, they serve as the first line of defense in the CNS by orchestrating inflammation upon the recognition of pathogen-associated molecular pattern molecules by innate immune receptors such asToll-like receptors (TLRs)[20]. TMEV-infected microglia secrete a large amount of type I IFNs (IFNα and IFNβ), pro-inflammatory cytokines (IL-6, IL-12, and TNFα), and chemokines (CCL2, CCL3, and CCL5). The chemokines attract infiltrating immune cells such dendritic cells and monocytes/macrophages to enter the CNS to partake in the inflammatory milieu. Microglia also express surface co-stimulatory molecules CD80, CD86, CD40 and MHC class II to present viral and myelin antigens to $CD4^+$ T cells[21]. Neuroinflammation persistently elicited by chronic viral infection can lead to bystander damage of neuronal structure, release of myelin epitopes, and consequently, demyelinating disease.

Exosomes have been shown to be exploited by viruses, specifically herpesviruses and hepatitis viruses for their transmission and latency[61, 62, 75, 76]. Our previous studies showed that microglia from TMEV-infected mice produced exosomes during the acute phase contain TMEV RNA and genome that could be transferred to uninfected bystander cells, independent of viral particles (Chapter 2). Moreover, these exosomes could induce an innate immune response in the uninfected cells and inflammation in the CNS of naive mice

(Chapter 2). These exciting data suggested that exosomes from microglia isolated during the acute infection may play an important role in upholding viral infection and neuroinflammation. However, TMEV-IDD is a complex model just as human MS, the profile and functions of exosomes collected 2 days after infection do not represent the exosomes collected at the chronic demyelinating disease phase. We hypothesized that exosomes secreted from microglia during the chronic phase of TMEV-IDD contain viral RNA which maintain persistent TMEV infection in the CNS and neuroinflammation by activating surrounding cells, contributing to demyelination. In summary, we found that during the chronic phase, exosomes isolated from microglia from the brains and spinal cord continued to contain replication-competent viral RNA. Further, these exosomes could continue to stimulate both bystander CNS resident and infiltrating cells to secrete type I IFNs, pro-inflammatory cytokines, and chemokines. Most importantly, these exosomes could induce an inflammatory response in recipient naïve mice brains. All of these findings provide a new insight into the mechanisms of how viruses can be persistent in the CNS via exosomes and continue to cause immune-mediated demyelinating disease.

RESULTS

Microglia secrete exosomes containing viral RNA during TMEV-IDD

Exosomes are constitutively secreted by cells as a means of communicating with other cells through cytoplasmic material exchange. We decided to look at exosomes secreted by microglia (***microglia exosomes***) from the brains and spinal cords separately because the microglia reside in the brain

have been reported to exhibit phenotypical and functional differences from the microglia reside in the spinal cord[77, 78]. Microglia exosomes were collected from both brains and spinal cords of mice at 63 days post TMEV infection i.e. during TMEV-IDD phase or age match naïve control mice using the standard procedures established by our lab, described in Chapter 2. Isolated microglia exosomes were identified by flow cytometry, western blot, and mass spectrometry. The size of microglia exosomes ranged from 30 to 150nm, verified by Nanosight (data not shown). The isolated microglia exosomes from both groups expressed exosomal marker CD63 (Figure 16A-D). Microglia exosomes isolated from the brains and spinal cords of mice during TMEV-IDD expressed higher level of surface activation molecules MHC class II, costimulatory molecules, CD80, CD86, and CD40 in comparison to naïve microglia exosomes (Figure 16E-L). Mass spectrometry revealed that these microglia exosomes expressed microglial marker, CD11b, exosome specific markers, CD63, CD9, CD81, TSG101, Rab, while lacking markers associated with other subsets of extravesicular vesicles (data not shown).

Next, we wanted to look into the content of microglia exosomes secreted during the full course of TMEV infection. From previous studies, microglia exosomes secreted 2 days post infection contain TMEV RNA/genome. Since TMEV establish a persistent infection in microglia, we queried whether microglia continue to encapsulate viral RNA inside exosomes throughout the full course of TMEV infection (approximately 96 days). Microglia exosomes were isolated from mice brains and spinal cords at 10 critical time points of TMEV-infection (1, 2, 3,

4, 7, 10, 14, 28, 42, 63, and 96 dpi). The microglia exosomes consistently contained viral RNA starting from day 1 until day 96 post infection (Figure 17A). The viral RNA level started high and then gradually decreased with no significant difference between the microglia exosomes from brains versus spinal cords at any given time point. Since we wanted to study the microglia exosomes produced during the chronic demyelinating disease phase, we focused on the microglia exosomes from 63dpi brains and spinal cords. Two pairs of primers were used to detect different regions on TMEV genome, 200bp upstream region and 5.4kbp coding region in the TMEV genome. The data showed that microglia exosomes isolated during TMEV-IDD contain viral RNA and genome (Figure 17B, C). The microglia exosomes from naïve brains were used as the control in the experiments because there was no any difference between exosomes from naïve brains and exosomes from naïve spinal cords. These findings indicated that microglia exosomes contain viral RNA/genome not only shortly after TMEV infection, but also throughout the TMEV-IDD. These studies suggested exosomes could be a way that viruses exploit to persist in host.

Viral RNA in microglia exosomes secreted during TMEV-IDD can be transferred to bystander uninfected CNS cells

One unique feature of exosomes is their host-derived cell membrane, which allows them to be endocytosed by a wide range of cell types, thus facilitating material exchange, including viral RNA. Microglia exosomes (100ug) isolated from mice brains and spinal cords during TMEV-IDD were added to uninfected microglia ($1x10^6$ cells) and cells were lysed after 24 hours of

incubation. Real-time PCR detected viral RNA transcripts in the bystander uninfected microglia after being exposed to microglia exosomes (Figure17D). Moreover, the viral RNA in the bystander microglia was able to replicate as the shown by level of viral RNA in cells amplified over the course of 20 hours (Figure 17G). Next, we investigated whether exosomes can be taken up and transfer viral RNA to other cell types in the CNS such as astrocytes and neurons. Again, microglia exosomes were added onto primary astrocytes ($1x10^6$ cells) and neurons ($1x10^6$ cells) and lysed the cells after 24 hours of incubation. Similar to microglia, astrocytes (Figure 17E) and neurons (Figure 17F) could take up the exosomes and obtain the viral RNA. These results suggest that microglia exosomes are capable of effectively transferring viral RNA to bystander cells, suggesting another persistence mechanism whereby infected cells could secrete exosomes containing viral RNA into the microenvironment which can be picked up by surrounding uninfected cells to facilitate the spread.

Viral RNA in microglia exosomes secreted during TMEV-IDD can activate bystander CNS cells

Microglia can be infected with TMEV *in vitro* and *in vivo* to become activated immune cells. The chronic inflammatory response against the virus is the key in TMEV-IDD pathogenesis[31]. We wanted to determine whether exosomes secreted from microglia isolated during the TMEV-IDD could exert a activate bystander CNS cells since they contain viral RNA. Microglia exosomes were isolated from mice brains and spinal cords during TMEV-IDD. Microglia exosomes were added to uninfected microglia, astrocytes, and neurons for 24

hours before getting lysed for RNA analysis. The number of exosomes added to the cells was determined by dose response curve experiments from our previous study (Chapter 2). Bystander cells were lysed for the real-time PCR analysis of type I IFNs, cytokines, chemokines, and effector molecules expression. These molecules are common markers associated with inflammation. First, the bystander microglia incubated with microglia exosomes from mice with TMEV-IDD expressed a higher level of type I IFNs, IFNα and IFNβ, pro-inflammatory cytokines, IL-1β, IL-6, IL-12, TNFα, and chemokines, CCL2, in comparison to cells incubated with to the microglia exosomes from naïve mice (Figure 18). Similarly, astrocytes (Figure 19A-F) and neurons (Figure 19G-L) also upregulated type I IFNs, IFNα and IFNβ, IL-1β, IL-6, TNFα, CCL2 after being incubated with microglia exosomes isolated from mice during TMEV-IDD.

The inflammatory response in bystander microglia were activated through innate immune receptors in response to viral RNA in exosomes

The inflammatory response can be triggered by a wide range of factors through the innate immune sensors on the surface and inside cells. Exosomes can package and deliver a myriad of host cell-derived materials to the recipient cells. In previous studies, we showed that the bystander cells become activated by viral RNA in exosome secreted by TMEV-infected cells. Exosomes from microglia infected with ultraviolet-inactivated TMEV were not able to elicit an immune response in bystander cells (data not shown). The current studies looked at microglia exosomes isolated during TMEV-IDD which may contain materials specific to chronic disease which acute phase may not have. Thus, we

wanted to determine whether viral RNA was still the key component in eliciting an innate immune response in bystander cells. To address this question, the innate receptors, MyD88 and MAVS, were silenced in microglia using a pool of four individual siRNAs for each receptor to assure an efficient knock-down. Then, microglia exosomes from TMEV-IDD mice were added to silenced cells for 24 hours before the cells were lysed for the PCR analysis. As the result, the expression of type I IFNs, IFNα and IFNβ, cytokines IL-1β, IL-6, TNFα, and chemokines CCL2 was greatly diminished in silenced cells, compared to the controls (Figure 20). These data show that viral RNA was able to activate an innate immune response that promoted an inflammatory response associated with TMEV-IDD.

The viral RNA in microglia exosomes can be transferred to infiltrating immune cells

TMEV establish a life-long infection in susceptible mice, particularly in microglia. Exosomes secreted by infected microglia contain viral RNA could be detected starting from day one post infection. Infiltrating immune cells including dendritic cells, monocytes, and macrophages can be detected within the first few days after the infection and continues through persistent disease, although at a lower level. We wanted to determine whether the infiltrating immune cells also take up the microglia exosomes containing viral RNA secreted during chronic TMEV-IDD. Microglia exosomes from TMEV-IDD mice brains and spinal cords were isolated as previously described and placed on cultures of dendritic cells, monocytes, and macrophages. After 24 hours of incubation, real time PCR was

able to identify viral RNA in dendritic cells (Figure 21A), monocytes (Figure 21B), and macrophages (Figure 21C). These data were particularly intriguing because they suggest that exosomes could transfer viral RNA to not only the local cells but also the immune cells that enter from the periphery.

Exosomes secreted by microglia during TMEV-IDD activate an innate immune response in infiltrating immune cells

Innate immune cell such as dendritic cells and monocytes/macrophages are sources of pro-inflammatory cytokines and chemokines following viral infection. These cells usually infiltrate into the CNS following viral infection and injury. The magnitude of inflammation seen in the CNS during TMEV-IDD suggests that infiltrating cells may also partake in substantiating the inflammation in the CNS during the chronic TMEV-IDD. Thus, we wanted to know whether microglia exosomes from the TMEV-IDD mice brains and spinal cords could activate the infiltrating cells. Microglia exosomes were added to uninfected dendritic cells, monocytes, and macrophages to determine if an immune response could be provoked. After 24 hours of incubation, cells were lysed. Real-time PCR analysis showed that type I IFNs, IFNα and IFNβ, pro-inflammatory cytokines, IL-1β, IL-6, IL-12, TNFα, and chemokines CCL2 were greatly increased in the dendritic cells (Figure 22A-E), monocytes (Figure 22F-J), and macrophages (Figure 22K-O) incubated with microglia exosomes from TMEV-IDD mice compared to the cells received naïve microglia exosomes. These data reveal that microglia exosomes could be mediating the inflammatory response in not only CNS-resident cells but also infiltrating immune cells during TMEV-IDD.

Microglia exosomes from mice with chronic TMEV-IDD into naïve mice causes neuroinflammation in naïve mice

The results from our *ex vivo* experiments showed that exosomes secreted by microglia during TMEV-IDD contain viral RNA that can be transferred to and activate an inflammatory response in uninfected bystander cells including microglia, astrocytes, neurons, dendritic cells, monocytes, and macrophages. The more important question is whether those phenomena could be repeated *in vivo*. Hence, microglia exosomes (500ug) from the TMEV-IDD mice brains or spinal cords was injected into the right hemisphere of naïve mice. Two days later, mice brains were dissected from mice and dissociated for RNA isolation. Viral RNA was detected using real time PCR in the brains of the injected mice (Figure 23A). Further, the presence of viral RNA in the brains of naïve mice was visualized using fluorescent TMEV RNA probe (Figure 23B). Most importantly, microglia exosomes from TMEV-IDD mice brains and spinal cords could increase the expression of type I IFNs, IFNα and IFNβ, and pro-inflammatory cytokines, TNFα, IL-6, IL-1β, and chemokine, CCL2 (Figure 24). Intracerebral injection of naïve microglia exosomes into naïve mice did not provoke an immune response. Overall, these data show that exosomes released by microglia during TMEV-IDD contained viral RNA and can promote neuroinflammation in naïve mice.

DATA

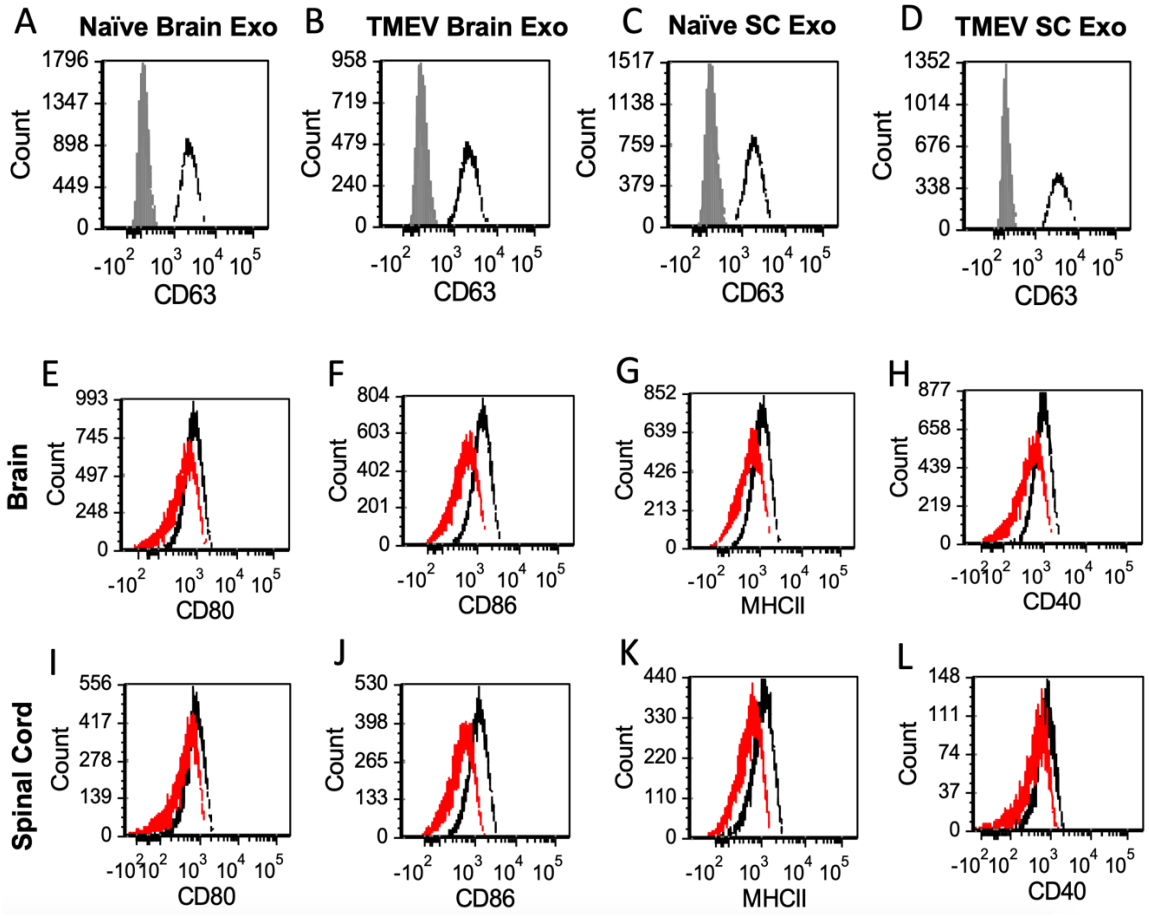

Figure 16. Microglia secrete exosomes during TMEV-IDD in mice express activation markers.

Exosomes were isolated from brains and spinal cords of naïve mice (Naïve Brain Exo, Naïve SC Exo) or mice with TMEV-IDD (TMEV Brain Exo, TMEV SC Exo) and sorted for microglial CD11b marker using magnetic bead. $CD11b^{+}$ exosomes (microglia exosomes) were fluorescently labeled with antibody for exosomal marker CD63 (A-D). Flow cytometry was done on the labeled exosomes for the expression of specific markers as shown in the **black lines** in comparison with isotype control antibodies in the **gray line**. Microglia exosomes

(CD11b^{+}CD63^{+}) from naïve brains (**red line**, E-H), TMEV-IDD brains (**black line**, E-H), naïve spinal cords (**red line,** I-L), and TMEV-IDD spinal cords (**black line,** I-L) were fluorescently labeled with antibodies for activation markers CD80, CD86, MHC class II, and CD40. Flow cytometry was done on the labeled exosomes for the expression of specific markers. These are representative graphs and images from one experiment of three independent experiments.

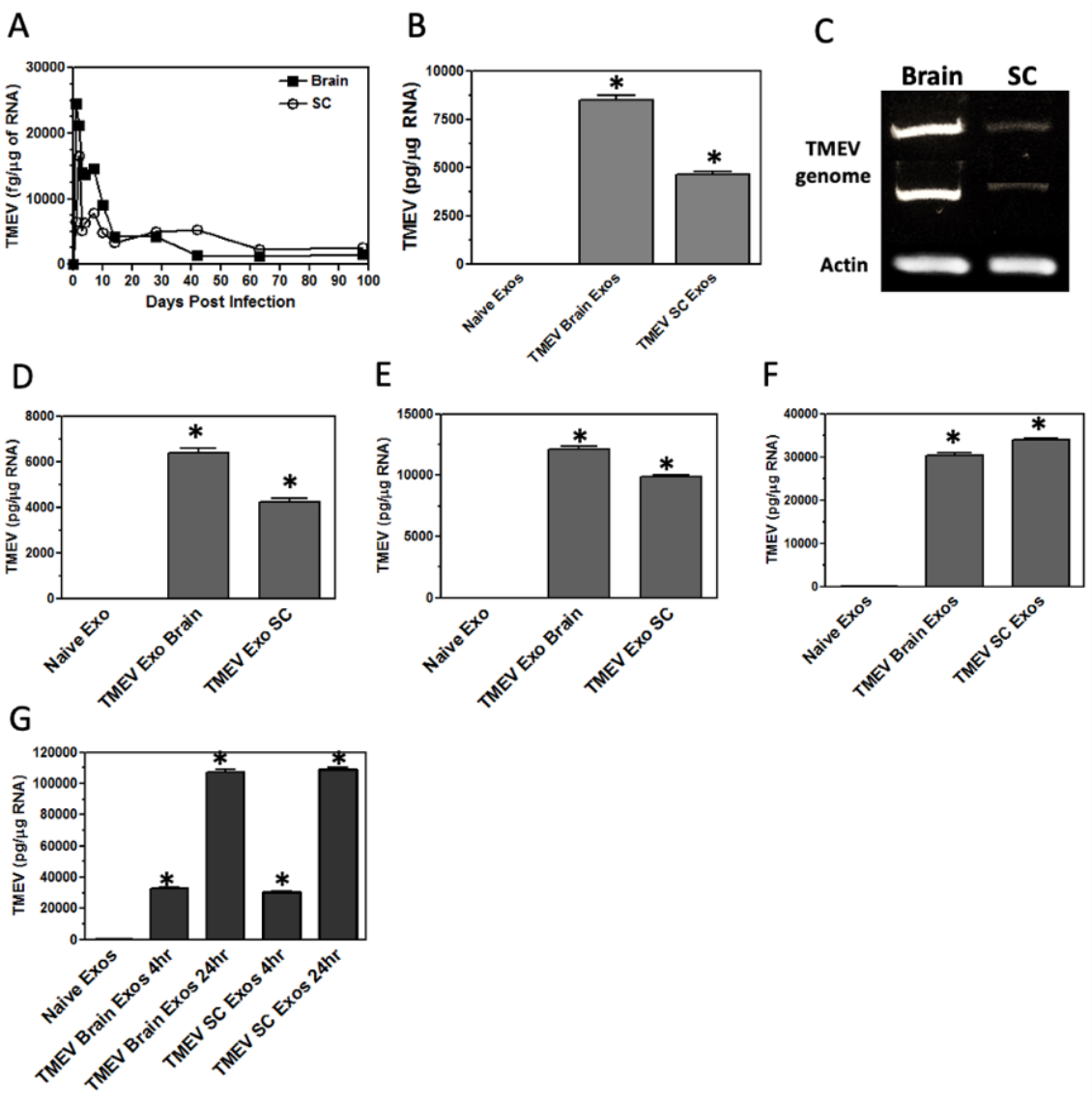

Figure 17. Exosomes secreted by microglia of mice with TMEV-IDD contain viral RNA genome that is transferred to bystander CNS cells.

Microglia exosomes were isolated from brains and spinal cords TMEV-infected mice at 1, 2, 3, 4, 7, 10, 28, 42, 63, and 96 dpi. Viral RNA was assessed by real-time PCR with TMEV primers (A). Microglia exosomes were isolated from brains and spinal cords of naïve mice or mice with TMEV-IDD (63dpi) contained viral RNA assessed by real-time PCR with TMEV primers (B) or by conventional PCR with primers for long TMEV (5.4kbp) product or for β-actin (C). In transfer experiments, microglia exosomes from mice brains and spinal cords isolated during TMEV-IDD were placed on microglia culture. Cells were lysed 24 hours later for RNA isolation and cDNA conversion. Real-time PCR was done with primers for TMEV (D). Similarly, RNA was assessed for TMEV from astrocytes (E) and neurons (F) that were incubated with microglia exosomes. Microglia exosomes isolated from brains and spinal cords of naïve mice or mice with TMEV-IDD were placed on naïve microglia. After 4 hours, the media containing exosomes was removed and replaced with fresh media. After 0 and 20 hours, cells were lysed and analyzed by real-time PCR for TMEV (G). Significant difference was determined by one-way ANOVA and Bonferroni's multiple comparison test ($p<0.001$) based on expression by naïve cells. These are representative graphs from one experiment of three individual experiments.

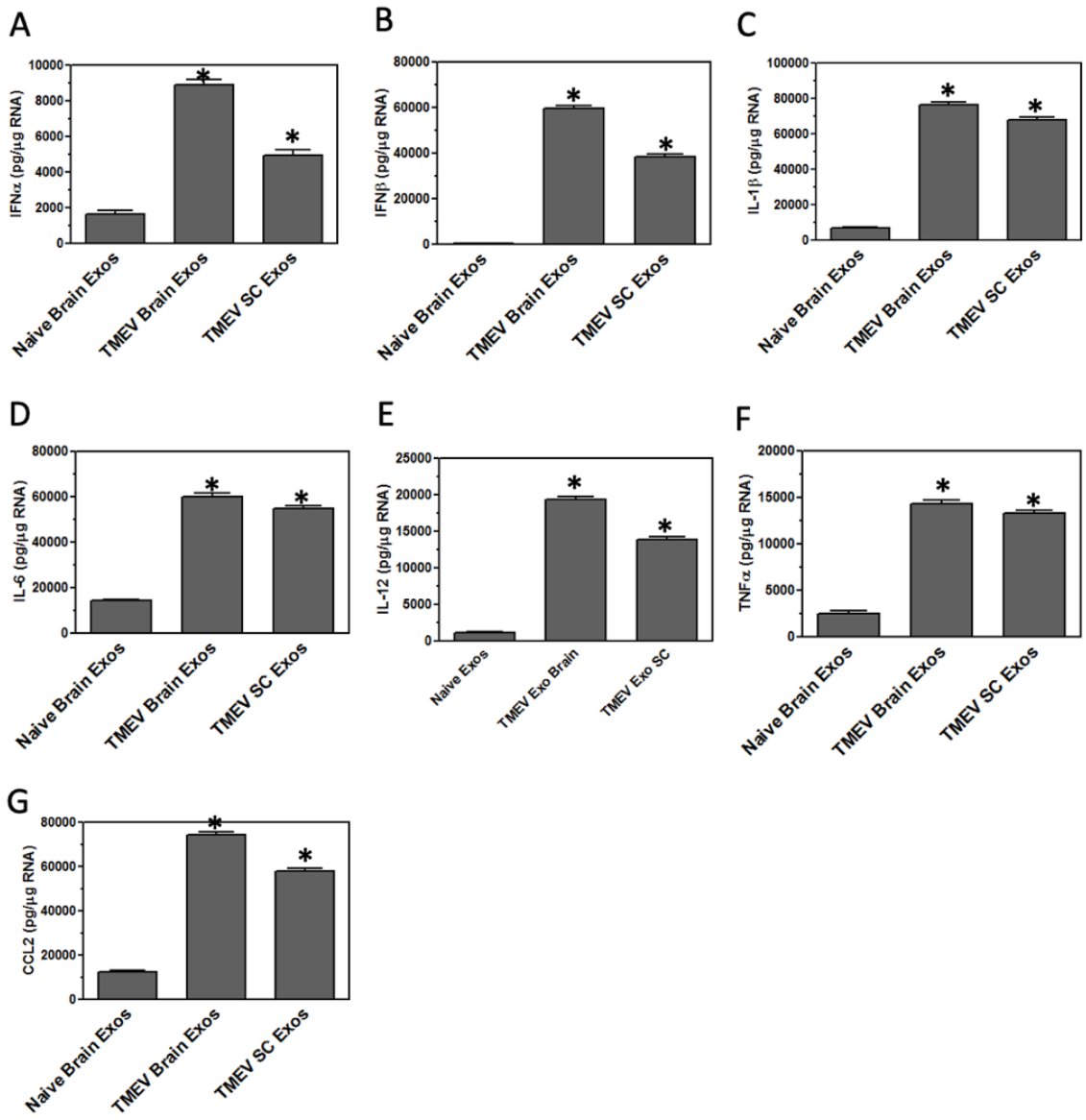

Figure 18. Activation of bystander microglia after taking up exosomes secreted by microglia during TMEV-IDD.

Microglia exosomes were isolated from mice brains and spinal cords from naïve or TMEV-IDD mice. The isolated exosomes were placed on naïve microglia ($1x10^6$) for 24 hours. Microglia were lysed, RNA isolated, converted to cDNA. Real time PCR was performed to measure the expression of IFNα (A), IFNβ (B), IL-1β (C), IL-6 (D), IL-12 (E), TNFα (F), and CCL2 (G). Significant differences

were determined by one-way ANOVA and Bonferroni's multiple comparison test ($p<0.001$) based on expression by naïve microglia. These are representative graphs from one experiment of four individual experiments.

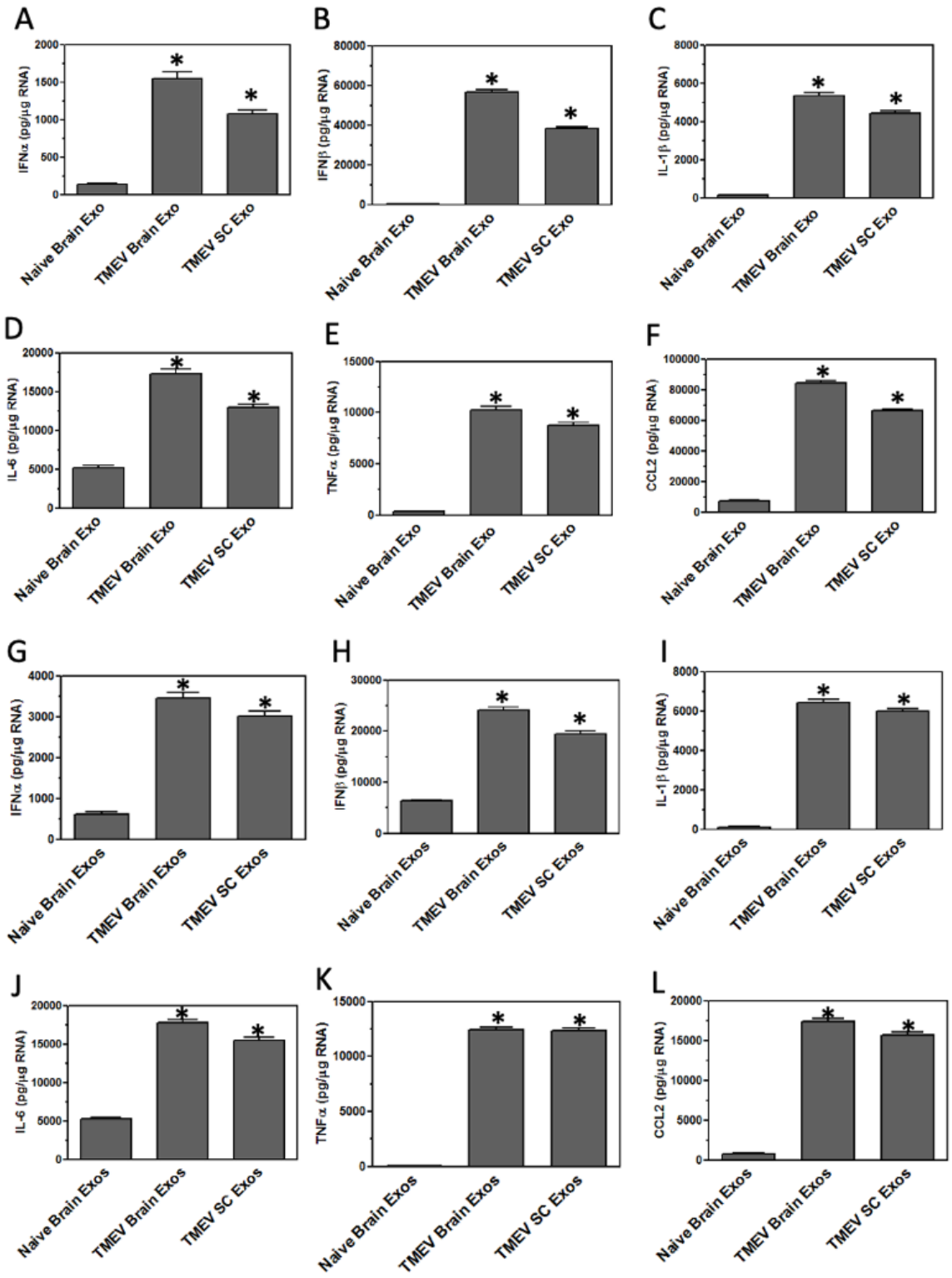

Figure 19. Activation of bystander astrocytes and neurons after the exposure to exosomes secreted by microglia during TMEV-IDD.

Microglia exosomes were isolated from naïve or TMEV-IDD mice brains and spinal cords. The isolated exosomes were placed on naïve (A-F) astrocytes and (G-L) neurons for 24 hours. Cells were lysed for RNA isolation and cDNA generation. Real time PCR was performed to measure the expression of IFNα (A and G), IFNβ (B and H), IL-1β, (C and I), IL-6 (D and J), TNF-α (E and K), and CCL2 (F and L). Significant difference was determined by one-way ANOVA and Bonferroni's multiple comparison test ($p<0.001$) based on expression by naïve astrocytes and neurons. These are representative graphs from one experiment of four individual experiments.

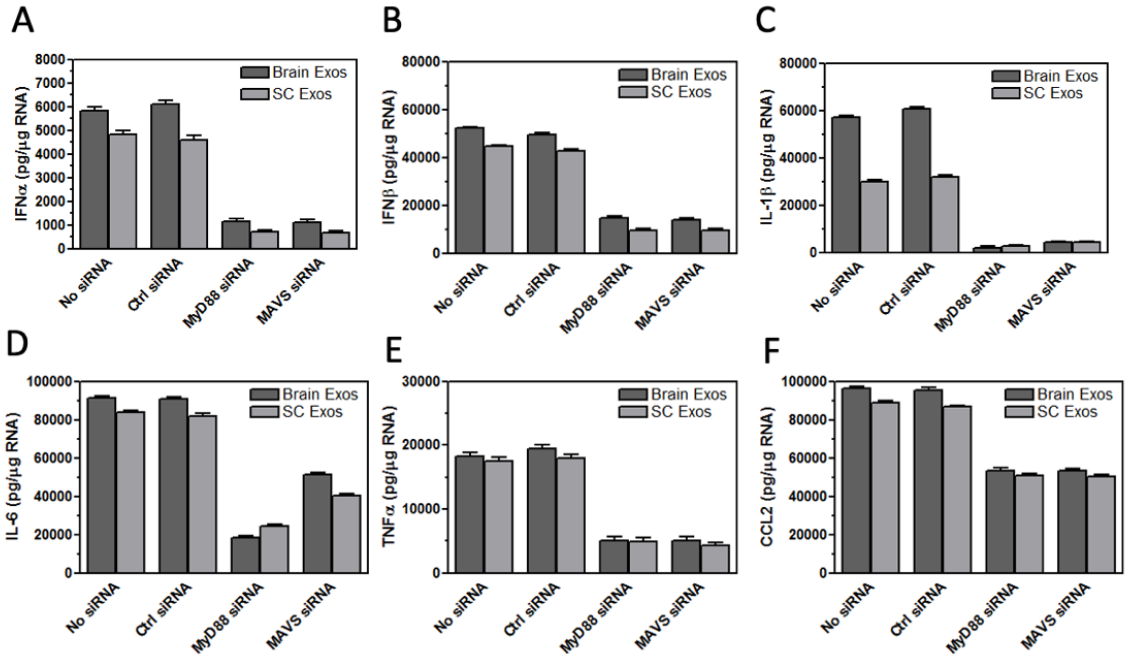

Figure 20. Bystander microglia are activated by exosomes from microglia isolated during TMEV-IDD via innate immune receptors.

Microglia were transfected with siRNA for MyD88, MAVS, control siRNA or no siRNA control (6 hours). Microglia exosomes were isolated naïve or TMEV-IDD mice brains and spinal cords. Exosomes were placed on the transfected

microglia for 24 hours. Microglia were lysed, RNA was isolated, and converted to cDNA for PCR analysis. The expression of IFNα (A), IFNβ (B), IL-1β (C), IL-6 (D), TNFα (E), and CCL2 (F) were measured and the significant differences were determined by one-way ANOVA and Bonferroni's multiple comparison test ($p<0.001$) based on control siRNA transfected microglia. These are representative graphs from one experiment of three independent repeated experiments.

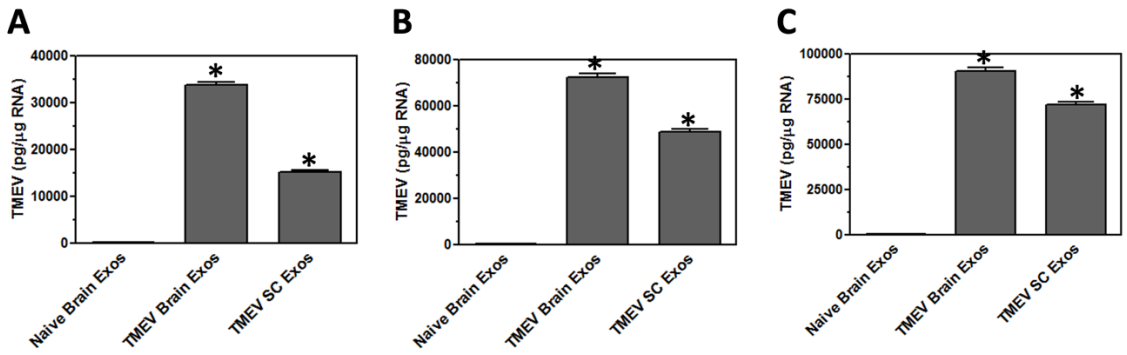

Figure 21. Exosomes from microglia during TMEV-IDD transfer viral RNA to infiltrating immune cells.

Microglia exosomes were isolated from brains and spinal cords of naïve mice or mice with TMEV-IDD. Microglia exosomes were placed on dendritic cells (A), monocytes (B), and macrophage (C). Cells were lysed 24 hours later for RNA isolation and cDNA conversion. Real-time PCR was done with primers for TMEV. Significant differences were determined by one-way ANOVA and Bonferroni's multiple comparison test ($p<0.001$) based on expression by naïve cells. These are representative graphs from one experiment of three individual experiments.

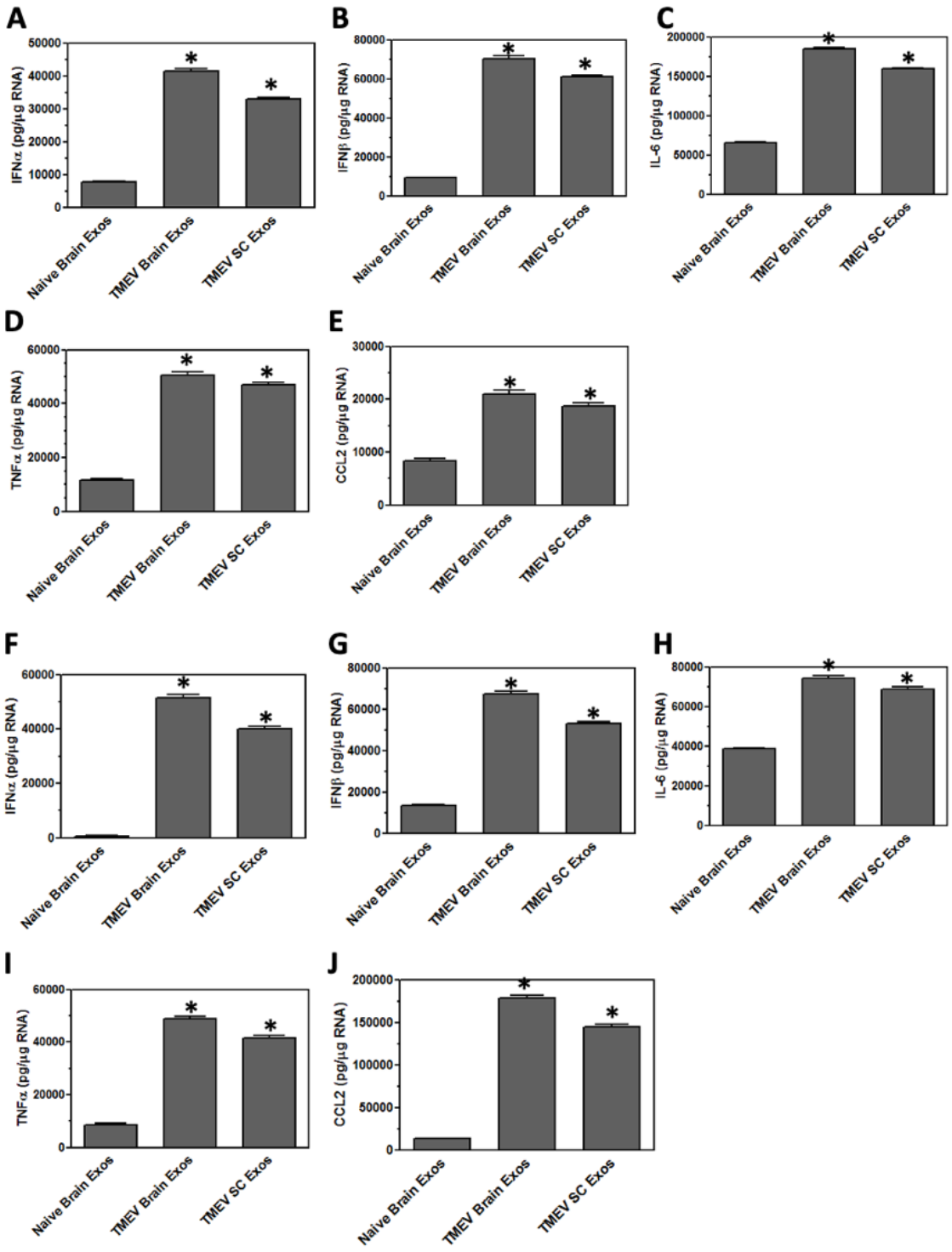
A
IFNα (pg/µg RNA)
50000
40000
30000
20000
10000
0
Naive Brain Exos
TMEV Brain Exos
TMEV SC Exos
B
IFNβ (pg/µg RNA)
80000
60000
40000
20000
0
C
IL-6 (pg/µg RNA)
200000
150000
100000
50000
0
D
TNFα (pg/µg RNA)
60000
40000
20000
0
E
CCL2 (pg/µg RNA)
30000
20000
10000
0
F
IFNα (pg/µg RNA)
G
IFNβ (pg/µg RNA)
H
IL-6 (pg/µg RNA)
I
TNFα (pg/µg RNA)
J
CCL2 (pg/µg RNA)

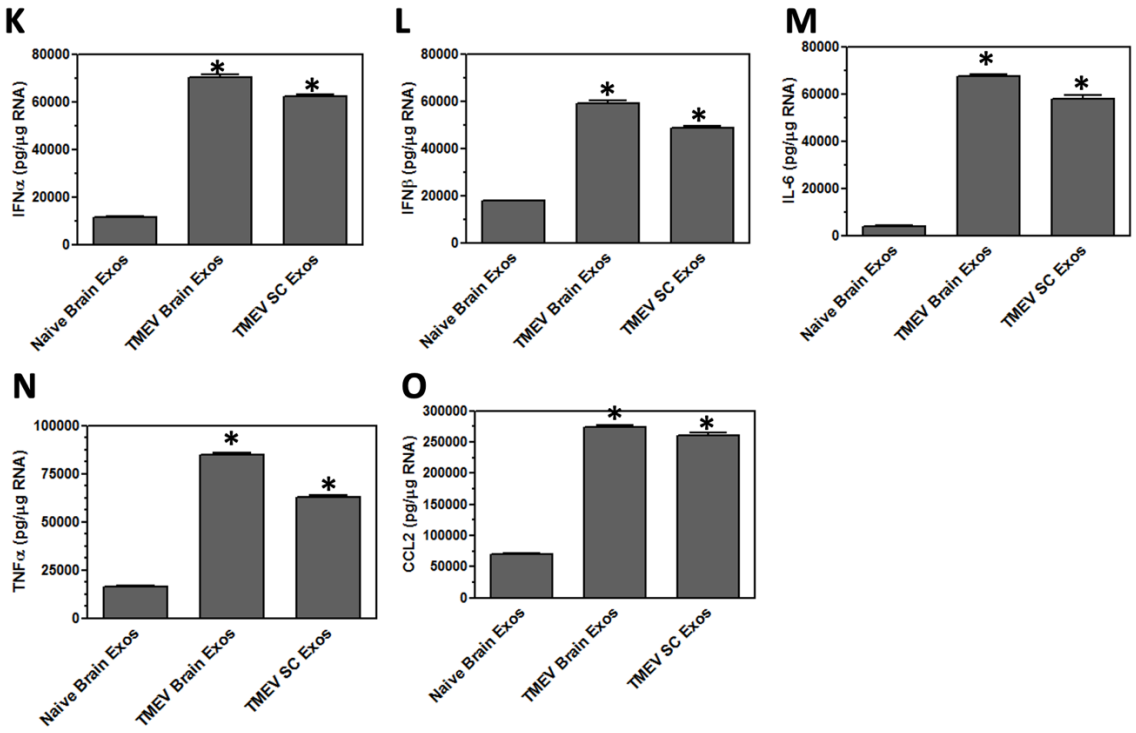

Figure 22. Exosomes secreted from microglia during TMEV-IDD activate infiltrating immune cells to express inflammatory mediators.

Microglia exosomes were isolated from naïve or TMEV-IDD mice brains and spinal cords and placed on naïve (A-E) dendritic cells, monocytes (F-J), and macrophages (K-O) for 24 hours. Cells were lysed for RNA isolation and cDNA generation. Real time PCR was performed to measure the expression of IFNα (A, F, K), IFNβ (B, G, L), IL-6 (C, H, M), TNFα (D, I, N), and CCL2 (E, J, O). Significant differences were determined by one-way ANOVA and Bonferroni's multiple comparison test ($p<0.001$) based on expression by unstimulated monocytes and macrophages. These are representative graphs from one experiment of three individual experiments.

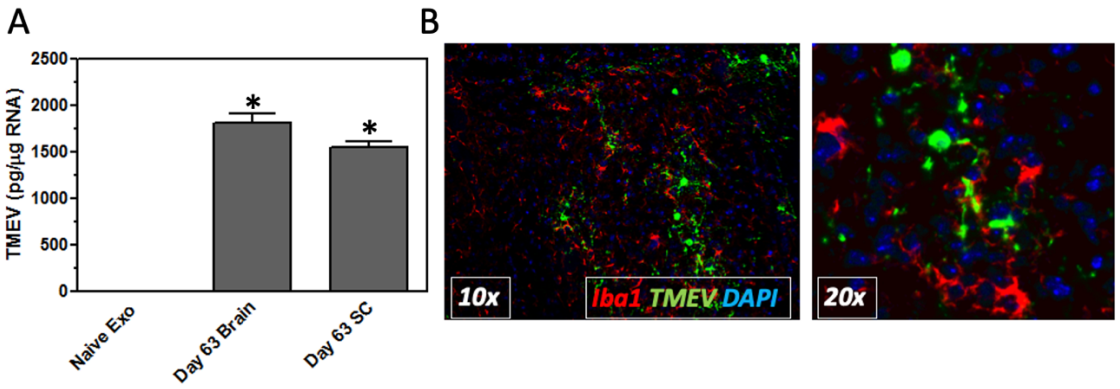

Figure 23. Exosomes secreted by microglia during TMEV-IDD transfer viral RNA to naïve mice. Microglia exosomes were isolated from naïve or TMEV-IDD mice brains and spinal cords. Exosomes (500µg) were injected intracranially into naïve mice. At 2 days post injection, brains were removed from mice (3 mice/group), and RNA was isolated, converted into cDNA and used in real time PCR with primers for TMEV (A). Significant differences were determined by the one-way ANOVA and Bonferroni's multiple comparison test ($p<0.001$) based on the naïve mouse brain. TMEV RNA (green), Iba1 (red), and DAPI (blue) were labeled with probe according to RNAScope *in situ* hybridization technique. Images were taken with confocal microscope at (B) 10x and 20x magnification.

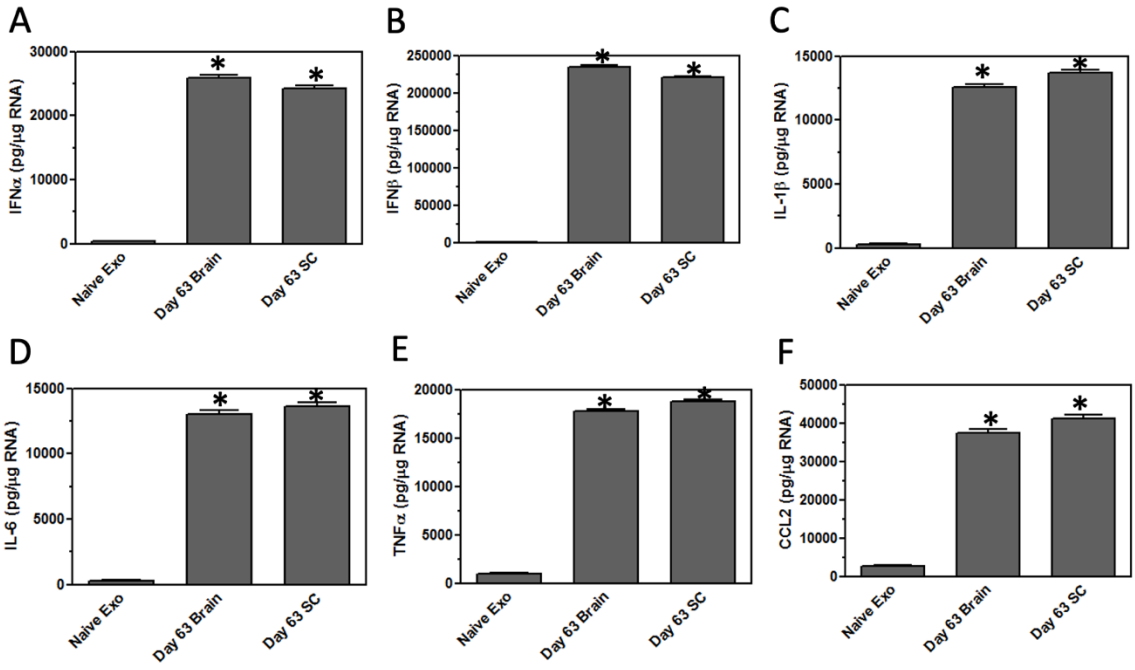

Figure 24. Exosomes secreted by microglia during TMEV-IDD induce neuroinflammation in naïve mice.

Microglia exosomes were isolated from naïve or TMEV-IDD mice brains and spinal cords. Exosomes (500µg) were injected intracranially into naïve mice. At 2 days post injection, the brains were removed from mice (3 mice/ group), and RNA was isolated, converted into cDNA to use in real time PCR. Expression of IFNα (A), IFNβ (B), IL-1β (C), IL-6 (D), TNFα (E), and CCL2 (F) were measured. Significant differences were determined by the one-way ANOVA and Bonferroni's multiple comparison test ($p<0.001$).

DISCUSSION

TMEV-IDD has been used as a valuable murine model to study the chronic progressive demyelinating phase of MS. This model closely recapitulates the hallmarks of disease as it starts with the initial inflammation in the CNS driven by viral infection followed by the progressive chronic demyelinating disease

associated with neuroinflammation due to persistent viral infection[11, 79]. TMEV infects and persists in microglia for the lifetime of susceptible mice[26]. Our previous studies showed that exosomes secreted by microglia (microglia exosomes) shortly after TMEV infection carry viral RNA and the viral RNA genome was transferred to bystander CNS cells including uninfected microglia, astrocytes, and neurons. Moreover, the bystander cells express pro-inflammatory mediators after being exposed to microglia exosomes containing viral RNA (Chapter 2).

These studies focus on the contribution of microglia exosomes secreted during the chronic phase of TMEV-IDD, which has differences from the acute phase[11]. Interestingly, previous studies have shown that the inflammation in the CNS, particularly the spinal cord, during the chronic phase is driven by an innate-like response, not adaptive immune response. This phenomenon might contribute to chronic inflammation and development of TMEV-IDD[32]. Persistent viral infection could be the key factor which accounts for the constant inflammatory response in the CNS as studies have shown that the administration of IFNβ could alleviate the severity and progression in mouse TMEV-IDD and human MS[41, 80]. Similar to the acute phase, in the chronic phase, microglia, continue to secret exosomes containing viral RNA and genome that allow for transfer of viral RNA to uninfected bystander CNS cells (microglia, astrocytes, and neurons) and infiltrating immune cells (dendritic cell, monocytes, and macrophages). The transfer is independent of viral particles as shown by the lack of viral capsid protein and plaque assay (data not shown). The viral RNA in

microglia exosomes were replication competent as the level of viral transcripts was amplified over time inside the recipient cells. Most importantly, these exosomes could elicit an inflammatory response in bystander cells and naïve mice, which was shown to be important in neuroinflammation and the development of TMEV-IDD.

Exosomes package messages including nucleic acids and proteins that can be carried from one cell to another[81]. The external and internal contents of exosomes is reflective of the activation stage of their cells of origin; thus, the proteomics and transcriptomics of exosomes can be potentially used as biomarkers of diseases. We found that microglia in the brains and spinal cords of mice during TMEV-IDD secrete exosomes. The exosomes expressed microglial marker, CD11b, and exosome markers CD63. The exosomes also expressed a high level of MHC class II molecule, costimulatory receptors, CD80 and CD86, and activation marker CD40, similar to the activation markers on microglia during TMEV-IDD.

During the acute infection, TMEV can infect several cell types such as microglia, monocytes/macrophages, astrocytes, and neurons. However, TMEV only persist long-term in microglia[26, 82]. The mechanism of how TMEV persists is not fully understood but most likely is due to inefficient viral clearance in susceptible mice. In the chronic demyelinating disease phase, viral RNA continues to be detected by sensitive PCR, and low level of infectious viral particles can be isolated (data not shown). In the last few years, viruses were found to exploit exosomes for their pathogenesis and spread. For examples,

exosomes released from enterovirus 71 virus-infected oral mucosal cells are enriched in miR-30a that can suppress type I IFNs through inhibiting MyD88 in macrophages, thus enabling viral replication[83]. Viruses such as hepatitis C virus, human immunodeficiency virus, and Dengue virus, can utilize vesicular secretion mechanism to enhance their replication and spread by loading exosomes with viral and host functional protein[61, 63, 84]. The current studies found that exosomes secreted by microglia contain viral RNA throughout TMEV infection. Ten critical time points were selected to collect exosomes. Day 1-4, the innate immunity becomes detectable. Day 7, virus-specific lymphocytes can be detected. Day 10-14, virus titers typically decline significantly in susceptible mice. Beyond day 28, infected mice enter the chronic infection phase. Day 42, demyelination occurs with assessable clinical symptoms. The scope of this chapter is day 63 post infection and onward. After day 63, it was observed that infected mice develop demyelinating disease with progressive clinical symptoms. These data suggest that exosomes could be one of the ways that viruses can persist in the host.

Due to their cell-derived membrane, exosomes can be taken up by other cells to facilitate the content exchange. The microglia exosomes isolated during TMEV-IDD could transfer viral RNA to bystander uninfected microglia. The viral RNA in the recipient cells was able to replicate, inferring replication had occurred. Since there is a crosstalk between cells in the CNS, we wanted to look at whether microglia exosomes could be taken up by astrocytes and neurons. Microglia exosomes from the brains and spinal cords of mice isolated during chronic TMEV-IDD were placed onto astrocytes and neuron. The viral RNA was

detected in bystander astrocytes and neurons. Thus, the persistence of TMEV viral RNA in the CNS could be facilitated via exosomes.

TMEV infection can lead to activation of an innate immune response in microglia[21]. Our studies showed that microglia exosomes elicited a pro-inflammatory response in the bystander microglia including the expression of type I IFNs, IFNα and IFNβ, pro-inflammatory cytokines IL-1β, IL-12, IL-6, TNFα, and chemokines CCL2. Microglia in spinal cord have been suggested to play a critical role in demyelinating disease as they are more reactive than those in the brain[77]. Microglia exosomes isolated from brains and spinal cords did not show significant differences in viral RNA level or functionality, as long as the same quantity of exosomes was used in the experiments. Silencing viral RNA-sensing innate immune receptors signaling, MYD88 and MAVS, decreased the expression of the cytokines and chemokines upon the exposure to microglia exosomes. These results suggest that bystander cells were activated by viral RNA in microglia exosomes secreted during TMEV-IDD.

The activation status of microglia might have a direct effect on astrocytes and neurons, especially in the context of neurodegenerative diseases and neurotoxicity. Supernatant from activated microglia alone is sufficient to activate astrocytes to release cytotoxic factors that cause dopaminergic neuron death, commonly seen in Parkinson's disease[85]. In EAE mouse model, the absence of aryl hydrocarbon receptor (Ahr) on microglia decreases NF-kB inhibitor, SOCS2 molecules, and can lead to the enrichment of VEGFB to induce the expression of CCL2, NOS2, IL1 β in astrocytes[86]. In the current studies, microglia exosomes

isolated during TMEV-IDD could activate astrocytes and neurons to secrete type I IFNs, pro-inflammatory cytokines, and chemokines, possibly contributing to the overall inflammatory milieu in the CNS during TMEV-IDD.

Infiltrating immune cells have been shown play a role in TMEV-IDD development[67]. However, no work has been done on the activities of infiltrating dendritic cells, monocytes, and macrophages in TMEV-IDD. In the current studies, microglia exosomes from TMEV-IDD could transfer viral RNA to dendritic cells, monocytes, and macrophages and activate the cells toward an inflammatory response. These results showed that exosomes can serve as vehicles to distribute viral RNA to not only CNS cells but also infiltrating immune cells.

Based on the *ex vivo* data, we wanted to determine if the microglia exosomes from the brains and spinal cords of mice during chronic TMEV-IDD could have a similar effect *in vivo*. Thus, microglia exosomes were injected directly into the right hemisphere of naïve mice to find that the viral RNA inside microglia exosomes was transferred to the naïve brains. Most importantly, microglia exosomes could induce inflammatory mediators, type I IFNs, pro-inflammatory cytokines, and chemokines, in the naïve mice brains, which is the hallmark of TMEV-IDD and human MS. Injection of microglia exosomes from naïve mice did not induce inflammation in mice. The chosen injection route of exosomes was intracerebral, albeit other routes such as intrathecal and intravenous injections could have been as effective as long as an effective dose was used.

In human, disease-modifying therapies (DMTs) have shown to only be more effective in relapse-remitting MS but not progressive MS[6]. Most of the available DMT such as natalizumab (blocking the infiltration of immune cells into the CNS) or rituximab and ocrelizumab (elimination of B cells) provide little to no therapeutic benefit in chronic progressive MS. One explanation is that in chronic progressive MS, only CNS resident microglia remain persistently active whereas infiltrating cells are no longer present or activated[23]. Thus, further investigations if microglia and the exosomes that microglia secrete, would enhance the understanding of the pathogenesis of chronic virus-initiated demyelinating disease or human chronic progressive MS.

MATERIALS AND METHODS

Mice

5 to 6-week-old female SJL/J mice and pregnant mice were purchased from Envigo (Madison, WI). Neonatal SJL mice were used for primary microglia and astrocytes isolation. Mice were housed and handled at University of Minnesota Research Animal Resource Center accredited by the American Association for Accreditation of Laboratory Animal Care.

Isolation and culture of cells

Isolation of primary glial cultures from neonatal mice was performed, as previously described[21]. Briefly, brains were removed from 1 to 3 days old mice, and the meninges were removed. The left and right hemispheres of the brain were dissociated in a nylon mesh bag. The cells were resuspended in DMEM-F12 media (Lonza) supplemented with 10% FCS (Invitrogen Life Technologies)

and 100U/ml penicillin and 100mg/ml streptomycin (Invitrogen Life Technologies). The cells were seeded in poly-D-lysine (Sigma- Aldrich) coated tissue culture flasks and incubated at 37°C. After 10-14 days of incubation, the microglia were shaken off from the astroglial layer on an orbital shaker for 24 hours. The primary microglia were removed from the flasks and placed in DMEM (Invitrogen Life Technologies) supplemented with 10% exosome-free FCS (Invitrogen Life Technologies) and 3ng/ml rGM-CSF (R&D Systems). Microglia were seeded in 24-well plates coated with poly-D-lysine. Dorsal root ganglia neurons (DRGs) were collected as described[87]. In summary, DRGs were dissected and aspirated in trypsin. The cells were resuspended in Ham's F12 media (Invitrogen Life Technologies) supplemented with 2mM L-glutamine, 10U/ml penicillin, 100U/ml streptomycin, and 0.15mg/ml DNAse I (Sigma) and placed in laminin coated flask.

Bone marrow derived monocytes (monocytes), bone marrow derived macrophages (macrophages), and bone marrow derived dendritic cells (dendritic cells) were isolated from femurs and tibia of adult mice. Briefly, both ends of femurs and tibias were incised to allow bone marrow cells to be flushed out by balanced salt solution (BSS) using a syringe with 27-gauge needle. Cells were washed with BSS twice, resuspended, and passed through a cell strainer. Bone marrow cells (14×10^6 cells per T75 flask) were cultured in complete DMEM with 3ng/ml of recombinant granulocyte-macrophage colony-stimulating factor (GM-CSF) (R&D System) for monocyte induction, 10ng/ml of GM-CSF for macrophage induction (based on $CD11b^+CD11C^-$ cells), and 20ng/ml of GM-CSF

and 10ng/ml IL-4 for dendritic cell induction[88]. On day 4, monocytes were re-stimulated with GM-CSF and ready for use. On day 7, macrophages were re-stimulated with GM-CSF and ready for use. For dendritic cells, on day 3, 75% of media including non-adherent cells was replaced with fresh dendritic cell media. On day 6, the adherent dendritic cells were stripped all using Versene, and replated. On day 10, dendritic cells were ready for use[88].

Transfection

Microglia were transfected with siRNAs specific for MyD88 or MAVS, 5mM SMARTpool siRNA (a mixture of 4 siRNAs in one reagent) or siCONTROL (Dharmacon) using Dharmafect 4 reagent according to manufacture protocol. Silencing was guaranteed by Dharmacon with 75% or better efficiency and 90% reduced off-targets.

TMEV-IDD induction

SJL female mice were intracranially injected with $2X10^6$ PFU of TMEV, BeAn 8386 strain. To detect viral RNA in microglia exosomes throughout TMEV infection, we sacrificed mice at 1, 2, 3, 4, 7, 10, 14, 28, 42, 63, and 96dpi to collect microglia exosomes from brains and spinal cords. Mice started to show clinical symptoms between 30-40 dpi and advanced into chronic progressive demyelinating disease around 63 dpi, akin to human primary progressive MS. Clinical symptoms include mild to severe gait abnormalities, righting inability, and worst, irreversible paralysis[89]. Infected mice were euthanized at 63 dpi. Brain and spinal cords were collected for microglia

exosomes isolation. Microglia exosomes isolated from brain and spinal cords of age-matched naïve mice were used as the controls.

Exosome isolation and analysis

The brains and spinal cords were dissociated through a metal screen (70mM pore) into Hank's balanced salt solution. The homogenates were first centrifuged at 2,000xG for 10 minutes and then increased to 4,200xG for another 45 minutes to remove cells and debris. The total exosomes were isolated from the clear homogenates with the Total Exosome Isolation reagent (Invitrogen). To select for exosomes from microglia, total exosomes were then incubated with antibody for CD11b (microglia marker) conjugated to magnetic beads and sorted on a column per manufacturer protocol (Miltenyi). CD11b+ exosomes (microglia exosomes) were then ready for further application. Pierce BCA protein assay (Thermo Fisher Scientific) was used to determine concentration of exosomes. Additional protein analysis was conducted using mass spectrometry using 120mg protein separated on 4-12% Bis-Tris gels (Invitrogen). Cysteine bonds were reduced and alkylated with 10nM DTT in 50mM ammonium bicarbonate and 55mM iodoacetamide: 50mM NH_4HCO_3. Proteins were digested in 50mM NH_4HCO_3, 5mM $CaCl_2$, 5ng/ml trypsin. The samples were eluted with acetonitrile: H_2O (6:4), 0.1% trifluoroacetic acid before analysis on Thermo Orbitrap Elite mass spectrometer at the University of Minnesota Center for Mass Spectrometry. 100mg or 500mg of isolated microglia exosomes were added to $1x10^6$ cultured cells or injected intracranially into mice, respectively. RNAScope RNA *in*

situ hybridization (ACD) was used to visualize TMEV RNA in cells or tissues. Images were captured with an Olympus BX51 confocal microscope at 10x and 20x magnification.

RNA isolation and PCR analysis

RNA was extracted from microglia exosomes using the Total Exosome RNA and protein isolation kit (Invitrogen). RNA was isolated from microglia, astrocytes, and neurons using SV Total RNA Isolation kit which contains a DNAse reaction (Promega). RNA was isolated from brain tissue using Trizol protocol followed by DNAse digestion (Thermo Fisher Scientific). First strand cDNA was made from 1µg of total RNA using oligo(dT)12-18 primers and Advantage for RT-PCR kit in a final volume of 100µl (Clontech). Real-time PCR was conducted in triplicate with Rotor-Gene SYBR green RT-PCR kit (Qiagen). Briefly, 0,5mM primers, 1X SYBR Green reagent, and 2µl of cDNA were combined in 10µl reactions. The primers for TMEV, IFNs, cytokines, and chemokines were previously described[20, 21]. Rotor-Gene Qiagen Q real time PCR was conducted using hot start with 40 cycles of 95°C for 15s; 60°C for 20s; 72°C for 15s, followed by a melt from 75°C to 95°C. Quantitation of the mRNA was based on standard curves derived from cDNA standards for each primer pair. Positive and negative cDNA controls were used for each primer pair using cells known to express or not express the specific mRNA. Samples from different groups were normalized based on expression of ß-actin. All samples were run in triplicate for each primer pair. Statistical analysis comparison between groups was determined by one-way analysis of variance (ANOVA) and Bonferroni's

multiple comparison test ($p<0.001$). PCR for viral genomes was conducted using cDNA in 25µl reactions with TMEV primers (0.5mM), dNTPs (200mM), 1X reaction buffer, and Q5 high fidelity DNA polymerase (0.02U/ml) (New England BioLabs) on Eppendorf Mastercycler with a hot start and 40 cycles: 95°C for 30s; 60°C for 30s; 72°C for 8 minutes, followed by a 20-minute extension. PCR products were separated on 0.8% agarose gel with Sybr Safe (Thermo Fisher Scientific) and imaged.

Flow Cytometry

Exosomes were isolated from both TMEV infected brains and spinal cords as described earlier. Exosomes were then incubated with latex beads (Invitrogen) for 2.5 hr at RT per the manufacturer protocol. Glycine was added to the mixture and then washed with PBS. Exosomes/beads were incubated for 45 minutes at 4°C with FITC-conjugated Abs specific for CD45, CD11b or CD4, PE conjugated Abs specific for CD63, I-As (MHC class II), CD86, CD80, and CD40 (BD). Following Ab binding, exosome/beads were washed and then fluorescence was analyzed on LSRII (BD).

CHAPTER 4

Extracellular vesicles secreted by tumor cells promote the generation of suppressive monocytes

Authors: Nhungoc Luong, Jennifer Lenz, and Julie K. Olson

*The first two authors contributed equally to this work.

*This work was submitted for publication in the journal ImmunoHorizons.

BACKGROUND

Monocytes are derived in the bone marrow and can differentiate into a wide spectrum of activation states, ranging from activated macrophages with inflammatory properties to immunosuppressive subsets, such as suppressive monocytes and myeloid-derived suppressor cells (MDSCs). Suppressor subsets strongly expand during tumor growth and play an important role in cancer evasion of the immune response. The presence of suppressor subsets in patients is associated with cancer progression, metastasis, and reduced response to therapy[90, 91]. Suppressive monocytes can regulate the function of other immune cell types, including T cells, dendritic cells, macrophages, and natural killer cells. The mechanisms by which monocytes acquire suppressive activity remains poorly defined, and it is uncertain whether suppressive monocytes represent a distinct myeloid lineage or a group of immature myeloid cell types with halted differentiation. Nonetheless, accumulation of suppressive monocytes inhibits antitumor immune responses necessary for controlling tumor

growth and metastasis[92]. In humans, $CD33^{+}CD11b^{+}CD14^{+}HLA\text{-}DR^{lo/neg}$ cells which are monocytes with low to no expression of MHC class II have been shown to be increased in several different types of cancer, including melanoma, glioblastoma, and renal cell carcinoma[93-95]. The $CD14^{+}HLA\text{-}DR^{lo/neg}$ monocytes have been shown to be immunosuppressive and increased numbers of these cells correlate with poor patient outcomes. Despite the known importance of suppressive monocytes in cancer progression, the mechanisms responsible for their generation remain unclear.

Tumors secrete a wide range of cytokines and metabolites that may directly promote the differentiation of suppressive monocytes. Tumors can secrete granulocyte-macrophage colony-stimulating factor (GM-CSF), prostaglandin E_2 and TGFβ that are capable of reaching the bone marrow and contributing to monocyte differentiation[94, 96]. Previous studies have shown that *in vitro* culture medium from tumor cells, glioma and renal cell carcinoma, contain factors that can promote differentiation of suppressive monocytes[97, 98]. Additional studies have demonstrated that suppressive monocytes can be differentiated from murine bone marrow when cultured in medium collected from cancer cell lines and supplemented with GM-CSF and IL-4[99, 100]. Thus, factors secreted by tumor cells have the ability to promote differentiation of suppressive monocytes.

Extracellular vesicles (EVs) are small membrane-bound vesicles released from cells and taken up by other cells as a means of intercellular communication. EVs contain proteins, mRNA, miRNA, and lipids that can then be transferred to another cell[70]. EVs play an important role in maintaining homeostasis under

healthy conditions. However, during disease states, EVs may transport contents that negatively impact surrounding cells. Tumor cells release EVs at a markedly increased rate compared to normal cell types[101, 102]. Tumor-derived EVs have been shown to regulate T cell function by mediating the apoptosis of cytotoxic T cells and promoting the expansion of T regulatory cells[103-105]. Tumor derived EVs have also been shown to reduce the cytotoxic activity of natural killer cells[103-105].

In the current study, we examined whether tumor derived EVs can affect monocyte differentiation. These studies show that EVs secreted by tumor cells can be taken up by bone marrow derived monocytes and promote the differentiation of monocytes toward a suppressive phenotype. Monocytes exposed to tumor derived EVs have reduced expression of MHC class II and costimulatory molecules as well increased expression of PD-L1. Most importantly, monocytes exposed to tumor derived EVs had reduced ability to activated antigen specific $CD4^+$ T cell responses compared to monocytes exposed to EVs from non-malignant cells. These studies were conducted with tumor cells from a variety of tumor types to demonstrate that EVs are a common mechanism used by tumors for promoting suppressive monocytes. These findings suggest that tumors secrete EVs to promote an immunosuppressive microenvironment.

RESULTS

EVs secreted by tumor cells promote bone marrow derived monocytes to express suppressive cytokines and effector molecules

Monocytes that infiltrate into areas of tumor have been shown to have suppressive features and are often referred to myeloid- derived suppressor cells (MDSCs). Tumors may promote the generation of MDSCs through secreted products. Thus, we wanted to determine whether EVs secreted by tumor cells may promote the suppressive properties of monocytes. EVs were isolated from various types of tumor cells lines, including osteosarcoma (K12), glioma (GL261), colon carcinoma (CT26), sarcoma (NCTC), and melanoma (B16OVA). As controls for the tumor cells, EVs were isolated from primary cultured cells of the cell types from which the tumor cells were derived. The isolated EVs were confirmed for size by Nanosight analysis and expression of EVs markers, including CD63, by flow cytometry and confirmed by western blot for all EVs (Figure 25J-M, shows glia and GL261). The EVs were labeled with florescent dye and added to bone marrow derived monocytes to determine whether the monocytes were able to take up the EVs secreted by tumor cells (Figure 25A-I). The monocytes were able to take up EVs secreted from the tumor cells as well as the primary cell controls for all the different types of cells.

Next, we wanted to determine whether EVs secreted by tumor cells could alter the activation of monocytes. EVs were isolated from tumor cells and primary cells, and the EVs were added to bone marrow derived monocytes for 4 days. After 4 days, the monocytes were analyzed for expression of cytokines and effector molecules by real time PCR (Figure 26 and 27). EVs secreted by osteosarcoma (K12) cells decreased the expression of pro-inflammatory cytokines IL-12 and TNFα and increased the expression of suppressive cytokine

IL-10 and TGFβ as well as suppressive molecules, arginase and inducible nitric oxide synthase (iNOS), by bone marrow derived monocytes as compared to EVs secreted by osteoblast cells (Figure 26). The glioma cells (GL261) were grown in stem cell as well as differentiated state to represent the different stages in tumors. The EVs secreted by glioma cells (GL261S and GL261D) decreased the expression of pro-inflammatory cytokines, IL-12 and TNFα and increased the expression of suppressive cytokines, IL-10 and TGFβ as well as suppressive molecules, arginase, and iNOS, by monocytes as compared to EVs secreted by glia cells (Figure 26). EVs secreted by colon carcinoma (CT26) and sarcoma (NCTC) cells decreased the expression of pro-inflammatory cytokines, IL-12 and TNFα and increased the expression of suppressive cytokines, IL-10, and TGFβ as well as suppressive molecules, arginase and iNOS, by bone marrow derived monocytes as compared to EVs secreted by fibroblast (Figure 27). EVs secreted by melanoma cells (B16OVA) decreased the expression of pro-inflammatory cytokines, IL-12 and TNFα and increased the expression of suppressive cytokines, IL-10 and TGFβ as well as suppressive molecules, arginase and iNOS, by monocytes as compared to EVs secreted by melanocytes (Figure 27). These results show that EVs secreted by various types of tumor cells decreases the expression of pro-inflammatory cytokines by monocytes and promotes the expression of suppressive cytokines and effector molecules by monocytes.

A recent study showed that media from GL261 glioma cells reduced the pro-inflammatory cytokines expressed by bone marrow derived monocytes via suppressor of cytokines 3 (SOCS3) dependent mechanism. SOCS3 is a

negative regulator of the Janus Kinase (JAK)/Signal Transducer and Activator of Transcription (STAT) and NFkB signaling pathways which promote expression of pro-inflammatory cytokines[106, 107]. Therefore, we wanted to determine whether EVs isolated from GL261 glioma cells as well as from other tumor cells upregulated SOCS3 expression. EVs were isolated from tumor cell lines and primary cells, the EVs were placed on bone marrow derived monocytes for 4 days as described above. After 4 days, the monocytes were analyzed by real time PCR for SOCS3 expression (Figure 28). EVs secreted by osteosarcoma, glioma, colon carcinoma, sarcoma, and melanoma increased the expression of SOCS3 in monocytes. Meanwhile, monocytes exposed to EVs secreted by corresponding primary cells did not change the expression of SOCS3. These results show that EVs secreted by several different types of tumor cells promote the upregulation of SOCS3 in monocytes which reduces the expression of pro-inflammatory cytokines.

EVs secreted by tumor cells alter the cell surface markers on monocytes

Previous studies have shown that monocytes that infiltrate into the tumor microenvironment have reduced expression of MHC class II and co-stimulatory molecules and can have increased expression of inhibitory molecules, such as PD-L1. Thus, we wanted to determine whether EVs secreted by tumor cells can alter the cell surface markers on monocytes. EVs secreted by the tumor cells were isolated and placed on bone marrow derived monocytes. After 4 days, the monocytes were washed and labeled with fluorescently labeled antibodies for CD11b and Ly6C, CD80, MHC class II, and PD-L1. The monocytes were

analyzed by flow cytometry to determine expression levels on the surface of the cells (Figure 29 and Table 2). Monocytes exposed to EVs secreted by tumor cells, including osteosarcoma, glioma, sarcoma, colon carcinoma, and melanoma, had decreased expression of MHC class II as well as co-stimulatory molecule, CD80, as compared to monocytes that were exposed to EVs secreted by primary cells, including osteoblast, glia, fibroblast, and melanocytes. Further, monocytes exposed to EVs from tumor cells had increased expression of PD-L1 as well as Ly6C as compared to monocytes exposed to EVs from primary cells. These results show that EVs secreted by tumor cells promote monocytes to increase Ly6C and PD-L1 and to decrease MHC class II and co-stimulatory molecules on their cell surface.

EVs secreted by tumor cells promote generation of monocytes that suppress CD4$^+$ T cells

Previous studies have shown that monocytes that infiltrate into tumor areas can suppress activated T cells. Several mechanisms have been proposed for suppression of T cells by monocytes including increased secretion of suppressive cytokines and negative immune mediators as well as decreased expression of MHC class II and co-stimulatory molecules. Based on our flow cytometry data, monocytes exposed to EVs from tumor cells decreased the expression of MHC class II and co-stimulatory molecules as well upregulated the expression of inhibitory molecule PD-L1 on the cell surface. Based on our cytokine data, monocytes exposed to EVs from tumor cells increased the expression of suppressive cytokines and immune mediators, including IL-10,

TGFβ, arginase, and iNOS. Thus, we wanted to determine whether EVs secreted by tumor cells promote the generation of monocytes that suppress activated $CD4^+$ T cells. Antigen- specific $CD4^+$ T cells were activated against a known mouse virus epitope in C57BL6 mice, TMEV $VP4_{21-40}$. EVs were isolated from tumor cells, including osteosarcoma, glioma, colon carcinoma, sarcoma, and melanoma, and from primary cell controls, osteoblast, glia, fibroblast, and melanocytes. The EVs were placed on bone marrow derived monocytes continually for 4 days. After 4 days, the monocytes were removed and placed in culture with the activated $VP4_{21-40}$- specific $CD4^+$ T cells in a T cell proliferation assay with or without peptide. The $CD4^+$ T cells were analyzed by flow cytometry for CFSE levels indicating proliferation (Figure 30A-M). When monocytes were added that had been incubated with EVs from primary cell cultures, the $VP4_{21-40}$ specific $CD4^+$ T cells proliferated similar to $VP4_{21-40}$ specific $CD4^+$ T cells that had monocytes incubated with no EVs added to the culture. Most interesting, $VP4_{21-40}$ specific $CD4^+$ T cells that were incubated with monocytes that were exposed to EVs from the tumor cells had greatly reduced proliferation compared to $VP4_{21-40}$ specific $CD4^+$ T cells that had monocytes incubated with no EVs added to the culture. Similarly, $VP4_{21-40}$ specific $CD4^+$ T cells secreted less IL-2 when incubated with monocytes that were exposed to EVs from tumor cells compared to monocytes exposed to EVs from primary cells or monocytes with no EVs (Figure 30N-O). These results show that tumor cells secrete EVs that convert monocytes into suppressive cells that inhibit activated $CD4^+$ T cells.

DATA

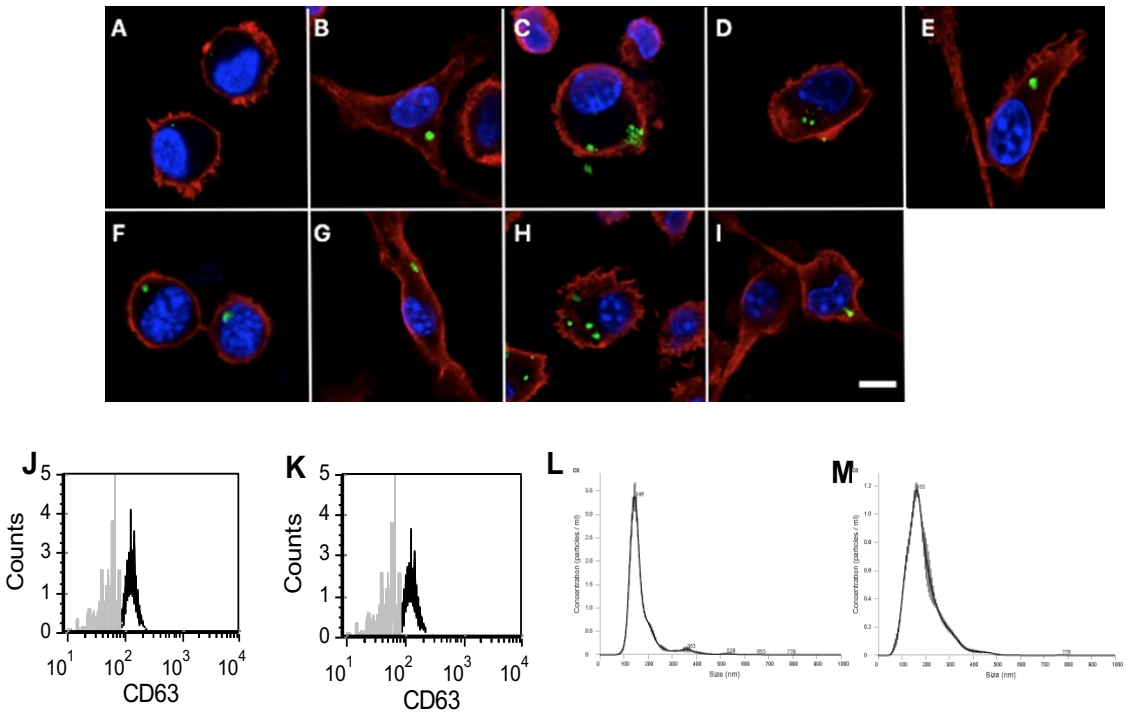

Figure 25. **EVs secreted by tumor cells can be taken up by monocytes.**

EVs were isolated from tumor cells GL261 (A), NCTC (C), CT26 (D), K12 (F), B16 (H) and control glia (B), fibroblast (E), osteoblast (G), and melanocytes (I) and labeled with CFSE (green). The EVs were placed on bone marrow derived monocytes for 2 hours, and the monocytes were labeled with antibody for CD11b (red). DAPI (blue) stained cellular nuclei. The cells were imaged on a confocal microscope, scale bar= 10μm. EVs were isolated and incubated with fluorescently labeled antibody for CD63 and analyzed by flow cytometry (black line) compared to isotype control (gray) shown for glia (J) and GL261 (K). EVs were isolated and analyzed on NanoSight to determine size, shown for glia (L)

and GL261 (M). These are representative images from one experiment of four independent repeated experiments.

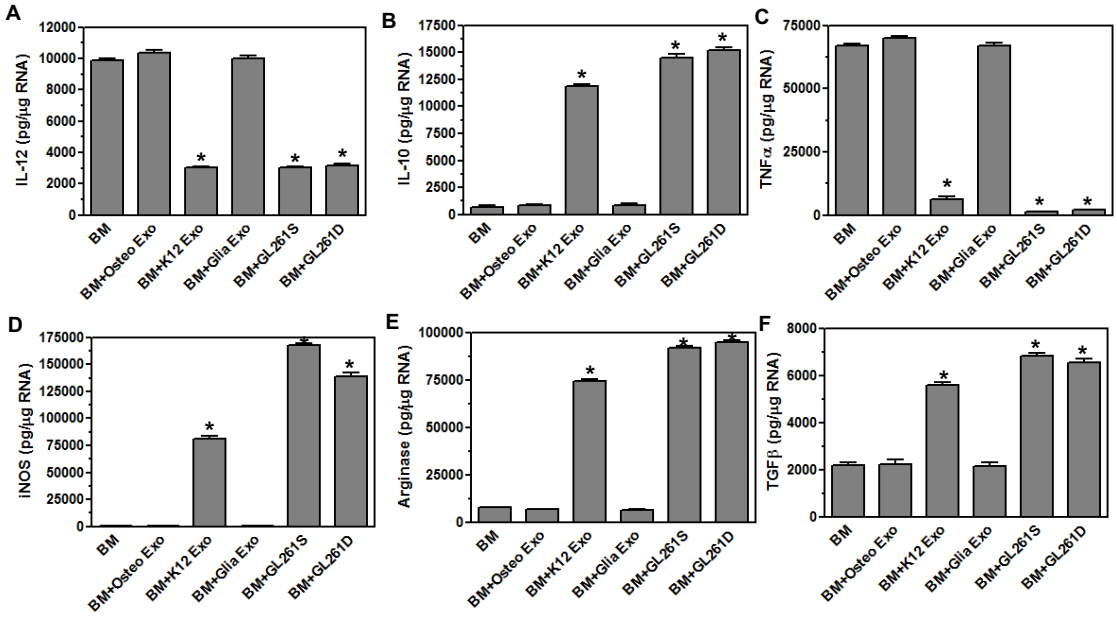

Figure 26. EVs secreted by glioma and osteosarcoma tumor cells promote the expression of suppressive cytokines and effector molecules by monocytes.

EVs were isolated from osteoblast (osteo), K12, mixed glia, GL261 stem cell (GL261S), GL261 differentiated (GL261D) cells. The EVs were placed on bone marrow- derived monocytes for 4 days, and the cells were lysed. The RNA was isolated from lysates, converted to cDNA and used in real time PCR with primers for IL-12 (A), IL-10 (B), TNFα (C), iNOS (D), arginase (E), and TGFβ (F). Significant difference was determined by the one-way ANOVA and Bonferroni's multiple comparison test ($p<0.001$) based on bone marrow derived monocytes without EVs added. These are representative graphs from one experiment of five independent repeated experiments.

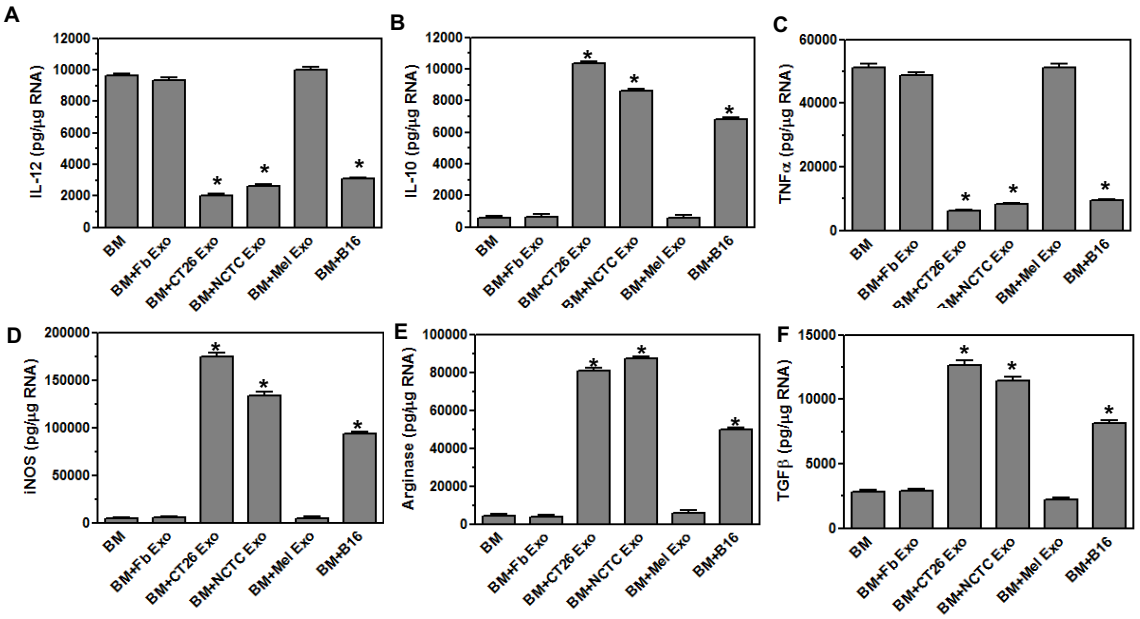

Figure 27. EVs secreted by colon carcinoma, sarcoma, and melanoma tumor cells promote expression of suppressive cytokines and effector molecules by monocytes.

EVs were isolated from fibroblast (Fb), CT26, NCTC 2472, melanocytes (Mel), and B16OVA cell lines. The EVs were placed on bone marrow- derived monocytes for 4 days, after which the cells were lysed. The RNA was isolated from lysates, converted to cDNA and used in real time PCR with primers for IL-12 (A), IL-10 (B), TNFα (C), iNOS (D), arginase (E), and TGFβ (F). Significant difference was determined by the one-way ANOVA and Bonferroni's multiple comparison test ($p<0.001$) based on bone marrow derived monocytes without EVs added. These are representative graphs from one experiment of five independent repeated experiments.

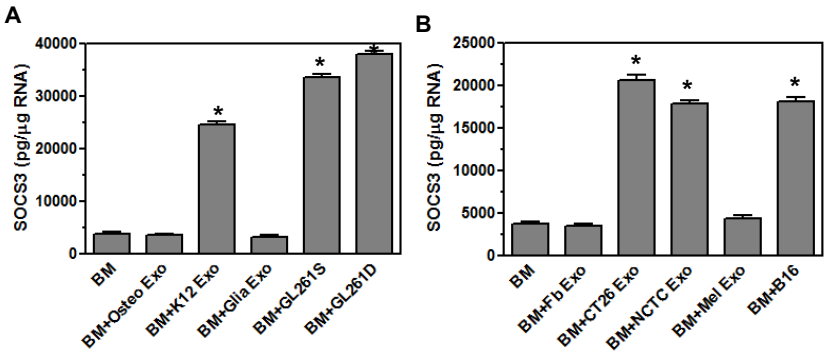

Figure 28. EVs secreted by tumor cells promote the upregulation of SOCS3 in monocytes.

EVs were isolated from osteoblast (osteo), K12, mixed glia, GL261 stem cell (GL261S), GL261 differentiated (GL261D) cells (A). EVs were isolated from fibroblast (Fb), CT26, NCTC 2472, melanocytes (Mel), and B16OVA cell lines (B). The EVs were placed on bone marrow-derived monocytes for 4 days. The monocytes were lysed, RNA isolated and converted to cDNA and used in real time PCR with primers for SOCS3. Significant difference was determined by the one-way ANOVA and Bonferroni's multiple comparison test ($p<0.001$) based on bone marrow derived monocytes without EVs added. These are representative graphs from one experiment of four independent repeated experiments.

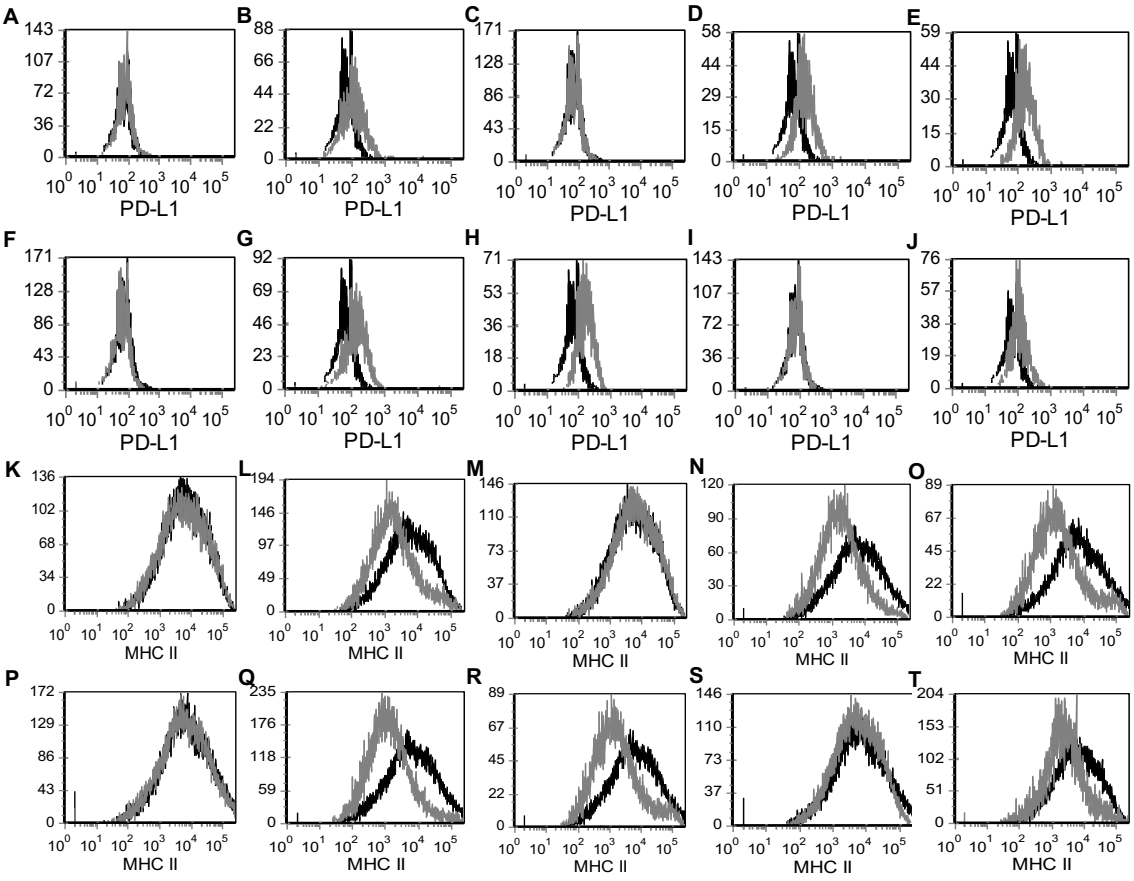

Figure 29. EVs secreted by tumor cells alter the surface markers on monocytes.

EVs were isolated from osteoblast (A, K), K12 (B, L), mixed glia (C, M), GL261 stem cells (D, N), GL261 differentiated cells (E, O), fibroblast (F, P), CT26 (G, Q), NCTC (H, R), melanocytes (I, S), and B16OVA (J, T) cell lines. The EVs were placed on bone marrow derived monocytes for 4 days. The monocytes were then incubated with fluorescently labeled antibody for CD11b and PD-L1 (A-J) or MHC class II (K-T). The monocytes were gated on $CD11b^+$ cells. Histogram plots show monocytes without EVs in the black lines and the monocytes with the EVs as listed above in the gray line. These are representative plots from one experiment of four independent repeated experiments.

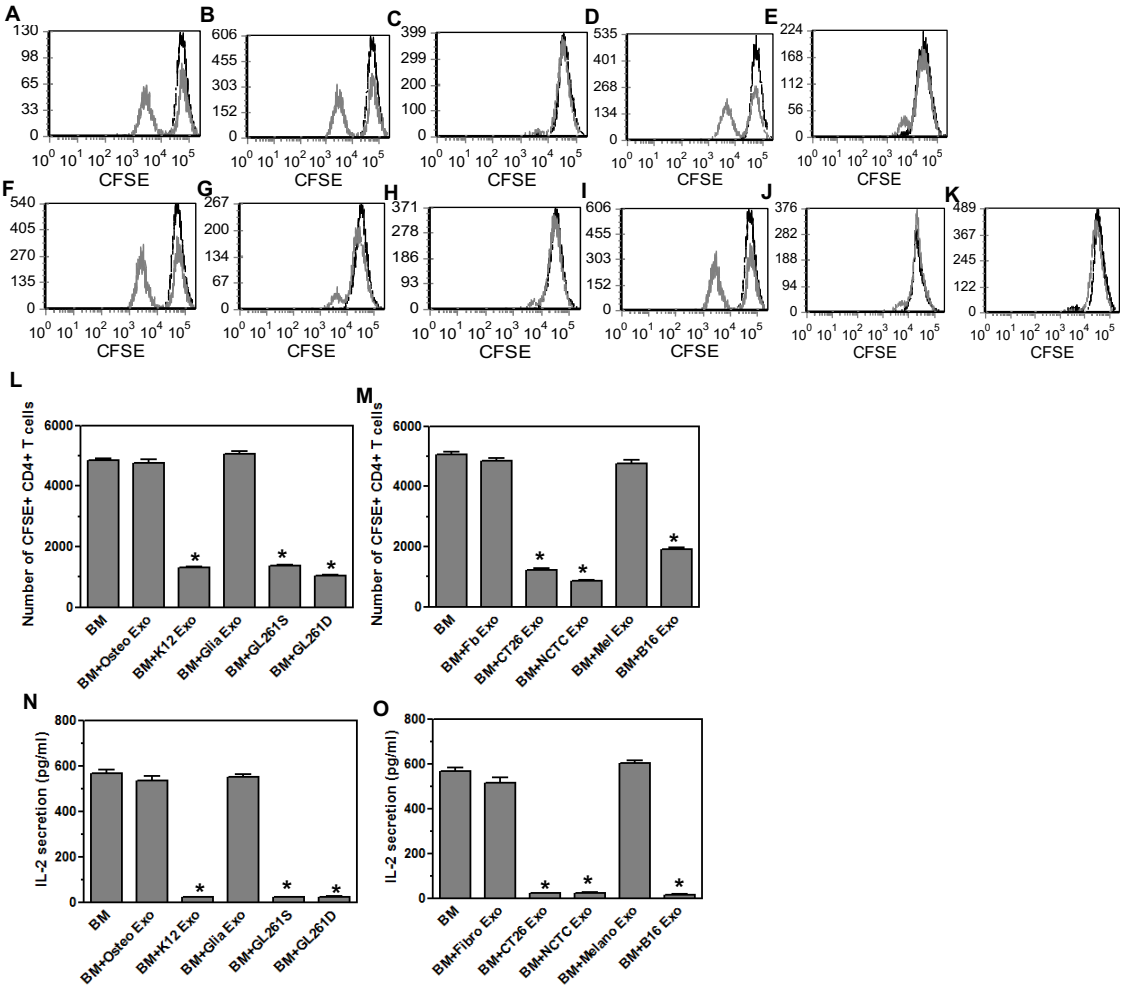

Figure 30. EVs secreted by tumor cells promote the generation of monocytes that suppress CD4⁺ T cell responses.

EVs were isolated from osteoblast (B), K12 (C), melanocytes (D), B16OVA (E), mixed glia (F), GL261 stem cells (G), GL261 differentiated cells (H), fibroblast (I), CT26 (J), NCTC (K) cell lines. The EVs were placed on bone marrow derived monocytes for 4 days. The monocytes were then washed and cultured with CFSE labeled $VP4_{21-40}$ -specific $CD4^+$ T cells with or without $VP4_{21-40}$ peptide. After 4 days in culture, the $CD4^+$ T cells were analyzed by flow cytometry for

CFSE shown in the histogram plots (A-K) with the black line showing VP_{21-40}-specific $CD4^+$ T cells without peptide added and gray line showing with VP_{21-10} peptide added. All groups were conducted in triplicate with one representative plot shown for each group. Results from triplicates are shown in graphs (L and M). Significant difference was determined by the one-way ANOVA and Bonferroni's multiple comparison test ($p<0.001$) based on bone marrow derived monocytes without EVs added. These are representative plots and graphs from one experiment of four independent repeated experiments.

	Osteo	K12	Glia	GL261S	GL261D	Fibro	CT26	NCTC	Melano	B16
Ly6C	+	++	+	+++	+++	+	+++	+++	+	+++
CD80	++	+	++	+	+	++	+	+	++	+
MHC II	++	+	++	+	+	++	+	+	++	+
PDL-1	+	++	+	++	++	+	++	++	+	++

Low expression +, medium expression ++, high expression +++

Table 2: Exosomes from tumor cells alter the surface markers on monocytes. Monocytes were exposed to EVs secreted by tumor cells, including osteosarcoma, glioma, sarcoma, colon carcinoma, and melanoma for 4 days. Monocytes were analyzed by flow cytometry to determine expression level of Ly6C, CD80, MHC II, PDL-1 on the surface of the cells.

DISCUSSION

Tumor growth and metastasis is dependent on the interaction between transformed tumor cells, the tumor microenvironment, and the host immune response[108]. Tumor cells evade detection by the host immune response by secretion of soluble factors to promote an immunosuppressive tumor microenvironment. Immunosuppression of monocytes, T cells, and NK cells

enables tumor growth. Circulating monocytes traffic to the site of tumor cell growth, however, in the tumor microenvironment, the monocytes then differentiate into suppressive monocytes and myeloid-derived suppressor cells (MDSCs). The mechanism by which tumor cells promote the differentiation of suppressive monocytes has not been determined, however, previous studies have suggested that tumor cells secrete factors that promote the differentiation of suppressive monocytes. In these studies, we wanted to determine whether EVs secreted by tumor cells can promote the differentiation of suppressive monocytes. Since several cancers have been associated with differentiation of suppressive monocytes, we investigated the contribution of tumor secreted EVs by a wide range of solid tumor cell types including osteosarcoma, glioma, colon carcinoma, sarcoma, and melanoma. These studies show that tumor secreted EVs can be taken up by bone marrow-derived monocytes. The monocytes exposed to tumor secreted EVs increased the expression of anti-inflammatory cytokines and mediators, IL-10, TGFβ, arginase, and iNOS, while decreasing the expression of pro-inflammatory cytokines and mediators, IL-12 and TNFα. The tumor secreted EVs also decreased the expression of MHC class II and co-stimulatory molecules on the monocytes while increasing the expression of PDL-1. Finally, monocytes exposed to tumor secreted EVs suppressed activated $CD4^+$ T cells. These results show that tumors secrete EVs that promote the differentiation of a suppressive phenotype in monocytes similar to suppressive monocytes that accumulate in cancer patients. Increased numbers of suppressive monocytes have been correlated with tumor growth, resistance to

chemotherapy, and increased risk of metastasis for a variety of different tumor types, including those chosen in the present study: osteosarcoma[109, 110], glioma[97, 111-115], colon carcinoma[116-118], fibrosarcoma[119], and melanoma[120, 121].

Recently EVs have been determined to play an important role in disease prognosis and pathogenesis, especially in cancer[122, 123]. EVs are a heterogeneous population of nano to micro-sized, membranous vesicles that are constitutively released by cells. EVs can be categorized by their biogenesis and size. Exosomes typically range from 30-150nm in diameter and are formed by the invagination of endosomes and subsequently released into the microenvironment by fusing with cell membrane. Microvesicles are typically bigger, 50-1000nm in diameter, and released by direct budding of cell membrane[124]. Large oncosomes represent an additional population of EVs characterized by their unusually large size (1-10um) and are released by cancer cells[125]. EVs express surface markers and carry a wide range of materials, including proteins, lipids, and genetic materials such as mRNA and miRNA, that are specific to their parental cell of origin[58]. Tetraspanins, such as CD63, CD9, and CD81, are enriched in EVs relative to their cell of origin. In this study, EVs were from a wide range of murine tumor cell lines, including osteosarcoma, glioma, colon carcinoma, fibrosarcoma, and melanoma, as well as EVs from correspondent control primary non-malignant cells. The EVs isolated from the tumor cells and normal cells expressed CD63 and ranged in size from 100-150nm, suggesting these EVs may be exosomes. When fluorescently labeled

tumor secreted EVs were added to monocytes, the EVs were observed in the cell cytoplasm of the monocytes, suggesting active internalization.

Monocytes are generated in the bone marrow from hematopoietic stem cells and then circulate in the blood. During times of inflammation, monocytes are recruited into tissue where they differentiate into macrophages. Macrophage express MHC class II and co-stimulatory molecules enabling them to function as antigen-presenting cells for $CD4^+$ T cells. Macrophage also secrete pro-inflammatory cytokines, such as IL-12 and TNFα, thus supporting both innate and adaptive immune responses. Pro-inflammatory cytokines have anti-tumor effects and have been administered to cancer patients in clinical trials with relative success[126-128]. In contrast, monocytes in the presence of tumors can promote the accumulation of immunosuppressive cell subsets, such as tumor-associated macrophages (TAMs) and myeloid derived suppressor cells (MDSCs)[129]. In the current studies, monocytes were exposed to EVs secreted by tumor cell lines that promoted the development of a suppressive phenotype by increasing the expression of anti-inflammatory mediators, IL-10, iNOS, arginase, and TGFβ, while decreasing the expression of pro-inflammatory cytokines, IL-12 and TNFα. TGFβ and IL-10 promote immune evasion by inducing T cell tolerance to tumor peptides and contributing to the generation of regulatory T cells[29]. TGFβ and IL-10 also downregulate the expression of MHC class II on monocytes converting them to suppressive monocytes[130, 131]. Notably, EVs isolated from the primary, non-malignant control cells did not promote the

monocytes to secrete anti-inflammatory cytokines and instead maintained the level of pro-inflammatory cytokine expression.

Several mechanisms may promote the differentiation of monocytes to suppressive monocytes by tumor derived EVs. The JAK/STAT pathway plays a key role in transcriptional control of cytokines. Activation of JAKs leads to phosphorylation of STAT transcription factors which promote the expression of immune molecules, including interferons and GM-CSF. JAK/STAT pathway is critical in the initiation of innate immunity and myeloid cell development[132, 133]. Suppressor of cytokine signaling 3 (SOCS3) is a negative regulator of the JAK/STAT pathway. IL-10 has been shown to increase the expression of SOCS3. SOCS3 targets JAKs for degradation via proteosomal degradation thus inhibiting STAT3 activation[106]. SOCS3 has also been determined to inhibit signaling in the NFkB pathway and enhancing signaling through the MAPK pathway[107, 134]. Macrophage derived from SOC3 deficient mice display enhanced expression of pro-inflammatory cytokines. The deletion of SOCS3 in myeloid cells delays tumor growth and increases survival of mice bearing orthotopic glioma tumors[135]. In these studies, monocytes exposed to EVs secreted by tumor cells had decreased expression of pro-inflammatory cytokines and increased expression of IL-10 compared to monocytes exposed to EVs secreted by non-malignant cells. Therefore, we wanted to determine whether SOCS3 which has been previously shown to be increased by IL-10 would be increased in monocytes that took up EVs secreted by tumor cells. The current studies show that monocytes exposed to EVs secreted by tumor cells had increased

expression of SOCS3 compared to monocytes exposed to EVs secreted by non-malignant cell controls. Thus, SOCS3 regulation may be one mechanism by which EVs secreted by tumors contribute to differentiation of suppressive monocytes.

Suppressive monocytes that arise during cancer have been shown to have decreased expression of MHC class II, and some have increased expression of PD-L1. The PD-1 receptor is expressed on nearly all immune cell types and, upon binding of PD-L1 ligand, results in decreased activity of the immune cells. Tumor cells have been shown to express PD-L1, and high levels of PD-L1 have been associated with poor patient prognoses[119, 136, 137]. Checkpoint inhibitors in the form of monoclonal antibodies that bind to PD-1/PD-L1 reinvigorate exhausted T cells and have resulted in remarkable responses for particular tumor types[138]. MDSCs characterized as monocytic suppressive cells express CD11b and have increased levels of Ly6C expression. In the current studies, monocytes exposed to EVs secreted by tumor cells lead to decreased expression of MHC class II and co-stimulatory molecules, CD80, and increased expression of PD-L1 and Ly6C on their cell. Monocytes exposed to EVs from non-malignant cells had no change in expression of MHC class II and costimulatory molecules and did not express PD-L1 on their surface. Thus, monocytes exposed to EVs from tumor cells would have reduced ability to present antigens to $CD4^+$ T cells and may promote tolerance and anergy in the $CD4^+$ T cells.

Although MDSCs are capable of suppressing a diverse repertoire of immune cells, they are most recognized for their potent ability to inactivate both $CD4^+$ and $CD8^+$ T cells[139, 140]. Mechanisms involved in MDSC-mediated immunosuppression of T cells include: elimination of key nutritional factors for T cells in the microenvironment via arginase 1 secretion, downregulation or desensitization of the T cell receptor and induction of T cell anergy through the production of reactive oxygen species (ROS) and inducible nitric oxide synthase (iNOS), secretion of immunosuppressive cytokines (IL-10, TGFβ), induction and recruitment of Tregs, and upregulation of inhibitory PDL1 on the MDSC surface . The results from the current studies showed that monocytes exposed to EVs secreted by tumor cells increased the expression of IL-10, TGFβ, iNOS, and arginase. The current studies further showed that monocytes exposed to EVs secreted by tumor cell had decreased expression of MHC class II and costimulatory concomitant with increased expression of PD-L1. Thus, we wanted to determine whether these monocytes could suppress activated $CD4^+$ Tells. Most significantly, the results from the current studies showed that monocytes exposed to EVs secreted by tumor cells decreased the proliferation of activated $CD4^+$ T cells compared to monocytes exposed to EVs from non-malignant cells. Thus, monocytes exposed to EVs secreted by tumor cells had decreased expression of MHC class II and increased expression of PD-L1 as well as increased expression of suppressive cytokines and effector mediators which contributed to the reduced activation and proliferation of antigen-specific $CD4^+$ T cells.

The current studies show that EVs secreted a variety of tumor cell types promote the differentiation of suppressive monocytes and may be a common mechanism used by tumors to create an immunosuppressive microenvironment. Future studies will characterize and compare the contents of EVs secreted by tumor cells to EVs that originate from non-malignant controls to identify specific proteins, mRNA, or miRNA that mediate the differentiation of suppressive monocytes. A better mechanistic understanding of how EVs secreted by tumors alter monocyte differentiation is critical in the discovery of novel therapeutic targets in cancer treatment to reduce immunosuppression and promote immune-based removal of cancer.

MATERIALS AND METHODS

Mice

Female 6-7 week old C57BL/6 mice were purchased from Jackson Laboratories and maintained in the Research Animal Resource (RAR) facility of the University of Minnesota. All mouse experiences were performed in compliance with RAR and Institutional Animal Care and Use Committee (IACUC) guidelines.

Tumor cell lines and primary cell cultures

Immortalized tumor cell lines osteosarcoma (K12), glioma (GL261), melanoma (B16OVA), and colonic carcinoma (CT26) were obtained from the National Cancer Institute. Fibrosarcoma (NCTC 2472) was provided by Dr. Donald Simone (University of Minnesota). Mouse osteosarcoma (K12), glioma

(GL261), melanoma (B16OVA), and colonic carcinoma (CT26) cell lines were cultured in Dulbecco's modified Eagle medium (DMEM, Sigma), supplemented with 10% EVs-free fetal bovine serum (FBS, Gibco), 100 U/ml penicillin, and 100 ug/ml streptomycin. The GL261 cells were cultured in serum-free DMEM/F12 supplemented with N2, 20 ng/ml mouse epidermal growth factor (EGF, Sigma), and 20 ng/ml mouse basic fibroblast growth factor (FGF, Sigma) to expand the population of $CD133^+$ stem-like cells. Mouse fibrosarcoma (NCTC 2472) cells were cultured in NCTC135 medium (Sigma) supplemented with 10% EVs- free serum. In all experiments, cells were maintained at 37°C in a humidified incubator at 5% CO_2.

Primary cultures of murine glia, fibroblasts, melanocytes, and osteoblasts were created using previously described protocols and served as non-malignant controls for each corresponding tumor cell line. Glia cells were isolated from the brain of 1-3 day old neonatal mice[21]. The resulting cell suspension was cultured in complete DMEM/F12 medium (Lonza) supplemented with 10% EVs-free fetal bovine serum (FBS, Gibco), 100 U/ml penicillin, and 100 ug/ml streptomycin and seeded in poly-D-lysine-coated tissue culture flasks (Sigma Aldrich). The medium was replaced every 3 days and cells were ready for use for experiments after removal of the microglia at 14 days of incubation. The glia cells in culture are <90% astrocytes (GFAP positive by florescence microscopy). Melanocytes were harvested from the dorsolateral skin of 1-3 day old neonates[141]. Epidermal and dermal layers were separated by incubating with 0.25% trypsin for 1 hour at 37°C. Single cells were obtained by forcing the digested tissues through a cell

strainer and the cells were suspended in melanocyte growth medium (Sigma Aldrich) containing 5% FBS. FBS was excluded from the medium after the first two days to allow cell selection for the next 14 days. Cells were then cultured in medium supplemented with 5% EVs-free FBS and antibiotics (purity based on anti- melanocyte antibody). Osteoblasts were isolated from the calvarium of 5-6 day old neonatal mice[141]. Each calvarium was removed from the surrounding soft tissue, washed in PBS, and digested in trypsin-EDTA (0.05%) and type II collagenase (0.3 Wünsch units/ml). The mixture was agitated at 37°C and 150rpm for 15 min. The digestion was repeated 3 more times for 45 minutes each. Cells from the last 2 digestions were collected by centrifugation, passed through a strainer, and incubated in complete DMEM (purity based on osteocalcin expression). Embryonic fibroblasts were isolated from mouse embryos at day 14[142]. Embryos were removed from the placenta and washed with PBS. Heads, heart, and liver were removed. The rest of the embryo was minced in a 0.25% trypsin EDTA solution with a scalpel blade and then pipetted up and down for several times. A trypsin EDTA (0.05%)-DNase I (100 Kunitz units) solution was added and incubated at 37°C for 15 minutes with occasional mixing. The activity of trypsin was deactivated by adding 1 volume of complete DMEM. Cells were then centrifuged, and cell pellet were resuspended in complete DMEM, passed through a cell strainer, and seeded in a gelatin coated flask. Pure cultures of embryonic fibroblasts were achieved after the third passage (purity based on anti-fibroblast staining).

Bone marrow derived monocytes (BDMCs) were isolated from femurs and tibia of adult mice. Briefly, both ends of femurs and tibias were incised to allow bone marrow cells to be flushed out by balanced salt solution (BSS) using a syringe with 27-gauge needle. Cells were washed with BSS twice, resuspended, and passed through a cell strainer. Bone marrow cells (14×10^6 cells per T75 flask) were cultured in complete DMEM with 3ng/ml of recombinant granulocyte-macrophage colony-stimulating factor (GM-CSF) (R&D System) to promote the maturation of monocytes (based on $CD11b^{+}CD11C^{-}$ cells). On day 4 of incubation, cultures were re-stimulated with GMCSF and were used for the addition of EVs.

EVs isolation and analysis

Supernatants from tumor and control cells were collected every 24 hrs. Supernatants were centrifuged twice at 4,200xg for 30 minutes to remove cell debris. Total EVs isolation reagent (Invitrogen) was added to the debris-free supernatant and EVs isolated according to the manufacture protocol. The size of EVs which ranged from 80-150nm was confirmed by NanoSight analysis. EVs were analyzed by flow cytometry for surface protein expression, CD63. Briefly, EVs were incubated with aldehyde/sulfate latex beads (Invitrogen) per the manufacturer protocol. The EVs were then incubated with fluorescently labeled antibodies for CD63. The EVs were washed and analyzed on LSRII (BD). Isolated EVs were also analyzed for CD63 by western blot (BioRad) following lysis using Total EVs RNA and protein isolation kit (Life Sciences). To determine concentration of EVs, Bradford assay was performed. Florescent imaging of EVs

was conducted by labeling EVs with carboxyfluorescein succinimidyl ester (2μM) (Thermo Fisher Scientific) and added to 50,000 monocytes grown on coverslips. After 2 hours, monocytes were washed and fixed with 4% paraformaldehyde. Monocytes were then incubated with biotin-conjugated rat anti-mouse CD11b antibody (BD Biosciences) followed by prediluted streptavidin-HRP solution (BD Biosciences). Signal was amplified by TSA Plus Cyanine 3 system (Perkin Elmer). Cells were visualized using the Zeiss LSM 700 confocal microscope.

Real-time PCR

EVs were isolated as described above and added to bone marrow derived monocyte cultures for 3 consecutive days (100μg to $1x10^6$ monocytes). On day 4, EVs-treated monocytes were washed twice with PBS, scraped, and lysed for RNA isolation using SV Total RNA Isolation Kit (Promega). First strand cDNA was generated from 1μg of total RNA using oligo(dT)12–18 primers and Transcriptor First Strand cDNA Synthesis Kit (Clontech). Real time PCR reactions were conducted with FastStart SYBR Green Master Mix (Qiagen Rotor-Gene Q). Briefly, 0.5μM primers, 1X SYBR Green Master Mix, and 2μl diluted cDNA were combined. The primers sequences were previously published, IL-10, IL-12, TNFα, TGFβ, iNOS, arginase I, and SOCS3[21, 143]. Real time PCR was conducted on a Qiagen-Q using a hot start with cycle conditions, 40 cycles; 95°C 15 seconds, 60°C 10 seconds, and 72°C 15 seconds; followed by a melt from 75°C to 95°C. Quantitation of the mRNA was based on standard curves derived from cDNA standards for each primer set that are run with the samples. Samples were normalized based on β-actin expression. All samples were run in

triplicate. Statistical analysis comparison between groups was determined by one-way ANOVA and Bonferroni's multiple comparison test ($p<0.001$).

Flow Cytometry on bone marrow derived monocytes

EVs were isolated as described above and added to the bone marrow derived monocytes for 4 days. After 4 days, the monocytes were removed from culture, washed with FACS buffer, and blocked with antibody to CD16/32 (BD Bioscience). The cells were then incubated with fluorescently labeled antibodies specific for CD11b and Ly6C, CD80, PD-L1, or MHC class II. Monocytes were analyzed by flow cytometry on LSRII (BD) gating on live cells and $CD11b^+$ cells.

T cell proliferation and cytokine assays

Mice were primed with Theiler's murine encephalomyelitis virus (TMEV) capsid epitope $VP4_{21-40}$ in complete Freund's adjuvants emulsion containing respective peptide and *Mycobacterium tuberculosis* H37Ra (Difco Laboratories). Seven days later, spleens were removed from mice and dissociated to obtain a homogenous cell suspension. The red blood cells were lysed with ammonium chloride solution, and $CD4^+$ T cells were sorted with magnetic beads. The $CD4^+$ T cells were labeled with 4μM CFSE and $5x10^5$ cells were placed in each well of a 96-well plate. Next, monocytes treated with EVs were prepared as described above and were added to $CD4^+$ T cells in the plate at 1:5 ratio. The controls consist of monocytes from cultures not treated with EVs or no monocytes added to the $CD4^+$ T cells. The cultures were stimulated with or without specific peptides $VP4_{21-40}$. After 4 days of incubation, $CD4^+$ T cells were removed and

analyzed by flow cytometry to determine proliferation based on CFSE staining. CFSE staining was gated on $CD4^+$ T cells and live cells. The supernatant from the $CD4^+$ T cell cultures was used for IL-2 ELISA per the manufacturers protocol (Invitrogen).

CHAPTER 5

Significance and future directions

MS is a chronic demyelinating disease with unknown etiology and unpredictable clinical course that predominantly affect women and young adults[1, 2]. MS is categorized as immune-mediated demyelinating disease as innate immune cells and autoreactive myelin-specific $CD4^+$T cells cause bystander damage to the myelin sheet. In MS patients, microglia have been consistently found in the lesions, independent of the disease stages[23]. These CNS-resident innate immune cells are found to be activated and have been linked to both demyelination and remyelination due to their phenotypical and functional plasticity[144].Viral infection(s) as the trigger for microglia activation has been comprehensively postulated[8, 9, 13, 145-147]. Although specific viruses associated with the disease has not been determined, the use of antiviral molecule, IFNβ, is widely accepted as a beneficial disease management for MS[80]. As the target is unspecified, current therapeutic interventions are only meant to alleviate symptoms, slow down progression, but unable to provide a cure.

TMEV-IDD serves as a tool to investigate the viral etiology of human MS as well as the role of microglia in the disease pathogenesis. TMEV is a virus that infects the CNS and establishes a persistent infection in the microglia. The microglia become activated during TMEV infection to secrete inflammatory cytokines and effector molecules which promote neuroinflammation. Persistent TMEV infection leads to the development of a demyelinating disease in mice that

is similar to human MS. These studies reveal that microglia secrete exosomes during the acute TMEV infection and chronic TMEV-IDD phases. These results suggest that a novel mechanism in which exosomes secreted by microglia may play a role in maintaining viral persistence and chronic inflammation in the CNS.

Following TMEV infection in SJL mice, the viral loads are high during the first few days in the brain but quickly dissipate to the spinal cord and stay at a low level throughout the lifetime of the animal[26]. Although TMEV persists in microglia, infected microglia produce low levels of infectious viral particles, which does not correlate with the high viral RNA/genome loads detected in the CNS[72]. Exosomes are nano-sized vesicles which contain a wide range of cellular components released from one cell to be taken up by another to facilitate communication. We found that exosomes secreted by microglia in both brains and spinal cord of TMEV-infected mice at 2 days and as late as 63 days contain viral RNA. Importantly, the viral particles and viral proteins were not present in exosomes. These exosomes were taken up and transferred to uninfected CNS resident cells (microglia, astrocytes, and neurons) and infiltrating cells (dendritic cells, monocytes, and macrophages). Moreover, the viral RNA was present in the cells that took up these exosomes and was shown to replicate. These findings do not only agree with the previous published literature, and also propose that exosomes may be one of the strategies that TMEV viral RNA can be transported between cells independent of viral particles and promote persistent infection in the CNS.

The innate immune response, particularly secretion of type I IFNs, induced by TMEV infection has been shown to be essential in the development of TMEV-IDD[41]. The expression of innate immune cytokines and chemokines is the predominant driver of neuroinflammation present in both acute and chronic stages of TMEV infection[32]. Type I IFNs, cytokines, and chemokines are induced in TMEV-IDD via the recognition of viral RNA by innate immune receptors, such as TLR3, TLR7, and MDA5, leading to NF-kB activation. In these studies, exosomes secreted by microglia during the acute TMEV infection or chronic demyelinating disease could activate the expression of type 1 IFNs, IFNα and IFNβ, pro-inflammatory cytokines, IL-6, IL-12, and TNFα, and chemokines, CCL2, in the uninfected bystander cells. This activation was induced by the viral RNA inside exosomes as shown by innate receptor silencing experiments. When MyD88 (activated by TLR7), or MAVS (activated by MDA5) were silenced with siRNAs, the expression of type I IFNs and cytokines were greatly decreased. The rest of the immune response could be triggered by other cellular materials inside the exosomes such as miRNA, mRNA, and proteins, which was not the scope of this work. These data suggest that the innate immune response can be activated in uninfected bystander cells at all phases of TMEV infection by exosomes secreted from microglia.

CNS inflammation induced by innate immune response is associated with the development of TMEV-IDD and several neurological diseases including MS. These studies showed that exosomes released by microglia isolated from both brains and spinal cords at the acute TMEV infection or during chronic

demyelinating disease were able to promote inflammation in the CNS of naïve mice. Thus, microglia exosomes may also be important in driving inflammation in human MS. TMEV-IDD is a useful mouse model to study human chronic progressive MS. The knowledge from this model may provide additional insight into better understanding the pathophysiology of MS.

Future studies may further explore the ability of exosomes to communicate with peripheral immune cells to mount an immune response and promote CNS infiltration of those cells. Additionally, future studies can investigate the proteins and the miRNA profile of exosomes secreted by microglia during the chronic TMEV-IDD in comparison to other phases using mass spectrometry and RNA sequencing, respectively. Exosomes secreted during this phase may contain suppressive or activation markers and miRNA that can affect the immune response of infiltrating immune cells such as virus-specific $CD4^+$T cells and myelin-specific $CD4^+$T. Since these works focused on how exosomes secreted by microglia containing viral RNA is involved in the inflammation, contributing to TMEV-IDD, the integrity of viral RNA remains to be investigated. Future studies could look into how the viral RNA inside of exosomes replicate in the recipient cells and whether viral proteins could be synthesized inside the recipient cells.

Besides studying the role of EVs in neurological diseases, the role of EVs in tumor microenvironment was also investigated in this thesis work. During pathologic conditions like cancers, tumor cells increase their EVs production containing miRNA, mRNA, and proteins that may mediate the immune cell response, contributing to the immunosuppressive microenvironment. Monocytes

are among the first cells to infiltrate the tumor microenvironment. The conversion of monocytes to suppressor cells is crucial in evasion of the immune response and tumor maintenance. The recent studies showed that EVs secreted by a wide range of tumor cells including osteosarcoma, glioma, colon carcinoma, sarcoma, and melanoma, could be taken up by bone marrow-derived monocytes. Further, the monocytes that took up the EVs secreted by tumors matured toward an immune-suppressive phenotype by upregulating the expression of suppressive cytokine (IL-10 and TGFβ) and effector molecules (arginase and iNOS). The monocytes also down regulated MHC class II and costimulatory molecules, CD80, while increasing the expression of PD-L1 and Ly6C on their surface after taking up EVs from tumor cells. Most importantly, monocytes exposed to EVs secreted by tumor cells suppressed activated antigen- specific $CD4^+$ T cells. These results demonstrate the important role of tumor derived EVs in promoting suppressive tumor environment by acting on immune cells such as monocytes. Future studies can further explore the content of these tumor derived EVs and their mechanisms of suppression. From a translational perspective, EVs/exosomes may advance prognostic and treatment approaches in cancers, and other diseases.

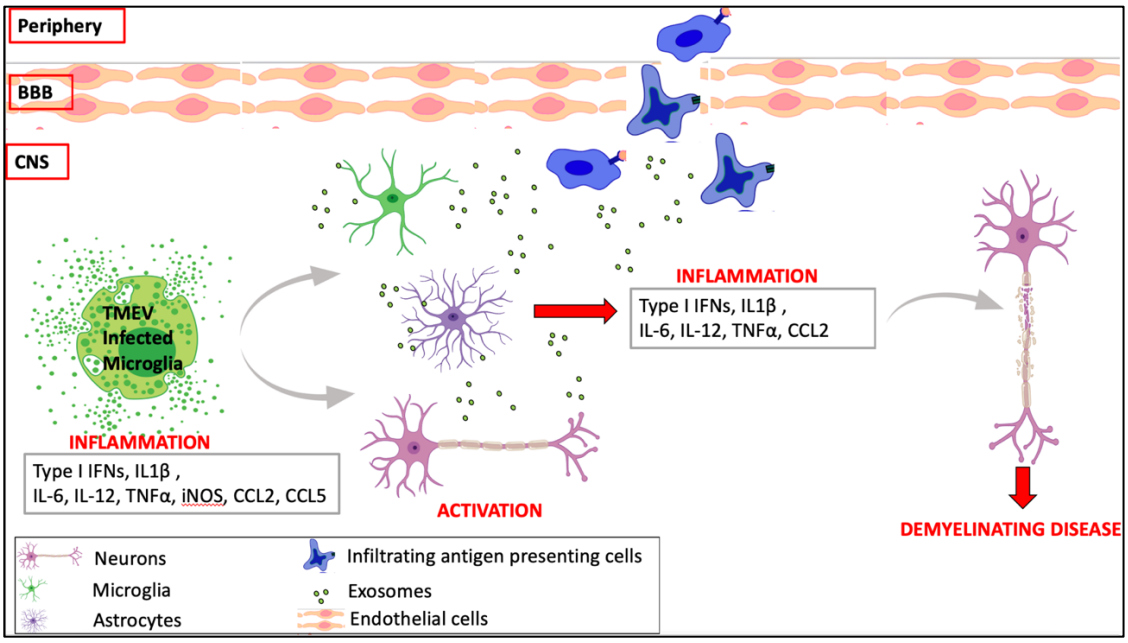

Figure 31. Exosomes secreted by microglia contribute to the TMEV-IDD pathogenesis.

TMEV infection in susceptible mice leads to a persistent infection of microglia in the CNS. TMEV-infected microglia secrete type I IFNs, pro-inflammatory cytokines, and chemokines associated inflammation. TMEV-infected microglia also secrete exosomes containing viral RNA that can be taken up by uninfected bystander CNS cells (microglia, astrocytes, and neurons) and infiltrating immune cells (dendritic cells, monocytes, and macrophages). The viral RNA inside the microglia exosomes can be transferred to uninfected bystander cells and activate an innate immune response in the cells, contributing to the inflammatory milieu in the CNS and the development of demyelinating disease.

BIBLIOGRAPHY

1. Koch-Henriksen N, Sørensen PS. The changing demographic pattern of multiple sclerosis epidemiology. Lancet Neurol 2010; 9:520-32.
2. Harbo HF, Gold R, Tintoré M. Sex and gender issues in multiple sclerosis. Ther Adv Neurol Disord 2013; 6:237-48.
3. Jeong A, Oleske DM, Holman J. Epidemiology of Pediatric-Onset Multiple Sclerosis: A Systematic Review of the Literature. J Child Neurol 2019; 34:705-12.
4. Kaunzner UW, Kang Y, Zhang S, Morris E, Yao Y, Pandya S, et al. Quantitative susceptibility mapping identifies inflammation in a subset of chronic multiple sclerosis lesions. Brain 2019; 142:133-45.
5. Ghasemi N, Razavi S, Nikzad E. Multiple Sclerosis: Pathogenesis, Symptoms, Diagnoses and Cell-Based Therapy. Cell J 2017; 19:1-10.
6. Wingerchuk DM, Carter JL. Multiple sclerosis: current and emerging disease-modifying therapies and treatment strategies. Mayo Clin Proc 2014; 89:225-40.
7. Karussis D, Petrou P. Immune reconstitution therapy (IRT) in multiple sclerosis: the rationale. Immunol Res 2018; 66:642-8.
8. Olival GS, Lima BM, Sumita LM, Serafim V, Fink MC, Nali LH, et al. Multiple sclerosis and herpesvirus interaction. Arq Neuropsiquiatr 2013; 71:727-30.
9. Kakalacheva K, Münz C, Lünemann JD. Viral triggers of multiple sclerosis. Biochim Biophys Acta 2011; 1812:132-40.
10. Kurtzke JF. Epidemiologic evidence for multiple sclerosis as an infection. Clin Microbiol Rev 1993; 6:382-427.
11. Lipton HL. Theiler's virus infection in mice: an unusual biphasic disease process leading to demyelination. Infect Immun 1975; 11:1147-55.
12. Simon KC, O'Reilly EJ, Munger KL, Finerty S, Morgan AJ, Ascherio A. Epstein-Barr virus neutralizing antibody levels and risk of multiple sclerosis. Mult Scler 2012; 18:1185-7.
13. Simpson S, Taylor B, Dwyer DE, Taylor J, Blizzard L, Ponsonby AL, et al. Anti-HHV-6 IgG titer significantly predicts subsequent relapse risk in multiple sclerosis. Mult Scler 2012; 18:799-806.
14. Li H, Cuzner ML, Newcombe J. Microglia-derived macrophages in early multiple sclerosis plaques. Neuropathol Appl Neurobiol 1996; 22:207-15.
15. Luo C, Jian C, Liao Y, Huang Q, Wu Y, Liu X, et al. The role of microglia in multiple sclerosis. Neuropsychiatr Dis Treat 2017; 13:1661-7.
16. Louveau A, Herz J, Alme MN, Salvador AF, Dong MQ, Viar KE, et al. CNS lymphatic drainage and neuroinflammation are regulated by meningeal lymphatic vasculature. Nat Neurosci 2018; 21:1380-91.
17. Nayak D, Roth TL, McGavern DB. Microglia development and function. Annual review of immunology 2014; 32:367.

18. Ginhoux F, Greter M, Leboeuf M, Nandi S, See P, Gokhan S, et al. Fate mapping analysis reveals that adult microglia derive from primitive macrophages. Science 2010; 330:841-5.
19. Schulz C, Gomez Perdiguero E, Chorro L, Szabo-Rogers H, Cagnard N, Kierdorf K, et al. A lineage of myeloid cells independent of Myb and hematopoietic stem cells. Science 2012; 336:86-90.
20. Olson JK, Miller SD. Microglia initiate central nervous system innate and adaptive immune responses through multiple TLRs. J Immunol 2004; 173:3916-24.
21. Olson JK, Girvin AM, Miller SD. Direct activation of innate and antigen-presenting functions of microglia following infection with Theiler's virus. J Virol 2001; 75:9780-9.
22. van Horssen J, Singh S, van der Pol S, Kipp M, Lim JL, Peferoen L, et al. Clusters of activated microglia in normal-appearing white matter show signs of innate immune activation. J Neuroinflammation 2012; 9:156.
23. Kuhlmann T, Ludwin S, Prat A, Antel J, Brück W, Lassmann H. An updated histological classification system for multiple sclerosis lesions. Acta Neuropathol 2017; 133:13-24.
24. Satoh J, Kino Y, Asahina N, Takitani M, Miyoshi J, Ishida T, et al. TMEM119 marks a subset of microglia in the human brain. Neuropathology 2016; 36:39-49.
25. Zrzavy T, Hametner S, Wimmer I, Butovsky O, Weiner HL, Lassmann H. Loss of 'homeostatic' microglia and patterns of their activation in active multiple sclerosis. Brain 2017; 140:1900-13.
26. Lipton HL, Twaddle G, Jelachich ML. The predominant virus antigen burden is present in macrophages in Theiler's murine encephalomyelitis virus-induced demyelinating disease. J Virol 1995; 69:2525-33.
27. Neville KL, Padilla J, Miller SD. Myelin-specific tolerance attenuates the progression of a virus-induced demyelinating disease: implications for the treatment of MS. J Neuroimmunol 2002; 123:18-29.
28. Dal Canto MC, Calenoff MA, Miller SD, Vanderlugt CL. Lymphocytes from mice chronically infected with Theiler's murine encephalomyelitis virus produce demyelination of organotypic cultures after stimulation with the major encephalitogenic epitope of myelin proteolipid protein. Epitope spreading in TMEV infection has functional activity. J Neuroimmunol 2000; 104:79-84.
29. Akdis CA, Akdis M. Mechanisms of immune tolerance to allergens: role of IL-10 and Tregs. J Clin Invest 2014; 124:4678-80.
30. Clatch RJ, Melvold RW, Miller SD, Lipton HL. Theiler's murine encephalomyelitis virus (TMEV)-induced demyelinating disease in mice is influenced by the H-2D region: correlation with TEMV-specific delayed-type hypersensitivity. J Immunol 1985; 135:1408-14.
31. Olson JK. Effect of the innate immune response on development of Theiler's murine encephalomyelitis virus-induced demyelinating disease. J Neurovirol 2014; 20:427-36.

32. Gilli F, Li L, Pachner AR. The immune response in the CNS in Theiler's virus induced demyelinating disease switches from an early adaptive response to a chronic innate-like response. J Neurovirol 2016; 22:66-79.
33. Alexopoulou L, Holt AC, Medzhitov R, Flavell RA. Recognition of double-stranded RNA and activation of NF-kappaB by Toll-like receptor 3. Nature 2001; 413:732-8.
34. Lund JM, Alexopoulou L, Sato A, Karow M, Adams NC, Gale NW, et al. Recognition of single-stranded RNA viruses by Toll-like receptor 7. Proc Natl Acad Sci U S A 2004; 101:5598-603.
35. Diebold SS, Kaisho T, Hemmi H, Akira S, Reis e Sousa C. Innate antiviral responses by means of TLR7-mediated recognition of single-stranded RNA. Science 2004; 303:1529-31.
36. Heil F, Hemmi H, Hochrein H, Ampenberger F, Kirschning C, Akira S, et al. Species-specific recognition of single-stranded RNA via toll-like receptor 7 and 8. Science 2004; 303:1526-9.
37. Hargreaves DC, Medzhitov R. Innate sensors of microbial infection. J Clin Immunol 2005; 25:503-10.
38. Takeda K, Akira S. Toll receptors and pathogen resistance. Cell Microbiol 2003; 5:143-53.
39. Malakhova O, Malakhov M, Hetherington C, Zhang DE. Lipopolysaccharide activates the expression of ISG15-specific protease UBP43 via interferon regulatory factor 3. J Biol Chem 2002; 277:14703-11.
40. Sasai M, Matsumoto M, Seya T. The kinase complex responsible for IRF-3-mediated IFN-beta production in myeloid dendritic cells (mDC). J Biochem 2006; 139:171-5.
41. Olson JK, Miller SD. The innate immune response affects the development of the autoimmune response in Theiler's virus-induced demyelinating disease. J Immunol 2009; 182:5712-22.
42. Biron CA, Nguyen KB, Pien GC, Cousens LP, Salazar-Mather TP. Natural killer cells in antiviral defense: function and regulation by innate cytokines. Annu Rev Immunol 1999; 17:189-220.
43. Le Bon A, Schiavoni G, D'Agostino G, Gresser I, Belardelli F, Tough DF. Type i interferons potently enhance humoral immunity and can promote isotype switching by stimulating dendritic cells in vivo. Immunity 2001; 14:461-70.
44. Biron CA. Interferons alpha and beta as immune regulators--a new look. Immunity 2001; 14:661-4.
45. Tough DF, Borrow P, Sprent J. Induction of bystander T cell proliferation by viruses and type I interferon in vivo. Science 1996; 272:1947-50.
46. Pullen LC, Miller SD, Dal Canto MC, Kim BS. Class I-deficient resistant mice intracerebrally inoculated with Theiler's virus show an increased T cell response to viral antigens and susceptibility to demyelination. Eur J Immunol 1993; 23:2287-93.
47. Kang BS, Lyman MA, Kim BS. Differences in avidity and epitope recognition of CD8(+) T cells infiltrating the central nervous systems of

SJL/J mice infected with BeAn and DA strains of Theiler's murine encephalomyelitis virus. J Virol 2002; 76:11780-4.
48. Murray PD, Pavelko KD, Leibowitz J, Lin X, Rodriguez M. CD4(+) and CD8(+) T cells make discrete contributions to demyelination and neurologic disease in a viral model of multiple sclerosis. J Virol 1998; 72:7320-9.
49. Katz-Levy Y, Neville KL, Padilla J, Rahbe S, Begolka WS, Girvin AM, et al. Temporal development of autoreactive Th1 responses and endogenous presentation of self myelin epitopes by central nervous system-resident APCs in Theiler's virus-infected mice. J Immunol 2000; 165:5304-14.
50. Miller SD, Clatch RJ, Pevear DC, Trotter JL, Lipton HL. Class II-restricted T cell responses in Theiler's murine encephalomyelitis virus (TMEV)-induced demyelinating disease. I. Cross-specificity among TMEV substrains and related picornaviruses, but not myelin proteins. J Immunol 1987; 138:3776-84.
51. Karpus WJ, Pope JG, Peterson JD, Dal Canto MC, Miller SD. Inhibition of Theiler's virus-mediated demyelination by peripheral immune tolerance induction. J Immunol 1995; 155:947-57.
52. Record M, Carayon K, Poirot M, Silvente-Poirot S. Exosomes as new vesicular lipid transporters involved in cell-cell communication and various pathophysiologies. Biochim Biophys Acta 2014; 1841:108-20.
53. Simons M, Raposo G. Exosomes--vesicular carriers for intercellular communication. Curr Opin Cell Biol 2009; 21:575-81.
54. Janas T, Janas MM, Sapoń K. Mechanisms of RNA loading into exosomes. FEBS Lett 2015; 589:1391-8.
55. Schneider A, Simons M. Exosomes: vesicular carriers for intercellular communication in neurodegenerative disorders. Cell Tissue Res 2013; 352:33-47.
56. Zhang Y, Liu Y, Liu H, Tang WH. Exosomes: biogenesis, biologic function and clinical potential. Cell Biosci 2019; 9:19.
57. Barile L, Vassalli G. Exosomes: Therapy delivery tools and biomarkers of diseases. Pharmacol Ther 2017; 174:63-78.
58. Andreu Z, Yáñez-Mó M. Tetraspanins in extracellular vesicle formation and function. Front Immunol 2014; 5:442.
59. He C, Zheng S, Luo Y, Wang B. Exosome Theranostics: Biology and Translational Medicine. Theranostics 2018; 8:237-55.
60. Vella LJ, Sharples RA, Nisbet RM, Cappai R, Hill AF. The role of exosomes in the processing of proteins associated with neurodegenerative diseases. Eur Biophys J 2008; 37:323-32.
61. Bukong TN, Momen-Heravi F, Kodys K, Bala S, Szabo G. Exosomes from hepatitis C infected patients transmit HCV infection and contain replication competent viral RNA in complex with Ago2-miR122-HSP90. PLoS Pathog 2014; 10:e1004424.
62. Saha B, Kodys K, Adejumo A, Szabo G. Circulating and Exosome-Packaged Hepatitis C Single-Stranded RNA Induce Monocyte

Differentiation via TLR7/8 to Polarized Macrophages and Fibrocytes. J Immunol 2017; 198:1974-84.
63. Rahimian P, He JJ. Exosome-associated release, uptake, and neurotoxicity of HIV-1 Tat protein. J Neurovirol 2016; 22:774-88.
64. Hoshino A, Costa-Silva B, Shen TL, Rodrigues G, Hashimoto A, Tesic Mark M, et al. Tumour exosome integrins determine organotropic metastasis. Nature 2015; 527:329-35.
65. Zeng Z, Li Y, Pan Y, Lan X, Song F, Sun J, et al. Cancer-derived exosomal miR-25-3p promotes pre-metastatic niche formation by inducing vascular permeability and angiogenesis. Nat Commun 2018; 9:5395.
66. Zhou J, Li X, Wu X, Zhang T, Zhu Q, Wang X, et al. Exosomes Released from Tumor-Associated Macrophages Transfer miRNAs That Induce a Treg/Th17 Cell Imbalance in Epithelial Ovarian Cancer. Cancer Immunol Res 2018; 6:1578-92.
67. Bowen JL, Olson JK. Innate immune CD11b+Gr-1+ cells, suppressor cells, affect the immune response during Theiler's virus-induced demyelinating disease. J Immunol 2009; 183:6971-80.
68. Dal Canto MC, Lipton HL. Primary demyelination in Theiler's virus infection. An ultrastructural study. Lab Invest 1975; 33:626-37.
69. Lipton HL, S. D. Miller, R. Melvold, and R. S. Fujinami. Theiler's murine encephalomyelitis virus (TMEV) infection in mice as a model for MS: Springer-Verlag, NY; 1986.
70. Théry C, Witwer KW, Aikawa E, Alcaraz MJ, Anderson JD, Andriantsitohaina R, et al. Minimal information for studies of extracellular vesicles 2018 (MISEV2018): a position statement of the International Society for Extracellular Vesicles and update of the MISEV2014 guidelines. J Extracell Vesicles 2018; 7:1535750.
71. Nair S, Diamond MS. Innate immune interactions within the central nervous system modulate pathogenesis of viral infections. Curr Opin Immunol 2015; 36:47-53.
72. Trottier M, Kallio P, Wang W, Lipton HL. High numbers of viral RNA copies in the central nervous system of mice during persistent infection with Theiler's virus. J Virol 2001; 75:7420-8.
73. Tsunoda I, Fujinami RS. Neuropathogenesis of Theiler's murine encephalomyelitis virus infection, an animal model for multiple sclerosis. J Neuroimmune Pharmacol 2010; 5:355-69.
74. Denic A, Johnson AJ, Bieber AJ, Warrington AE, Rodriguez M, Pirko I. The relevance of animal models in multiple sclerosis research. Pathophysiology 2011; 18:21-9.
75. Sadeghipour S, Mathias RA. Herpesviruses hijack host exosomes for viral pathogenesis. Semin Cell Dev Biol 2017; 67:91-100.
76. Cosset FL, Dreux M. HCV transmission by hepatic exosomes establishes a productive infection. J Hepatol 2014; 60:674-5.
77. Olson JK. Immune response by microglia in the spinal cord. Ann N Y Acad Sci 2010; 1198:271-8.

78. Xuan FL, Chithanathan K, Lilleväli K, Yuan X, Tian L. Differences of Microglia in the Brain and the Spinal Cord. Front Cell Neurosci 2019; 13:504.
79. Murray PD, Krivacic K, Chernosky A, Wei T, Ransohoff RM, Rodriguez M. Biphasic and regionally-restricted chemokine expression in the central nervous system in the Theiler's virus model of multiple sclerosis. J Neurovirol 2000; 6 Suppl 1:S44-52.
80. Reder AT, Feng X. How type I interferons work in multiple sclerosis and other diseases: some unexpected mechanisms. J Interferon Cytokine Res 2014; 34:589-99.
81. Valadi H, Ekström K, Bossios A, Sjöstrand M, Lee JJ, Lötvall JO. Exosome-mediated transfer of mRNAs and microRNAs is a novel mechanism of genetic exchange between cells. Nat Cell Biol 2007; 9:654-9.
82. Clatch RJ, Miller SD, Metzner R, Dal Canto MC, Lipton HL. Monocytes/macrophages isolated from the mouse central nervous system contain infectious Theiler's murine encephalomyelitis virus (TMEV). Virology 1990; 176:244-54.
83. Wang Y, Zhang S, Song W, Zhang W, Li J, Li C, et al. Exosomes from EV71-infected oral epithelial cells can transfer miR-30a to promote EV71 infection. Oral Dis 2020.
84. Reyes-Ruiz JM, Osuna-Ramos JF, De Jesús-González LA, Hurtado-Monzón AM, Farfan-Morales CN, Cervantes-Salazar M, et al. Isolation and characterization of exosomes released from mosquito cells infected with dengue virus. Virus Res 2019; 266:1-14.
85. Liddelow SA, Guttenplan KA, Clarke LE, Bennett FC, Bohlen CJ, Schirmer L, et al. Neurotoxic reactive astrocytes are induced by activated microglia. Nature 2017; 541:481-7.
86. Rothhammer V, Borucki DM, Tjon EC, Takenaka MC, Chao CC, Ardura-Fabregat A, et al. Microglial control of astrocytes in response to microbial metabolites. Nature 2018; 557:724-8.
87. Scott BS. Adult mouse dorsal root ganglia neurons in cell culture. J Neurobiol 1977; 8:417-27.
88. Matheu MP, Sen D, Cahalan MD, Parker I. Generation of bone marrow derived murine dendritic cells for use in 2-photon imaging. J Vis Exp 2008.
89. Fuller KG, Olson JK, Howard LM, Croxford JL, Miller SD. Mouse models of multiple sclerosis: experimental autoimmune encephalomyelitis and Theiler's virus-induced demyelinating disease. Methods Mol Med 2004; 102:339-61.
90. Ostuni R, Kratochvill F, Murray PJ, Natoli G. Macrophages and cancer: from mechanisms to therapeutic implications. Trends Immunol 2015; 36:229-39.
91. Serafini P, Borrello I, Bronte V. Myeloid suppressor cells in cancer: recruitment, phenotype, properties, and mechanisms of immune suppression. Semin Cancer Biol 2006; 16:53-65.

92. Umansky V, Blattner C, Fleming V, Hu X, Gebhardt C, Altevogt P, et al. Myeloid-derived suppressor cells and tumor escape from immune surveillance. Semin Immunopathol 2017; 39:295-305.
93. Woiciechowsky C, Asadullah K, Nestler D, Schöning B, Glöckner F, Döcke WD, et al. Diminished monocytic HLA-DR expression and ex vivo cytokine secretion capacity in patients with glioblastoma: effect of tumor extirpation. J Neuroimmunol 1998; 84:164-71.
94. Valenti R, Huber V, Filipazzi P, Pilla L, Sovena G, Villa A, et al. Human tumor-released microvesicles promote the differentiation of myeloid cells with transforming growth factor-beta-mediated suppressive activity on T lymphocytes. Cancer Res 2006; 66:9290-8.
95. Gustafson MP, Lin Y, Bleeker JS, Warad D, Tollefson MK, Crispen PL, et al. Intratumoral CD14+ Cells and Circulating CD14+HLA-DRlo/neg Monocytes Correlate with Decreased Survival in Patients with Clear Cell Renal Cell Carcinoma. Clin Cancer Res 2015; 21:4224-33.
96. Morales JK, Kmieciak M, Knutson KL, Bear HD, Manjili MH. GM-CSF is one of the main breast tumor-derived soluble factors involved in the differentiation of CD11b-Gr1- bone marrow progenitor cells into myeloid-derived suppressor cells. Breast Cancer Res Treat 2010; 123:39-49.
97. Rodrigues JC, Gonzalez GC, Zhang L, Ibrahim G, Kelly JJ, Gustafson MP, et al. Normal human monocytes exposed to glioma cells acquire myeloid-derived suppressor cell-like properties. Neuro Oncol 2010; 12:351-65.
98. Okada SL, Simmons RM, Franke-Welch S, Nguyen TH, Korman AJ, Dillon SR, et al. Conditioned media from the renal cell carcinoma cell line 786.O drives human blood monocytes to a monocytic myeloid-derived suppressor cell phenotype. Cell Immunol 2018; 323:49-58.
99. Youn JI, Nagaraj S, Collazo M, Gabrilovich DI. Subsets of myeloid-derived suppressor cells in tumor-bearing mice. J Immunol 2008; 181:5791-802.
100. Cheng P, Corzo CA, Luetteke N, Yu B, Nagaraj S, Bui MM, et al. Inhibition of dendritic cell differentiation and accumulation of myeloid-derived suppressor cells in cancer is regulated by S100A9 protein. J Exp Med 2008; 205:2235-49.
101. Huber V, Fais S, Iero M, Lugini L, Canese P, Squarcina P, et al. Human colorectal cancer cells induce T-cell death through release of proapoptotic microvesicles: role in immune escape. Gastroenterology 2005; 128:1796-804.
102. Taylor DD, Lyons KS, Gerçel-Taylor C. Shed membrane fragment-associated markers for endometrial and ovarian cancers. Gynecol Oncol 2002; 84:443-8.
103. Whiteside TL. Immune modulation of T-cell and NK (natural killer) cell activities by TEXs (tumour-derived exosomes). Biochem Soc Trans 2013; 41:245-51.
104. Taylor DD, Gerçel-Taylor C, Lyons KS, Stanson J, Whiteside TL. T-cell apoptosis and suppression of T-cell receptor/CD3-zeta by Fas ligand-containing membrane vesicles shed from ovarian tumors. Clin Cancer Res 2003; 9:5113-9.

105. Wieckowski EU, Visus C, Szajnik M, Szczepanski MJ, Storkus WJ, Whiteside TL. Tumor-derived microvesicles promote regulatory T cell expansion and induce apoptosis in tumor-reactive activated CD8+ T lymphocytes. J Immunol 2009; 183:3720-30.
106. Boyle K, Zhang JG, Nicholson SE, Trounson E, Babon JJ, McManus EJ, et al. Deletion of the SOCS box of suppressor of cytokine signaling 3 (SOCS3) in embryonic stem cells reveals SOCS box-dependent regulation of JAK but not STAT phosphorylation. Cell Signal 2009; 21:394-404.
107. Baetz A, Frey M, Heeg K, Dalpke AH. Suppressor of cytokine signaling (SOCS) proteins indirectly regulate toll-like receptor signaling in innate immune cells. J Biol Chem 2004; 279:54708-15.
108. Hanahan D, Weinberg RA. Hallmarks of cancer: the next generation. Cell 2011; 144:646-74.
109. Horlad H, Fujiwara Y, Takemura K, Ohnishi K, Ikeda T, Tsukamoto H, et al. Corosolic acid impairs tumor development and lung metastasis by inhibiting the immunosuppressive activity of myeloid-derived suppressor cells. Mol Nutr Food Res 2013; 57:1046-54.
110. Jiang K, Li J, Zhang J, Wang L, Zhang Q, Ge J, et al. SDF-1/CXCR4 axis facilitates myeloid-derived suppressor cells accumulation in osteosarcoma microenvironment and blunts the response to anti-PD-1 therapy. Int Immunopharmacol 2019; 75:105818.
111. Wu A, Maxwell R, Xia Y, Cardarelli P, Oyasu M, Belcaid Z, et al. Combination anti-CXCR4 and anti-PD-1 immunotherapy provides survival benefit in glioblastoma through immune cell modulation of tumor microenvironment. J Neurooncol 2019; 143:241-9.
112. Guo X, Qiu W, Wang J, Liu Q, Qian M, Wang S, et al. Glioma exosomes mediate the expansion and function of myeloid-derived suppressor cells through microRNA-29a/Hbp1 and microRNA-92a/Prkar1a pathways. Int J Cancer 2019; 144:3111-26.
113. Domenis R, Cesselli D, Toffoletto B, Bourkoula E, Caponnetto F, Manini I, et al. Systemic T Cells Immunosuppression of Glioma Stem Cell-Derived Exosomes Is Mediated by Monocytic Myeloid-Derived Suppressor Cells. PLoS One 2017; 12:e0169932.
114. Gao C, Wang A. [The role of myeloid-derived suppressor cells in glioma microenvironment]. Sheng Wu Yi Xue Gong Cheng Xue Za Zhi 2019; 36:515-20.
115. Guo X, Qiu W, Liu Q, Qian M, Wang S, Zhang Z, et al. Immunosuppressive effects of hypoxia-induced glioma exosomes through myeloid-derived suppressor cells via the miR-10a/Rora and miR-21/Pten Pathways. Oncogene 2018; 37:4239-59.
116. Zhang B, Wang Z, Wu L, Zhang M, Li W, Ding J, et al. Circulating and tumor-infiltrating myeloid-derived suppressor cells in patients with colorectal carcinoma. PLoS One 2013; 8:e57114.
117. Shimura T, Shibata M, Gonda K, Hayase S, Sakamoto W, Okayama H, et al. Prognostic impact of preoperative lymphocyte-to-monocyte ratio in

patients with colorectal cancer with special reference to myeloid-derived suppressor cells. Fukushima J Med Sci 2018; 64:64-72.
118. OuYang LY, Wu XJ, Ye SB, Zhang RX, Li ZL, Liao W, et al. Tumor-induced myeloid-derived suppressor cells promote tumor progression through oxidative metabolism in human colorectal cancer. J Transl Med 2015; 13:47.
119. Chen G, Huang AC, Zhang W, Zhang G, Wu M, Xu W, et al. Exosomal PD-L1 contributes to immunosuppression and is associated with anti-PD-1 response. Nature 2018; 560:382-6.
120. Meyer C, Cagnon L, Costa-Nunes CM, Baumgaertner P, Montandon N, Leyvraz L, et al. Frequencies of circulating MDSC correlate with clinical outcome of melanoma patients treated with ipilimumab. Cancer Immunol Immunother 2014; 63:247-57.
121. de Coaña YP, Wolodarski M, Poschke I, Yoshimoto Y, Yang Y, Nyström M, et al. Ipilimumab treatment decreases monocytic MDSCs and increases CD8 effector memory T cells in long-term survivors with advanced melanoma. Oncotarget 2017; 8:21539-53.
122. Zhang HG, Grizzle WE. Exosomes and cancer: a newly described pathway of immune suppression. Clin Cancer Res 2011; 17:959-64.
123. Zhang HG, Grizzle WE. Exosomes: a novel pathway of local and distant intercellular communication that facilitates the growth and metastasis of neoplastic lesions. Am J Pathol 2014; 184:28-41.
124. Willms E, Cabañas C, Mäger I, Wood MJA, Vader P. Extracellular Vesicle Heterogeneity: Subpopulations, Isolation Techniques, and Diverse Functions in Cancer Progression. Front Immunol 2018; 9:738.
125. Minciacchi VR, Freeman MR, Di Vizio D. Extracellular vesicles in cancer: exosomes, microvesicles and the emerging role of large oncosomes. Semin Cell Dev Biol 2015; 40:41-51.
126. Tahara H, Lotze MT. Antitumor effects of interleukin-12 (IL-12): applications for the immunotherapy and gene therapy of cancer. Gene Ther 1995; 2:96-106.
127. Thamm DH, Kurzman ID, Clark MA, Ehrhart EJ, Kraft SL, Gustafson DL, et al. Preclinical investigation of PEGylated tumor necrosis factor alpha in dogs with spontaneous tumors: phase I evaluation. Clin Cancer Res 2010; 16:1498-508.
128. Luo JL, Maeda S, Hsu LC, Yagita H, Karin M. Inhibition of NF-kappaB in cancer cells converts inflammation- induced tumor growth mediated by TNFalpha to TRAIL-mediated tumor regression. Cancer Cell 2004; 6:297-305.
129. Richards DM, Hettinger J, Feuerer M. Monocytes and macrophages in cancer: development and functions. Cancer Microenviron 2013; 6:179-91.
130. Koppelman B, Neefjes JJ, de Vries JE, de Waal Malefyt R. Interleukin-10 down-regulates MHC class II alphabeta peptide complexes at the plasma membrane of monocytes by affecting arrival and recycling. Immunity 1997; 7:861-71.

131. Gonzalez-Junca A, Driscoll KE, Pellicciotta I, Du S, Lo CH, Roy R, et al. Autocrine TGFβ Is a Survival Factor for Monocytes and Drives Immunosuppressive Lineage Commitment. Cancer Immunol Res 2019; 7:306-20.
132. O'Shea JJ, Plenge R. JAK and STAT signaling molecules in immunoregulation and immune-mediated disease. Immunity 2012; 36:542-50.
133. Ding C, Sun X, Wu C, Hu X, Zhang HG, Yan J. Tumor Microenvironment Modulates Immunological Outcomes of Myeloid Cells with mTORC1 Disruption. J Immunol 2019; 202:1623-34.
134. Cacalano NA, Sanden D, Johnston JA. Tyrosine-phosphorylated SOCS-3 inhibits STAT activation but binds to p120 RasGAP and activates Ras. Nat Cell Biol 2001; 3:460-5.
135. McFarland BC, Marks MP, Rowse AL, Fehling SC, Gerigk M, Qin H, et al. Loss of SOCS3 in myeloid cells prolongs survival in a syngeneic model of glioma. Oncotarget 2016; 7:20621-35.
136. Wang X, Teng F, Kong L, Yu J. PD-L1 expression in human cancers and its association with clinical outcomes. Onco Targets Ther 2016; 9:5023-39.
137. Theodoraki MN, Yerneni SS, Hoffmann TK, Gooding WE, Whiteside TL. Clinical Significance of PD-L1. Clin Cancer Res 2018; 24:896-905.
138. Sunshine J, Taube JM. PD-1/PD-L1 inhibitors. Curr Opin Pharmacol 2015; 23:32-8.
139. Kumar V, Patel S, Tcyganov E, Gabrilovich DI. The Nature of Myeloid-Derived Suppressor Cells in the Tumor Microenvironment. Trends Immunol 2016; 37:208-20.
140. Gabrilovich DI, Ostrand-Rosenberg S, Bronte V. Coordinated regulation of myeloid cells by tumours. Nat Rev Immunol 2012; 12:253-68.
141. Owen TA, Pan LC. Isolation and culture of rodent osteoprogenitor cells. Methods Mol Biol 2008; 455:3-18.
142. Durkin ME, Qian X, Popescu NC, Lowy D. Isolation of Mouse Embryo Fibroblasts. Bio Protocol 2013; 3.
143. Boontanrart M, Hall SD, Spanier JA, Hayes CE, Olson JK. Vitamin D3 alters microglia immune activation by an IL-10 dependent SOCS3 mechanism. J Neuroimmunol 2016; 292:126-36.
144. Voss EV, Škuljec J, Gudi V, Skripuletz T, Pul R, Trebst C, et al. Characterisation of microglia during de- and remyelination: can they create a repair promoting environment? Neurobiol Dis 2012; 45:519-28.
145. Mouhieddine TH, Darwish H, Fawaz L, Yamout B, Tamim H, Khoury SJ. Risk factors for multiple sclerosis and associations with anti-EBV antibody titers. Clin Immunol 2015; 158:59-66.
146. Lucas RM, Ponsonby AL, Dear K, Valery P, Pender MP, Burrows JM, et al. Current and past Epstein-Barr virus infection in risk of initial CNS demyelination. Neurology 2011; 77:371-9.

147. Ascherio A, Munger KL, Lennette ET, Spiegelman D, Hernán MA, Olek MJ, et al. Epstein-Barr virus antibodies and risk of multiple sclerosis: a prospective study. JAMA 2001; 286:3083-8.